

INSTRUMENTATION & DETECTORS for HIGH ENERGY PHYSICS IV

isabelle.wingerter@lapp.in2p3.fr
Office: 40-4-D32 - tel: 16 4889

DETECTOR: LECTURE III QUIZZ

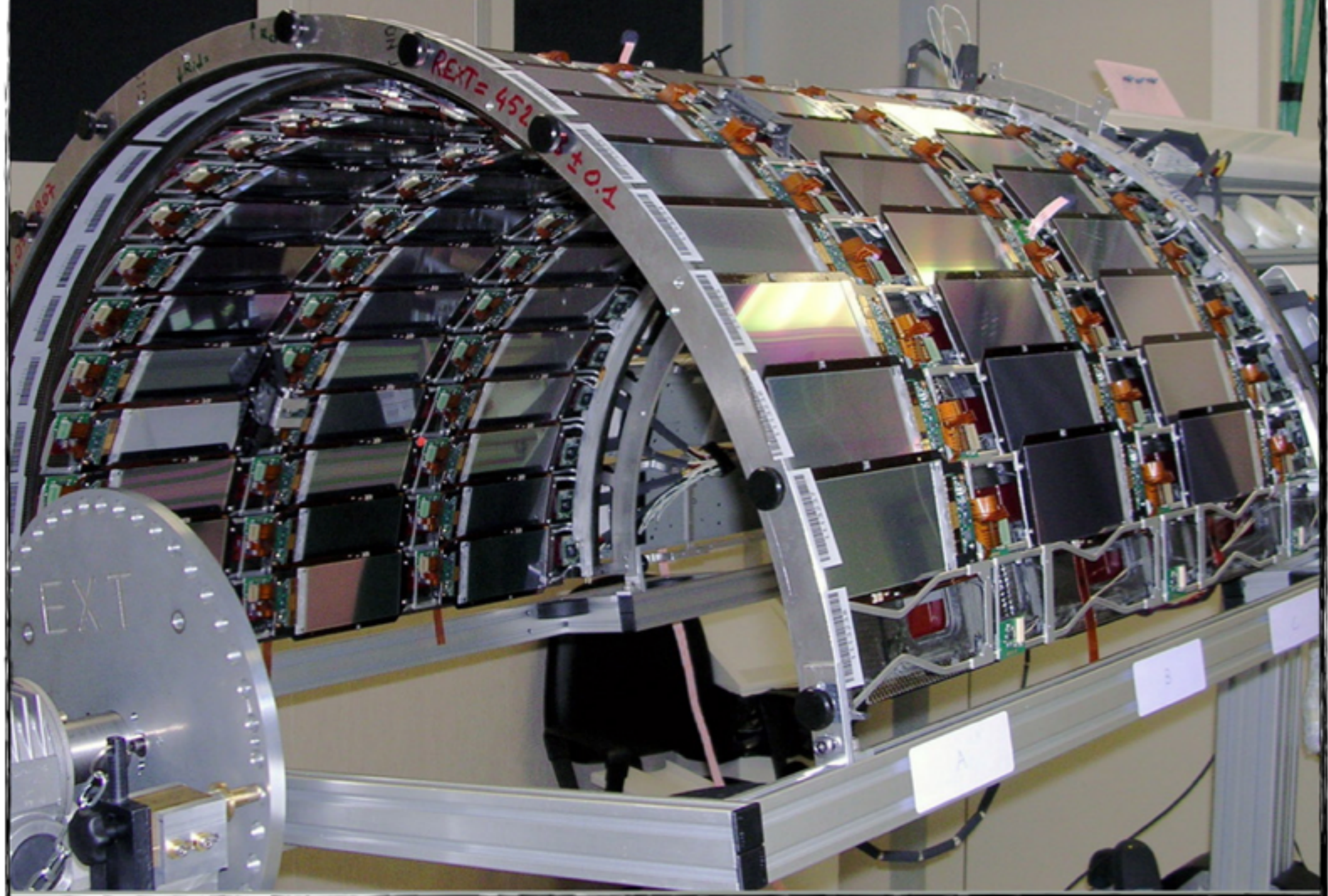
Gas vs solid state ionisation detector ?

Typical size of a cell in a silicium detector

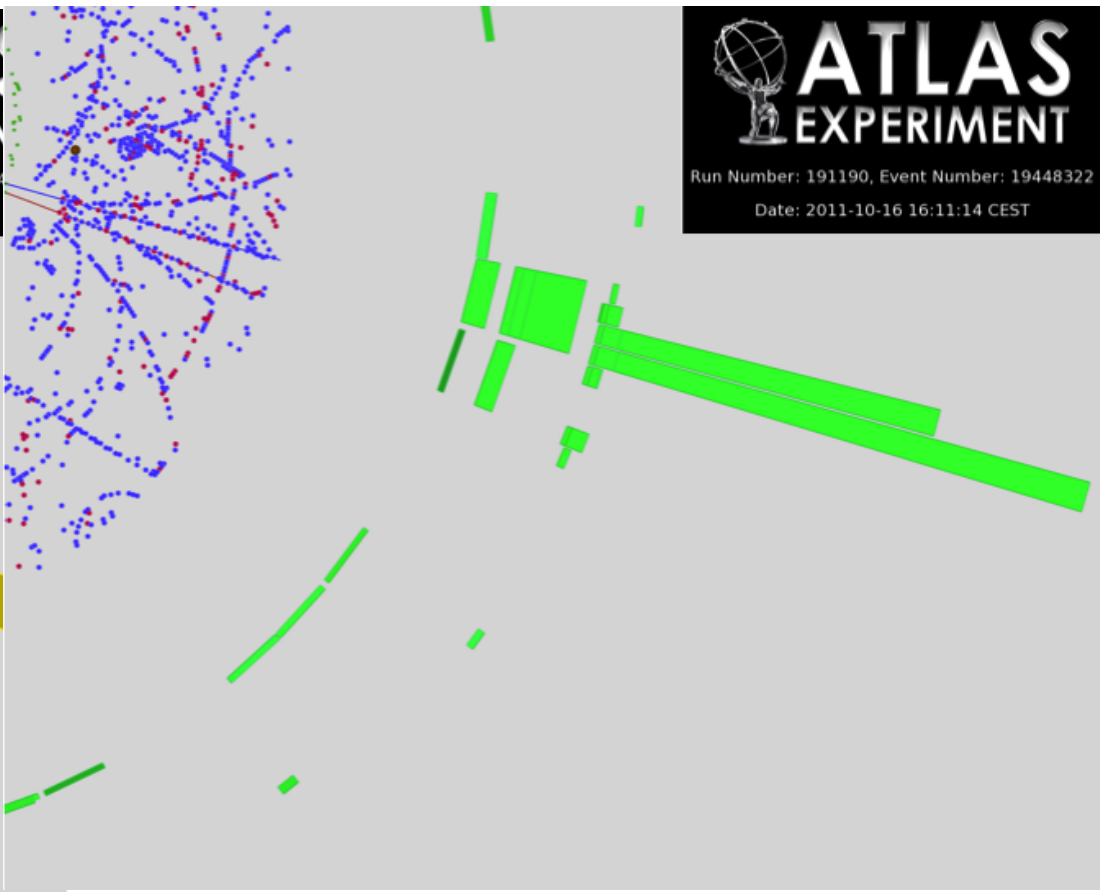
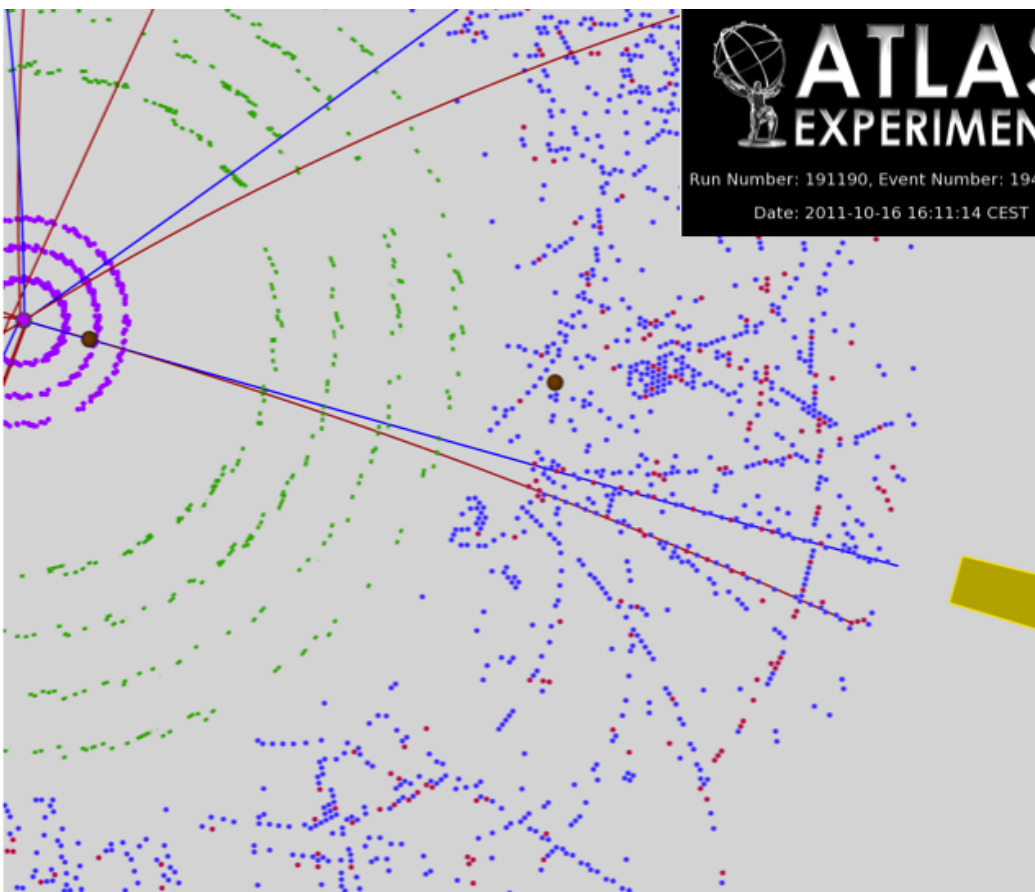
Why do experimentalists like small cell size ?

What is the consequence of small cell size ?

CMS Inner Barrel

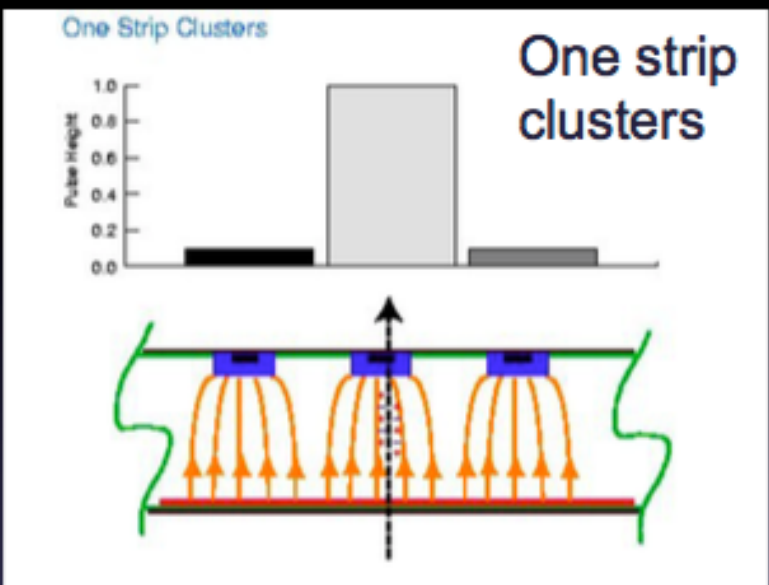


PHOTON CONVERSION

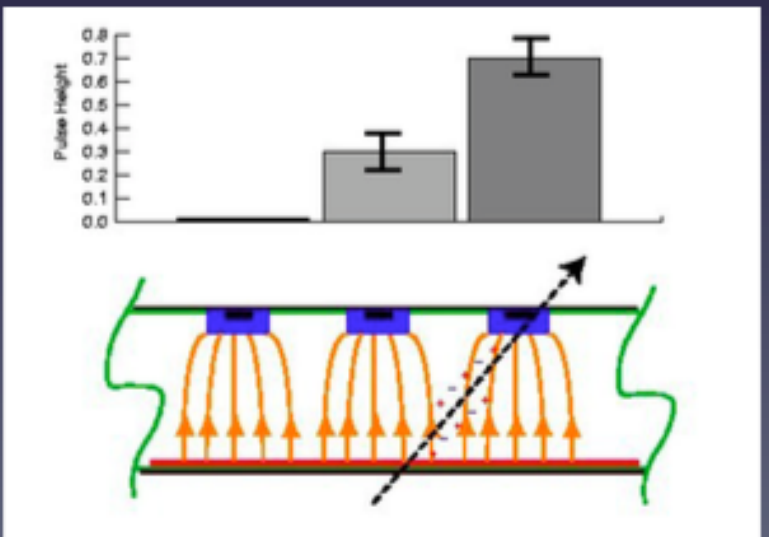
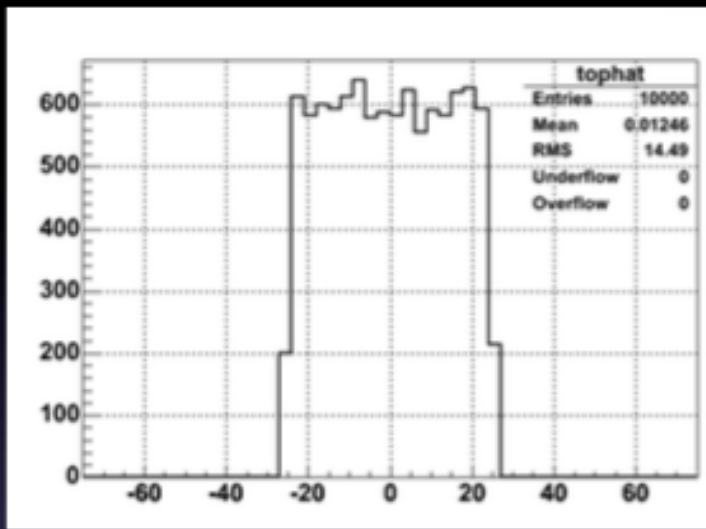


CHARGE SHARING

- Resolution is the spread of the reconstructed position minus the true position

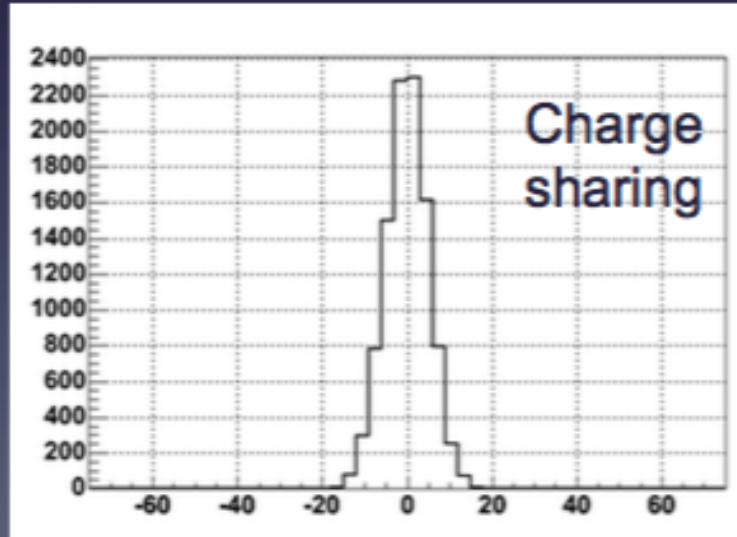


$$\sigma = \frac{pitch}{\sqrt{12}}$$



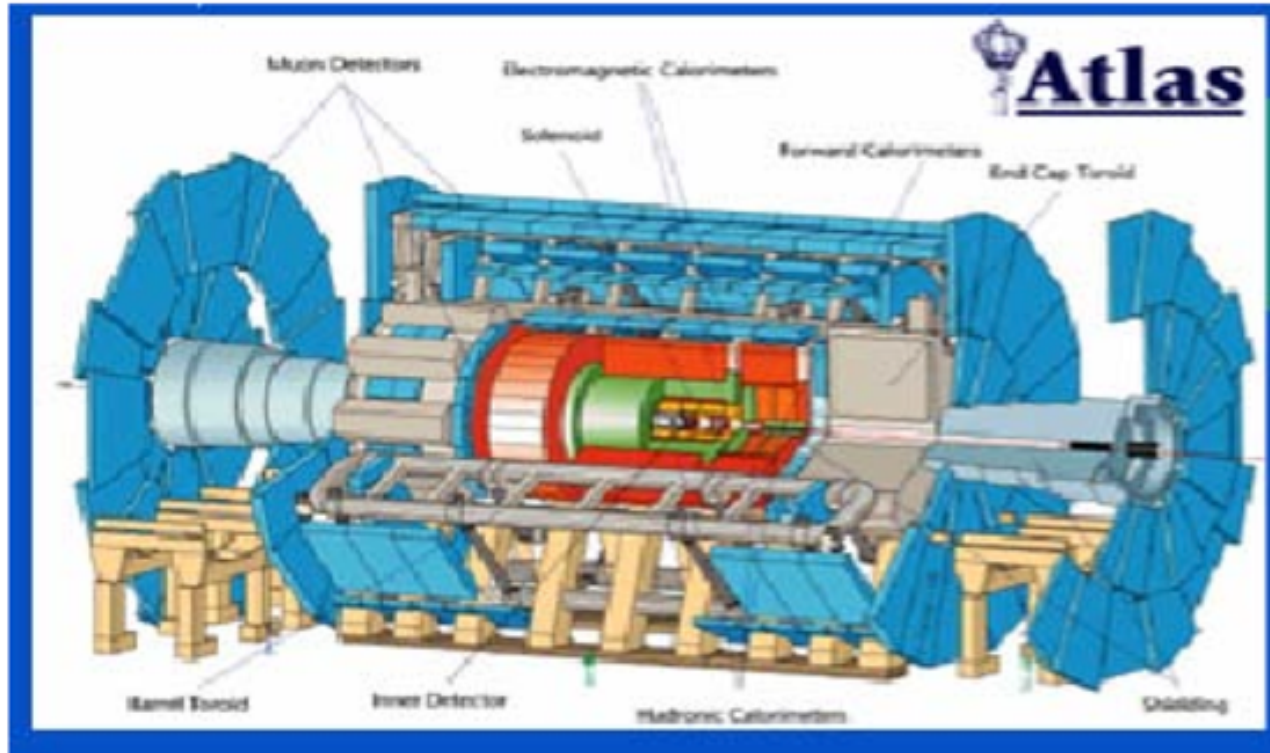
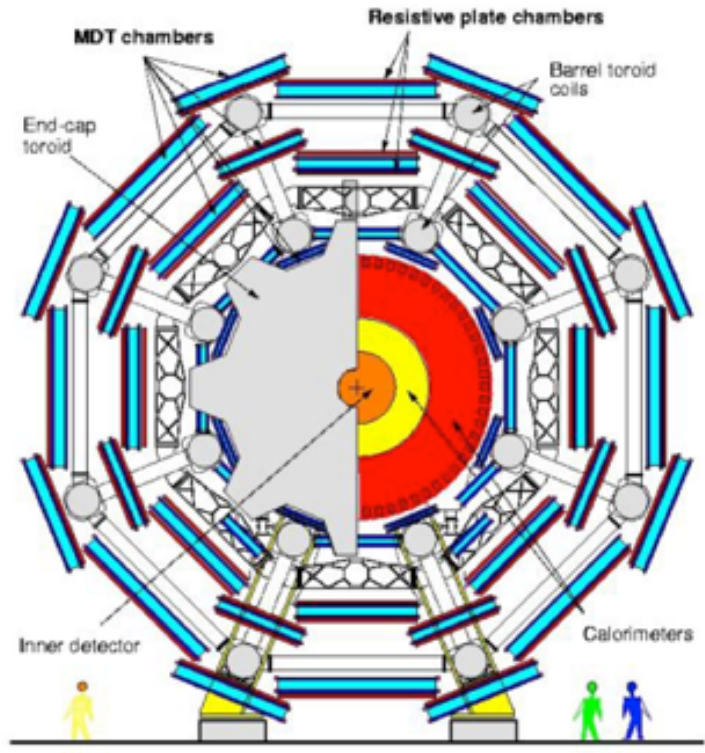
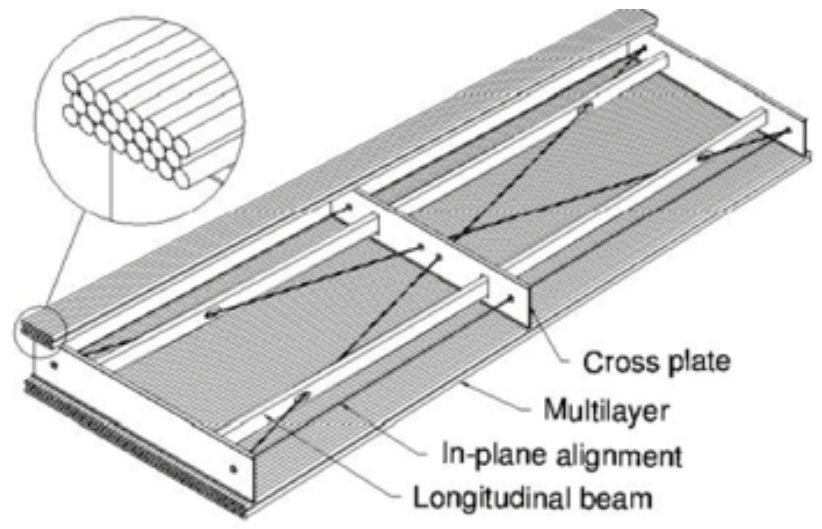
$$\sigma \approx \frac{pitch}{1.5 \cdot \sqrt{12}}$$

$$\eta = \frac{PH_R}{PH_L + PH_R}$$



ATLAS MUON SYSTEM

- Atlas Muon Spectrometer, 44m long, from $r=5$ to $11m$.
- 1200 Chambers
- 6 layers of 3cm tubes per chamber.
- Length of the chambers 1-6m !
- Position resolution: $80\mu m$ /tube, $<50\mu m$ /chamber (3 bar)
- Maximum drift time $\approx 700ns$
- Gas Ar/CO₂ 93/7



MOMENTUM RESOLUTION

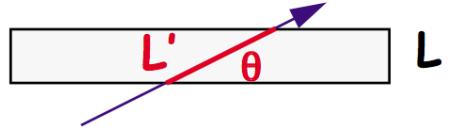
The contribution to the momentum error from MS is given by

$$\left. \frac{\sigma(p_T)}{p_T} \right|_{MS} = \frac{\sigma^{MS}(s)}{s} = \frac{\frac{L' 13.6 \times 10^{-3}}{\sqrt{3}} \frac{z}{p\beta} \sqrt{\frac{L'}{X_0}}}{0.3BL^2z/(8p_T)} = \frac{0.2}{\beta B \sqrt{LX_0} \sin \theta}$$

with

$$L' = L / \sin \theta$$

$$p_T = p \sin \theta$$

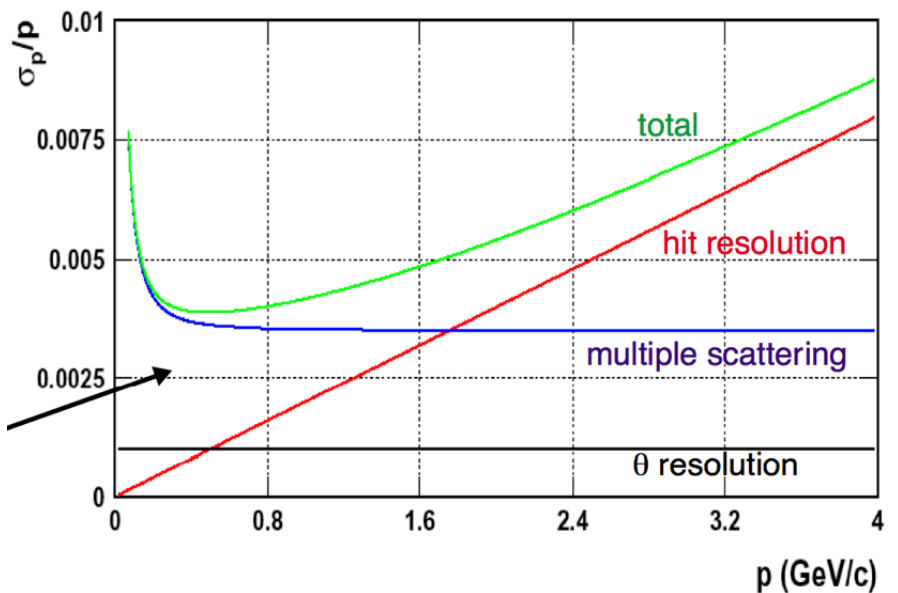


For $\beta \rightarrow 1$ this part is momentum independent.

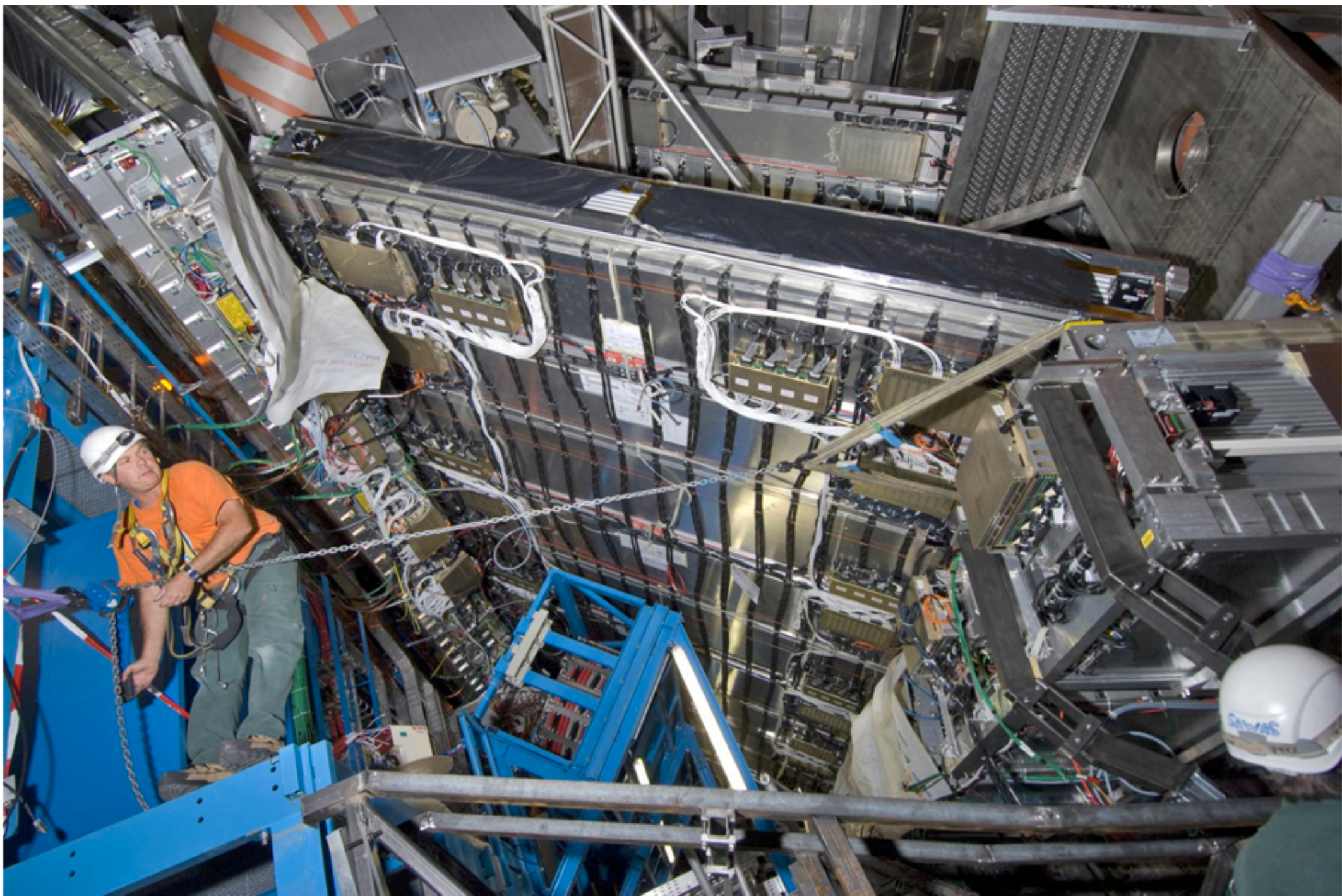
The combined total momentum error is:

$$\left(\frac{\sigma_p}{p} \right)^2 = \left(\sqrt{\frac{720}{N+4}} \frac{\sigma_x p \sin \theta}{0.3BL^2} \right)^2 + \left(\frac{0.2}{\beta B \sqrt{LX_0} \sin \theta} \right)^2$$

Example for momentum dependence of individual contributions

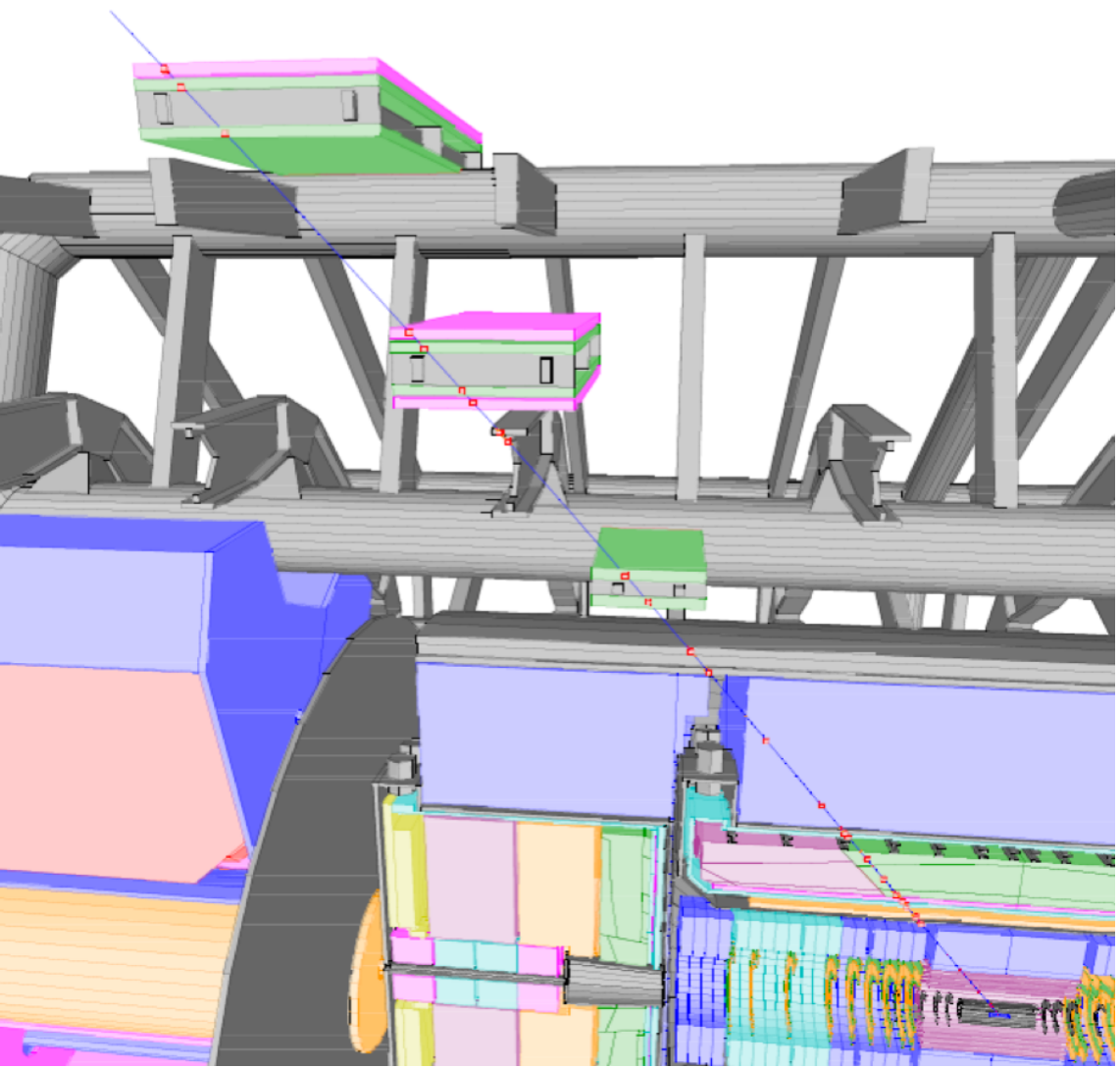


ATLAS RPC

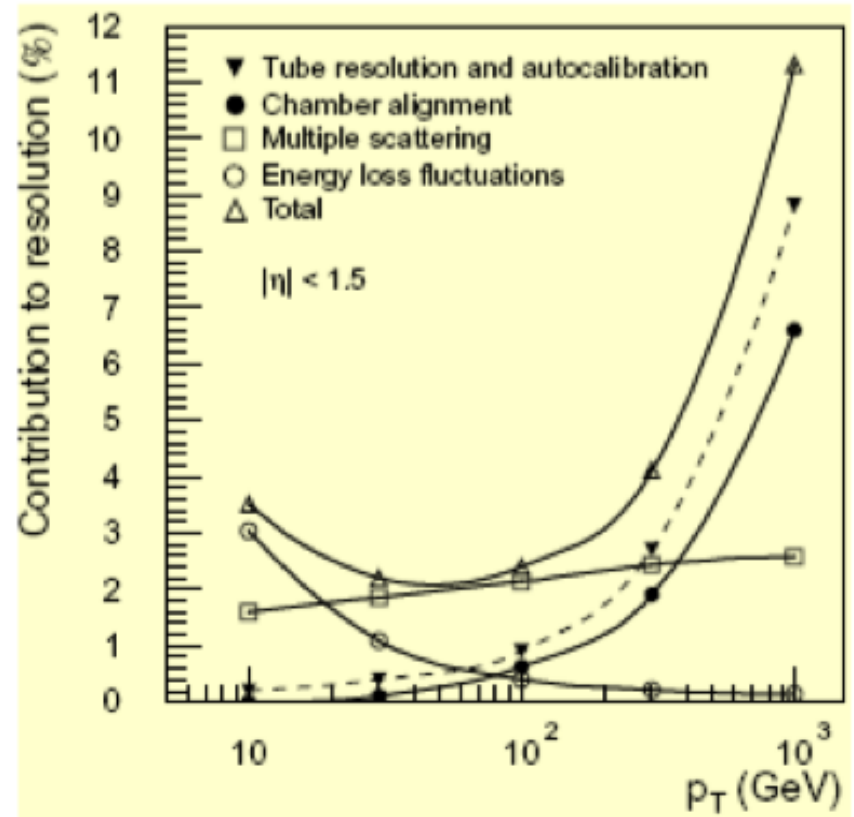


MUON MOMENTUM RESOLUTION

COMBINE Measurement from the tracker and the muon chambers



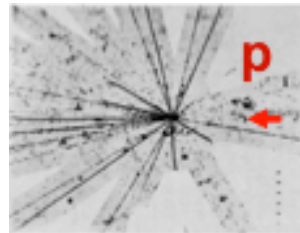
• $\delta p_T/p_T$ vs p_T



Contributions: $\text{measure} \propto p$
 $\text{diffusion} \sim \text{cte}$
 $\delta E/\text{loss} \propto 1/p$

FROM INTERACTIONS to DETECTOR

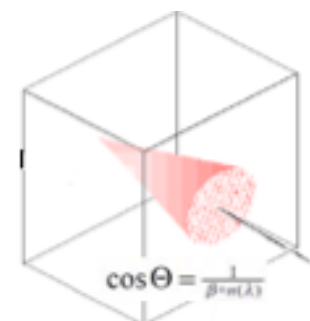
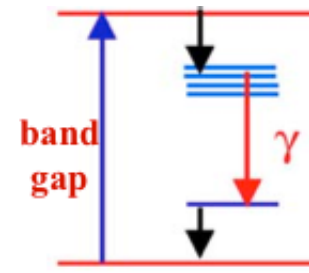
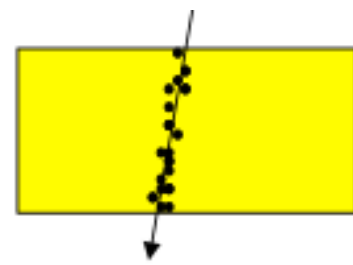
1. Particles interact with matter
depends on particle and material



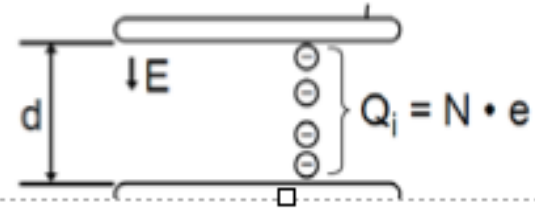
2. Energy loss transfer to detectable signal
depends on the material

Detecting emitted light

Detecting ionisation current

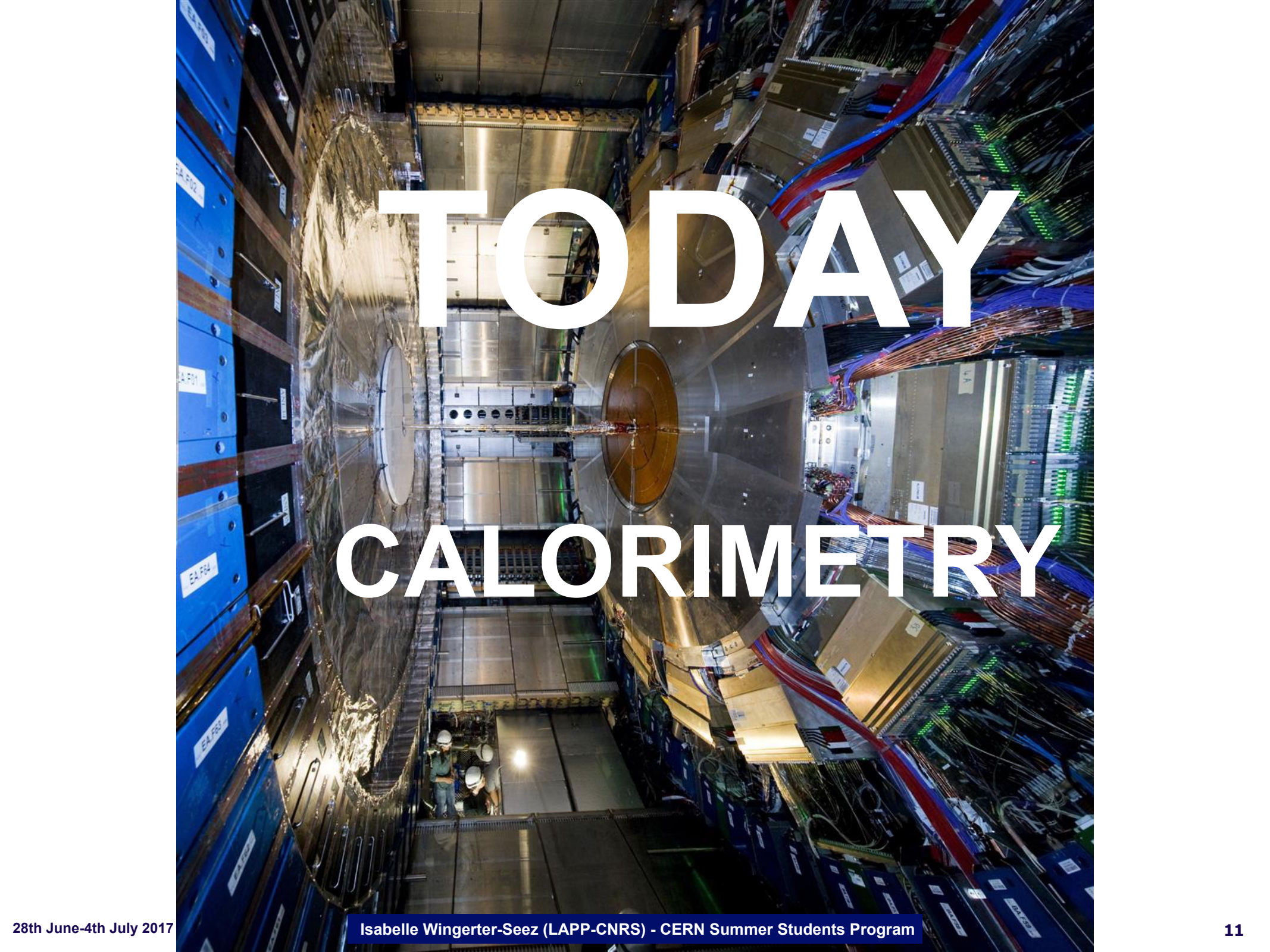


3. Signal collection
depends on signal and type of detection



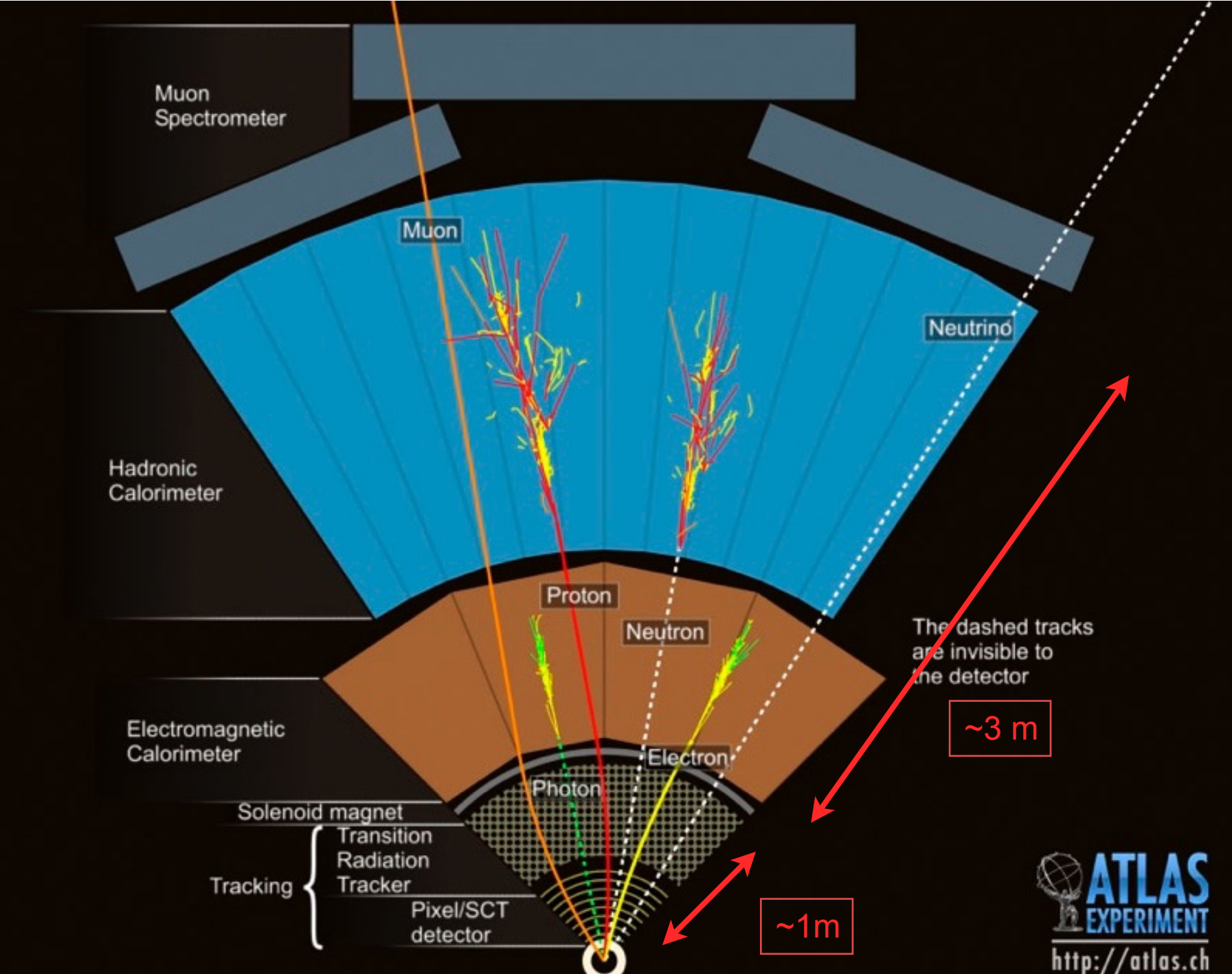
4. BUILD a SYSTEM
depends on physics, experimental conditions,....



A photograph of a large particle detector, likely the ATLAS calorimeter, showing a complex structure of metal and electronics. The text "TODAY CALORIMETRY" is overlaid in large white letters. The image shows a long, narrow tunnel-like structure with various components, including a large circular detector element in the center. The walls are lined with blue panels, and there are many cables and wires visible. The lighting is dim, with some green and red lights from the equipment. The overall scene is a technical and industrial environment.

TODAY CALORIMETRY

CALORIMETERS



CALORIMETER

Concept comes from thermo-dynamics:

A leak-proof closed box containing a substance which temperature is to be measured.

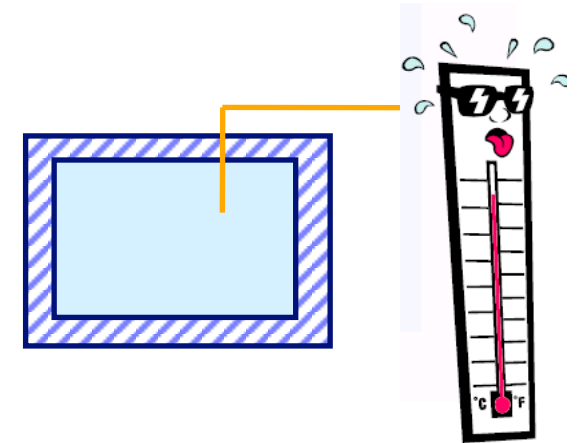
Temperature scale:

1 calorie (4.185J) is the necessary energy to increase the temperature of 1 g of water at 15°C by one degree

At hadron colliders we measure GeV (0.1 - 1000)

1 GeV = 10^9 eV $\approx 10^9 * 10^{-19}$ J = 10^{-10} J = $2.4 * 10^{-9}$ cal

1 TeV = 1000 GeV : kinetic energy of a flying mosquito



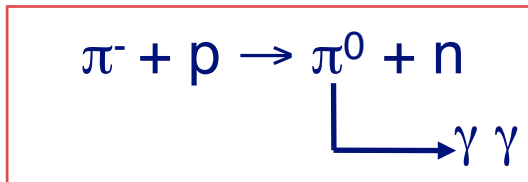
Required sensitivity for our calorimeters is
~ a thousand million times larger than
to measure the increase of temperature by 1°C of 1 g of water

WHY CALORIMETERS ?

First calorimeters appeared in the 70's:
need to measure the energy of all particles, charged and **neutral**.

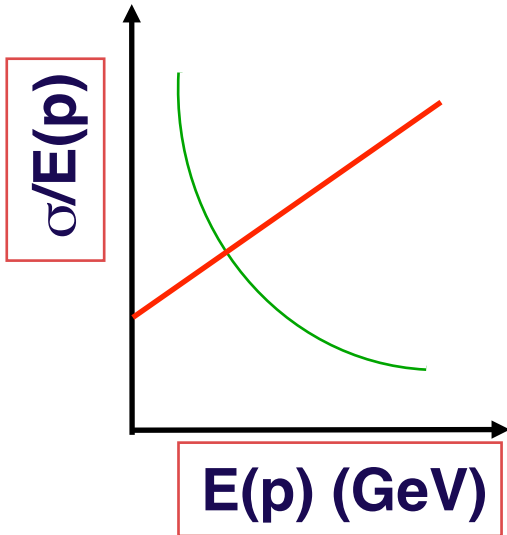
Until then, only the momentum of **charged particles** was measured using **magnetic analysis**.

The measurement with a calorimeter is destructive e.g.



Magnetic analysis

$$\frac{\sigma(p)}{p} = ap \oplus b$$



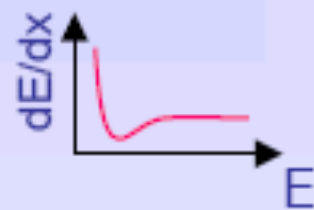
$$\frac{\sigma(E)}{E} \approx \frac{a}{\sqrt{E}}$$

Calorimetry

Particles (but μ and ν) do not come out alive of a calorimeter

e^+ / e^-

■ Ionisation



■ Bremsstrahlung

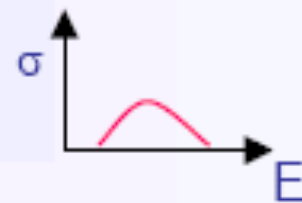


γ

■ Photoelectric effect



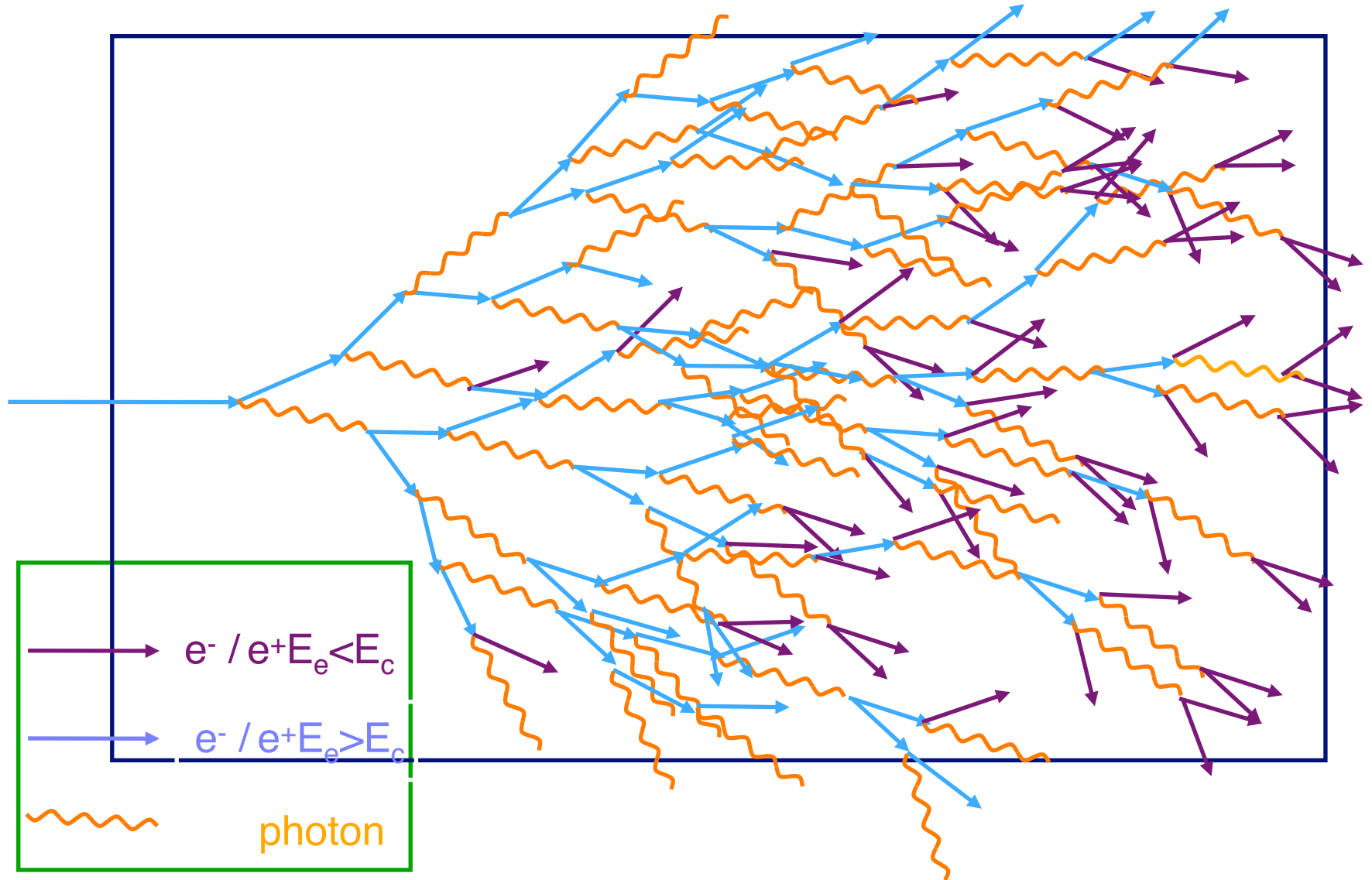
■ Compton effect



■ Pair production



ELECTROMAGNETIC SHOWER



ELECTROMAGNETIC SHOWER DEVELOPMENT

The shower develops as a **cascade** by **energy transfer** from the incident particle to a **multitude of particles** (e^\pm and γ).

The **number of cascade particles** is **proportional** to the **energy deposited** by the incident particle

The role of the calorimeter is to **count** these cascade particles

The relative occurrence of the various processes briefly described is a function of the material (Z)

The radiation length (X_0) allows to universally describe the shower development

CRITICAL ENERGY

Critical energy:

$$\left(\frac{dE}{dx}\right)_{\text{Tot}} = \left(\frac{dE}{dx}\right)_{\text{Ion}} + \left(\frac{dE}{dx}\right)_{\text{Brems}}$$

$$\left.\frac{dE}{dx}(E_c)\right|_{\text{Brems}} = \left.\frac{dE}{dx}(E_c)\right|_{\text{Ion}}$$

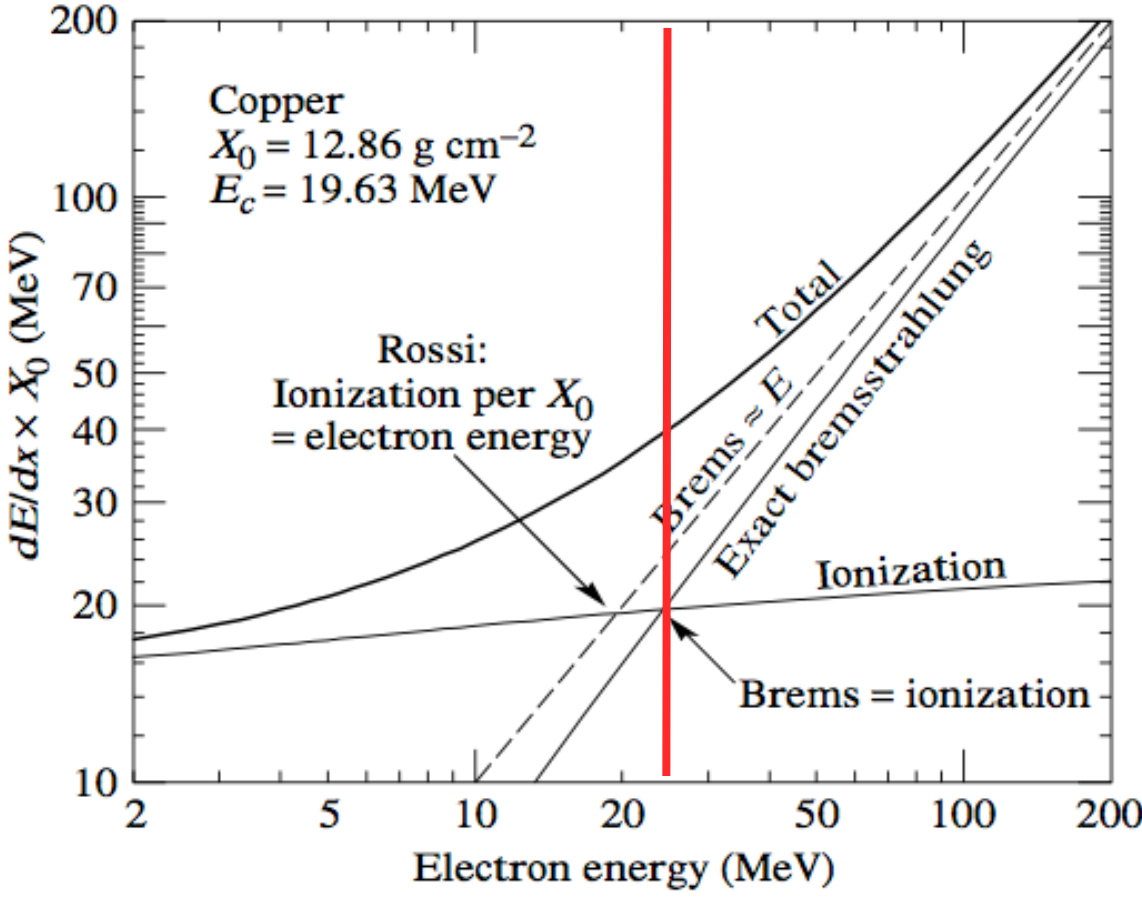
Approximation:

$$E_c^{\text{Gas}} = \frac{710 \text{ MeV}}{Z + 0.92}$$

$$E_c^{\text{Sol/Liq}} = \frac{610 \text{ MeV}}{Z + 1.24}$$

Example Copper:

$$E_c \approx 610/30 \text{ MeV} \approx 20 \text{ MeV}$$



EM SHOWER DEVELOPMENT: SIMPLE MODEL

The multiplication of the shower continues until the energies fall below the critical energy, E_c

A simple model of the shower uses variables scaled to X_0 and E_c

$$t = \frac{x}{X_0}, y = \frac{E}{E_c}$$

Electrons lose about 2/3 of their energy in $1X_0$, and the photons have a probability of 7/9 for conversion: $X_0 \sim$ generation length

After distance t :

$$\begin{aligned} \text{number of particles, } & n(t) = 2^t \\ \text{energy of particles, } & E(t) \approx \frac{E}{2^t} \end{aligned}$$

When $E \sim E_c$ shower maximum:

$$\begin{aligned} n(t_{\max}) &\approx \frac{E}{E_c} = y \\ t_{\max} &\approx \ln \left(\frac{E}{E_c} \right) \div \ln 2 = \ln y \end{aligned}$$

EM LONGITUDINAL DEVELOPMENT

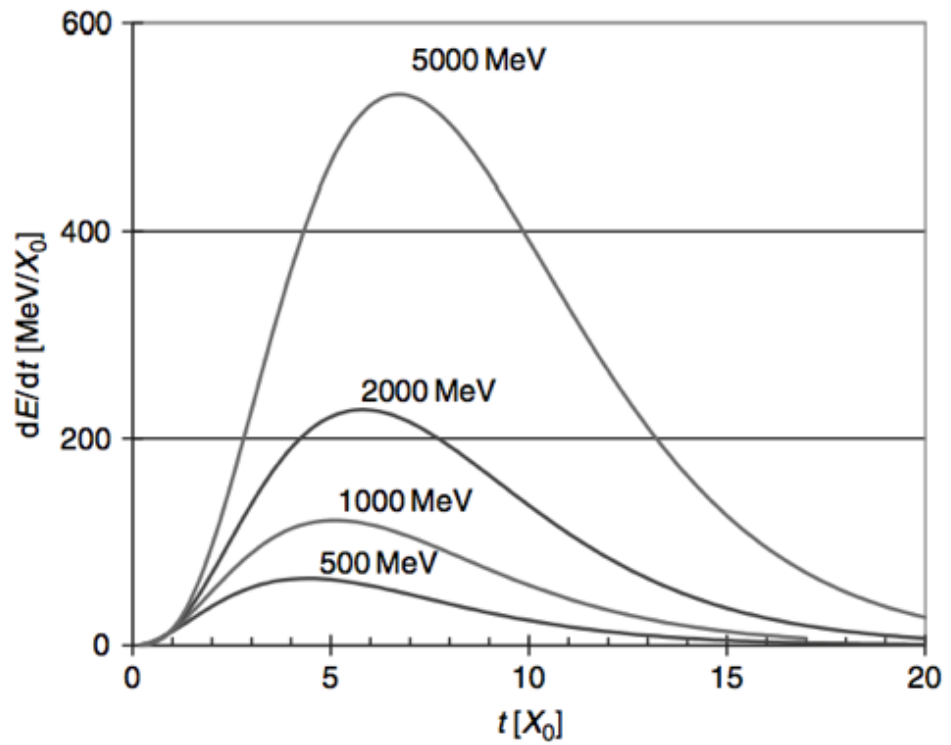
Longitudinal profile

Parametrization:
[Longo 1975]

$$\frac{dE}{dt} = E_0 t^\alpha e^{-\beta t}$$

- α, β : free parameters
- t^α : at small depth number of secondaries increases ...
- $e^{-\beta t}$: at larger depth absorption dominates ...

Numbers for $E = 2$ GeV (approximate):
 $\alpha = 2, \beta = 0.5, t_{\max} = \alpha/\beta$



More exact
[Longo 1985]

$$\frac{dE}{dt} = E_0 \cdot \beta \cdot \frac{(\beta t)^{\alpha-1} e^{-\beta t}}{\Gamma(\alpha)}$$

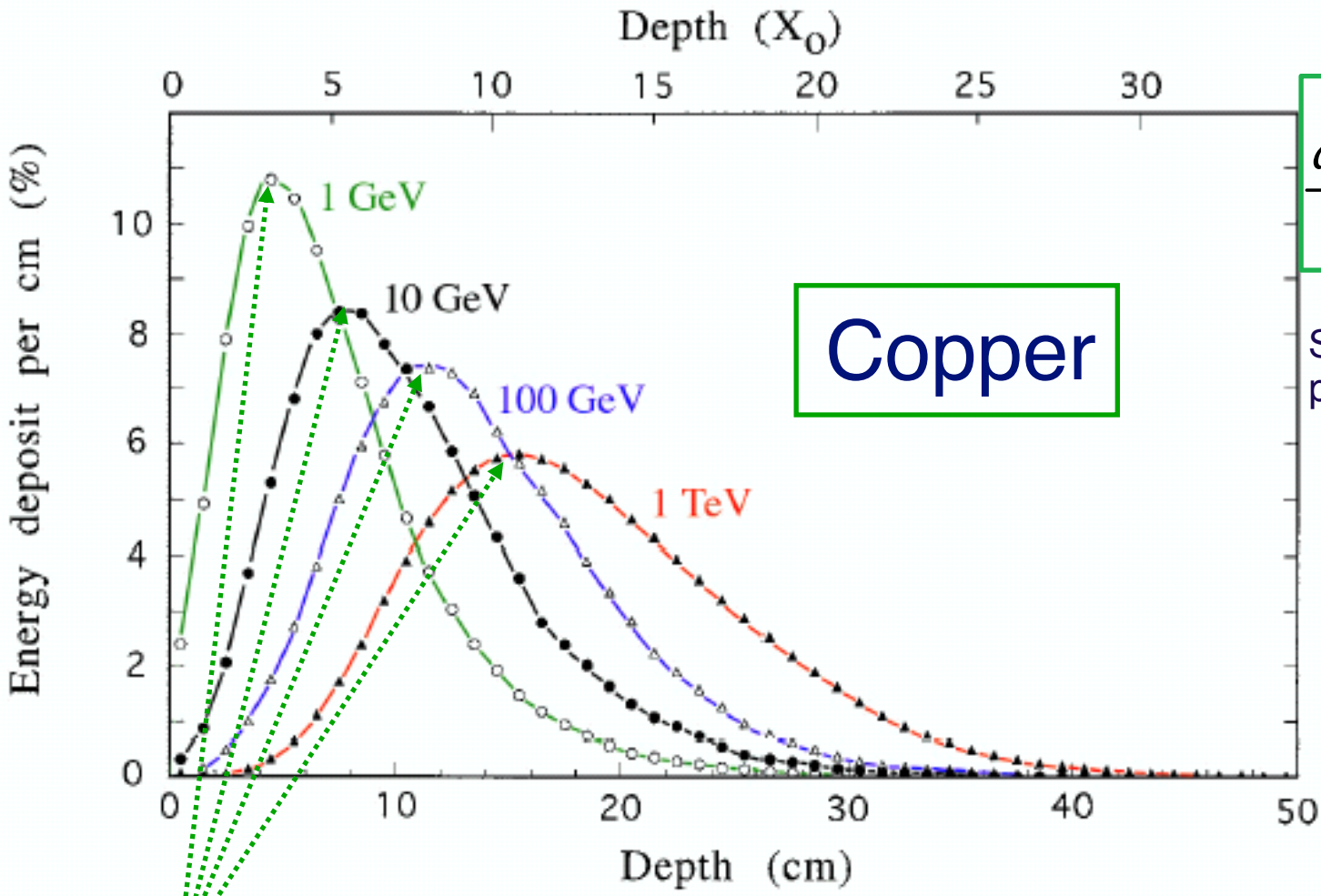
[Γ : Gamma function]

$$\rightarrow t_{\max} = \frac{\alpha - 1}{\beta} = \ln \left(\frac{E_0}{E_c} \right) + C_{e\gamma}$$

with:

- $C_{e\gamma} = -0.5$ [γ -induced]
- $C_{e\gamma} = -1.0$ [e-induced]

EM SHOWERS LONGITUDINAL DEVELOPMENT



$$\frac{dE}{dt} \propto E_0 b \frac{(bt)^{a-1} e^{-bt}}{\Gamma(a)}$$

Shower energy development parametrization

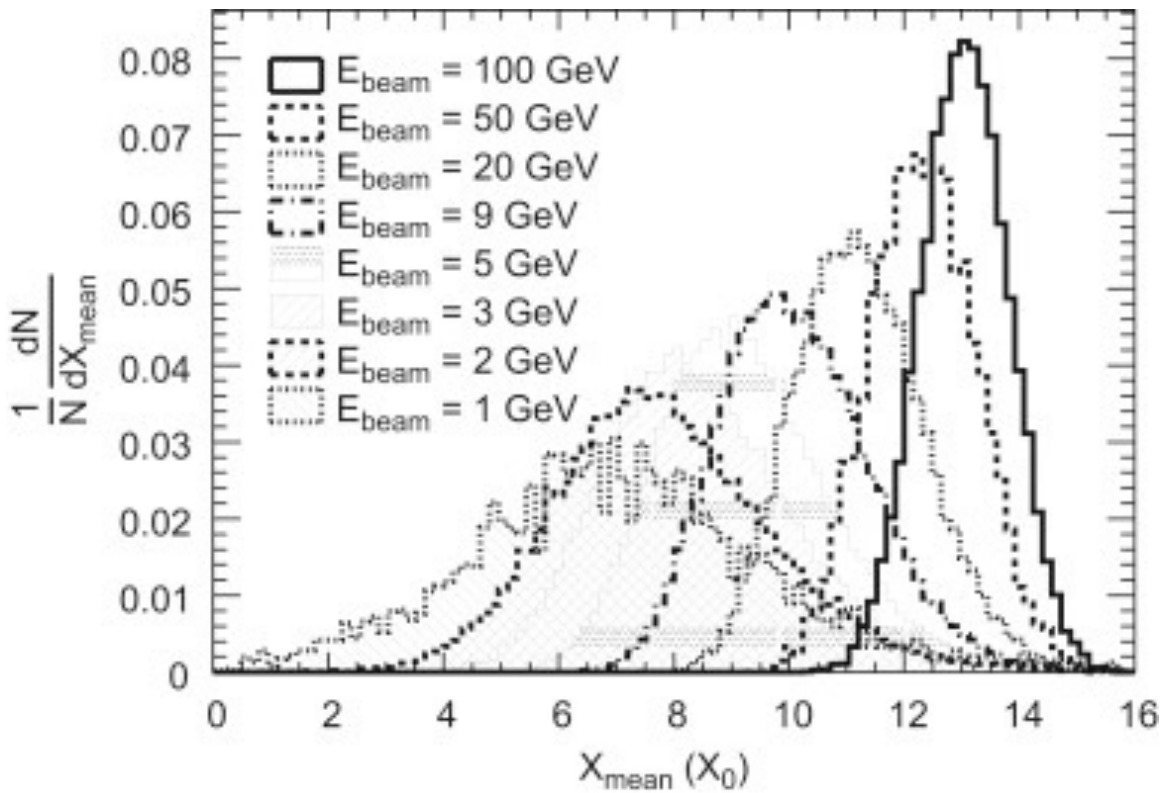
b: material

E.Longo & I.Sestili
(NIM128-1975)

$$X_{\max} = X_0 \ln\left(\frac{E}{E_c} + t_0\right)$$

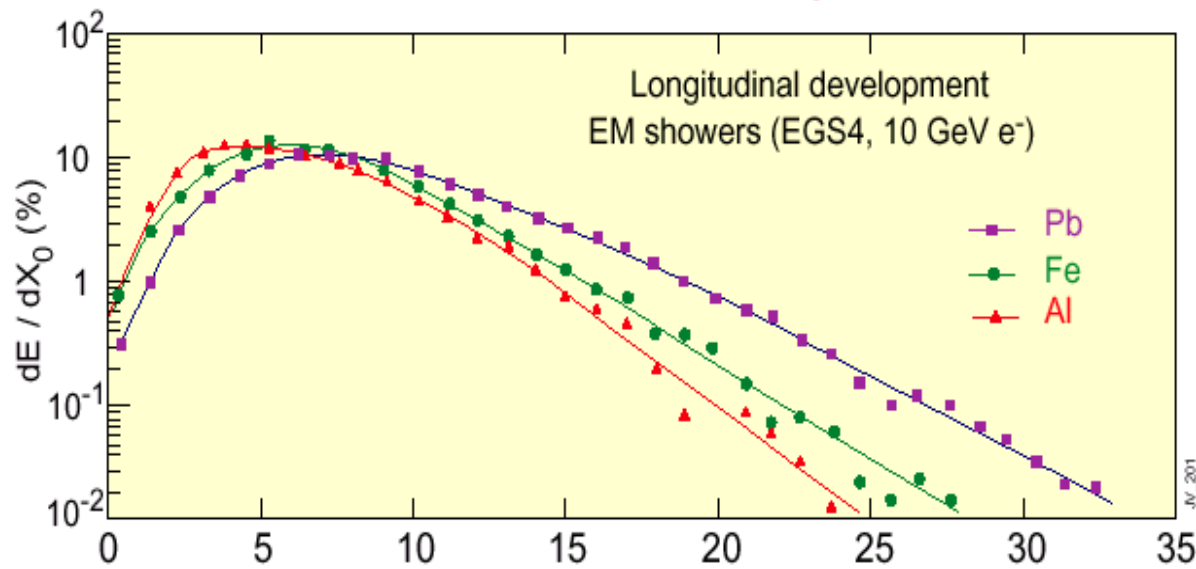
$$t_0 = \begin{matrix} -0.5 \text{ electrons} \\ +0.5 \text{ photons} \end{matrix}$$

EM SHOWERS LONGITUDINAL DEVELOPMENT



ATLAS combined testbeam
2004 setup

Electrons shower mean
depth in X_0 (MC)
1,2,3,5,9,20,50, 100 GeV



$E_c \propto 1/Z$

- Shower maximum
- Shower tails

$t_{95\%} = t_{\text{max}} + 0.08Z + 9.6$

SEARCH FOR DECAYS OF THE Z^0 INTO A PHOTON AND A PSEUDOSCALAR MESON

ALEPH Collaboration

D. DECAMP, B. DESCHIZEAUX, C. GOY, J.-P. LEES, M.-N. MINARD

Laboratoire de Physique des Particules (LAPP), IN2P3-CNRS, F-74019 Annecy-le-Vieux Cedex, France

.....
Measurement made by ALEPH

$$e^+e^- \rightarrow e^+e^-$$

$$e^+e^- \rightarrow \gamma\gamma$$

Electron/Photon longitudinal development: different

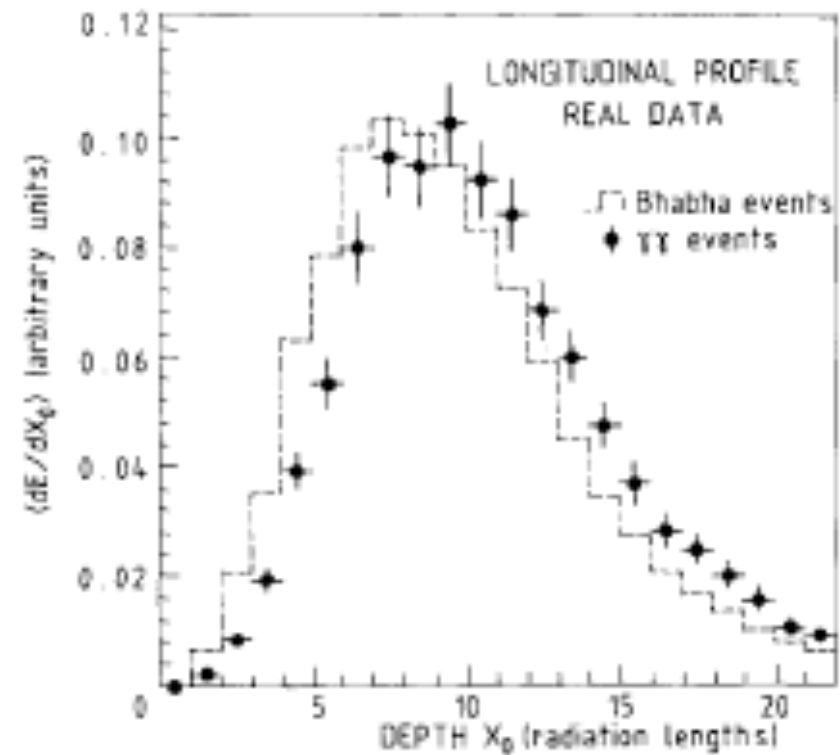


Fig. 1. Longitudinal profile of electromagnetic showers, both for electrons from $e^+e^- \rightarrow e^+e^-$ and for the $\gamma\gamma$ candidates. Both samples are real data. There is a clear shift by about 1 radiation length of the photon showers with respect to electron showers, as expected.

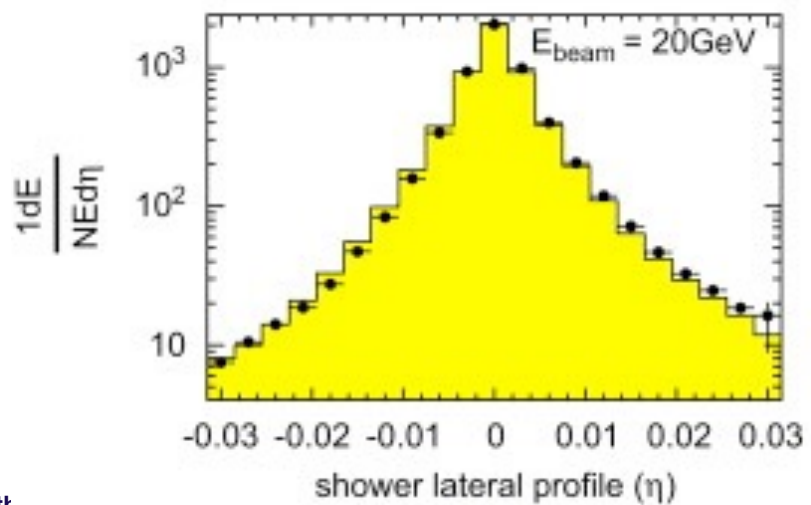
EM shower lateral development

Molière radius, R_m , scaling factor for lateral extent, defined by:

$$R_M = \frac{21 \text{MeV} \times X_0}{E_c} \approx \frac{7A}{Z} g \times \text{cm}^{-2}$$

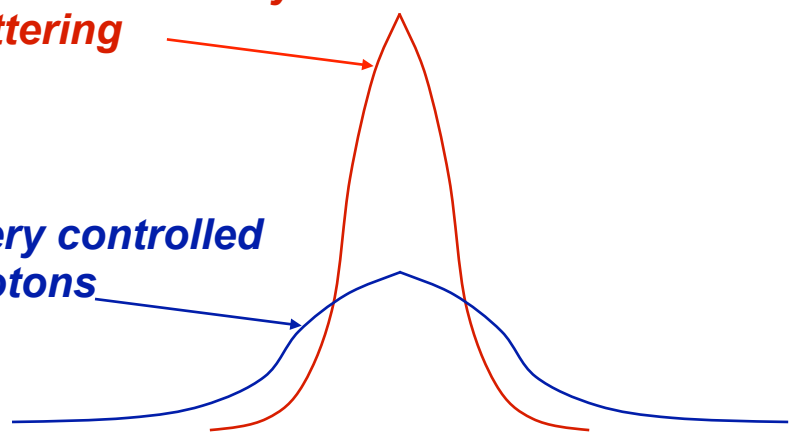
Gives the average lateral deflection of electrons of critical energy after $1X_0$

- 90% of shower energy contained in a cylinder of $1R_m$
- 95% of shower energy contained in a cylinder of $2R_m$
- 99% of shower energy contained in a cylinder of $3.5R_m$



Width of core controlled by multiple scattering of e^\pm

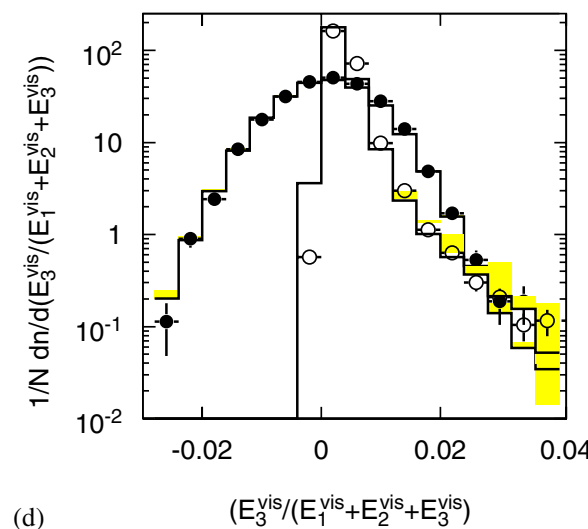
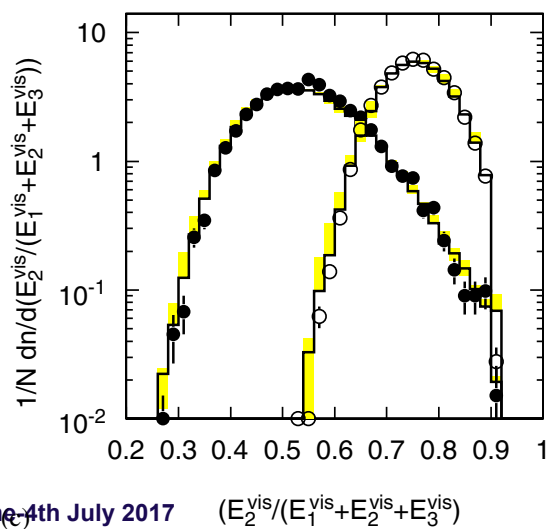
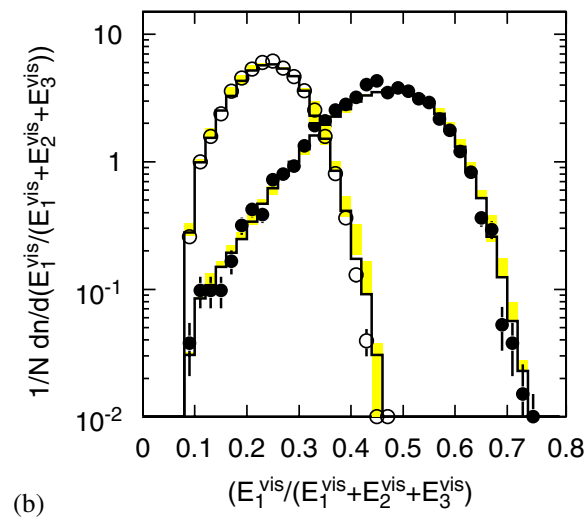
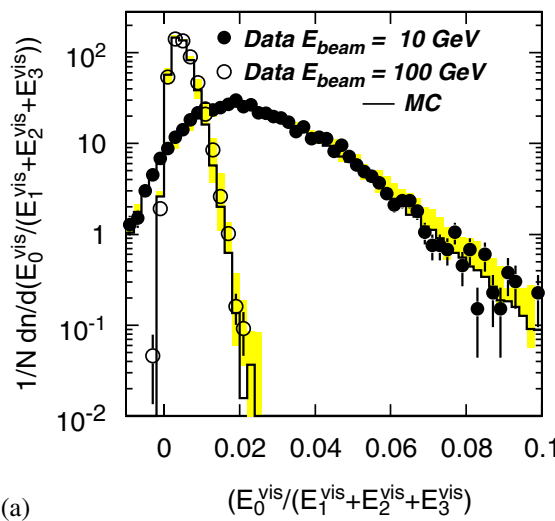
Width of periphery controlled by Compton photons



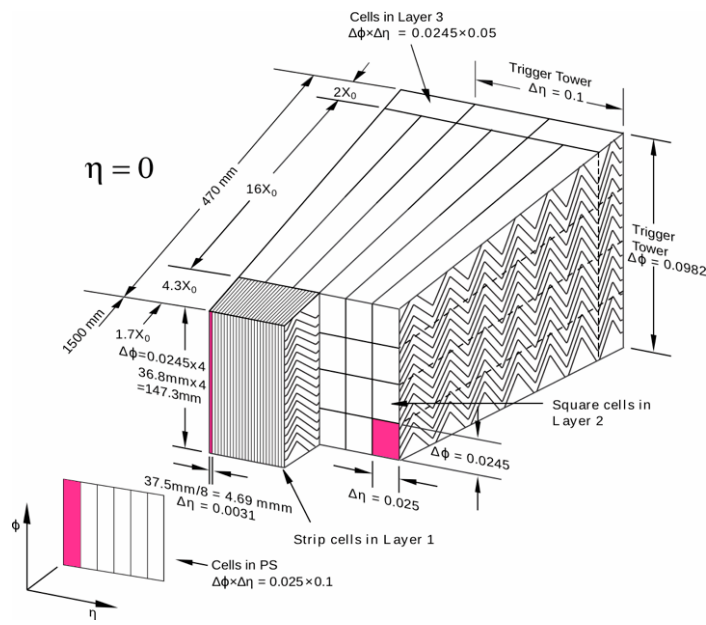
EM shower simulations

Electromagnetic processes are well understood and can be very well reproduced by MC simulation:

A key element in understanding detector performance



ATLAS EM calorimeter testbeam



PROPERTIES of ELECTROMAGNETIC CALORIMETERS

| Material | Z | Density [g cm ⁻³] | E _c [MeV] | X ₀ [mm] | ρ _M [mm] | λ _{int} [mm] | (dE/dx) _{mip} [MeV cm ⁻¹] |
|------------------|----|----------------------------------|-------------------------|------------------------|------------------------|--------------------------|---|
| C | 6 | 2.27 | 83 | 188 | 48 | 381 | 3.95 |
| Al | 13 | 2.70 | 43 | 89 | 44 | 390 | 4.36 |
| Fe | 26 | 7.87 | 22 | 17.6 | 16.9 | 168 | 11.4 |
| Cu | 29 | 8.96 | 20 | 14.3 | 15.2 | 151 | 12.6 |
| Sn | 50 | 7.31 | 12 | 12.1 | 21.6 | 223 | 9.24 |
| W | 74 | 19.3 | 8.0 | 3.5 | 9.3 | 96 | 22.1 |
| Pb | 82 | 11.3 | 7.4 | 5.6 | 16.0 | 170 | 12.7 |
| ²³⁸ U | 92 | 18.95 | 6.8 | 3.2 | 10.0 | 105 | 20.5 |
| Concrete | - | 2.5 | 55 | 107 | 41 | 400 | 4.28 |
| Glass | - | 2.23 | 51 | 127 | 53 | 438 | 3.78 |
| Marble | - | 2.93 | 56 | 96 | 36 | 362 | 4.77 |
| Si | 14 | 2.33 | 41 | 93.6 | 48 | 455 | 3.88 |
| Ge | 32 | 5.32 | 17 | 23 | 29 | 264 | 7.29 |
| Ar (liquid) | 18 | 1.40 | 37 | 140 | 80 | 837 | 2.13 |
| Kr (liquid) | 36 | 2.41 | 18 | 47 | 55 | 607 | 3.23 |
| Polystyrene | - | 1.032 | 94 | 424 | 96 | 795 | 2.00 |
| Plexiglas | - | 1.18 | 86 | 344 | 85 | 708 | 2.28 |
| Quartz | - | 2.32 | 51 | 117 | 49 | 428 | 3.94 |
| Lead-glass | - | 4.06 | 15 | 25.1 | 35 | 330 | 5.45 |
| Air 20°, 1 atm | - | 0.0012 | 87 | 304 m | 74 m | 747 m | 0.0022 |
| Water | - | 1.00 | 83 | 361 | 92 | 849 | 1.99 |

TOWARDS ELECTROMAGNETIC CALORIMETERS

Detectable signal is proportional to the number of potentially detectable particles in the shower $N_{\text{tot}} \propto E_0/E_c$

Total track length $T_0 = N_{\text{tot}} \cdot X_0 \sim E_0/E_c \cdot X_0$

$$\frac{\sigma(E)}{E} \propto \frac{1}{\sqrt{T_0}} \propto \frac{1}{\sqrt{E}}$$

Detectable track length $T_r = f_s \cdot T_0$ where f_s is the fraction of N_{tot} which can be detected by the involved detection process (Cerenkov light, scintillation light, ionization) $E_{\text{kin}} > E_{\text{th}}$

$$\frac{\sigma(E)}{E} \propto \frac{1}{\sqrt{E}} \frac{1}{\sqrt{f_s}}$$

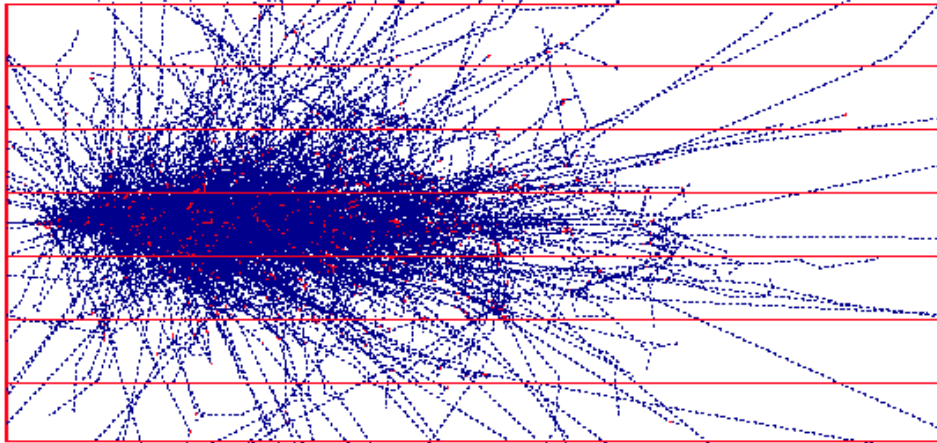
Converting back to materials ($X_0 \propto A/Z^2$, $E_c \propto 1/Z$) and fixing E

Maximize detection f_s

Minimize Z/A

$$\frac{\sigma(E)}{E} \propto \frac{1}{\sqrt{f_s}} \sqrt{\frac{E_c}{X_0}} \propto \frac{1}{\sqrt{f_s}} \sqrt{\frac{Z}{A}}$$

HOMOGENOUS CALORIMETERS



All the energy is deposited in the active medium

Excellent energy resolution

No longitudinal segmentation

All e^\pm with $E_{\text{kin}} > E_{\text{th}}$ produce a signal

Scintillating crystals

$$E_{\text{th}} \approx \beta \cdot E_{\text{gap}} \sim \text{eV}$$

$$\rightarrow 10^2 \div 10^4 \text{ } \gamma/\text{MeV}$$

$$\sigma/E \sim (1 \div 3)\% / \sqrt{E} \text{ (GeV)}$$

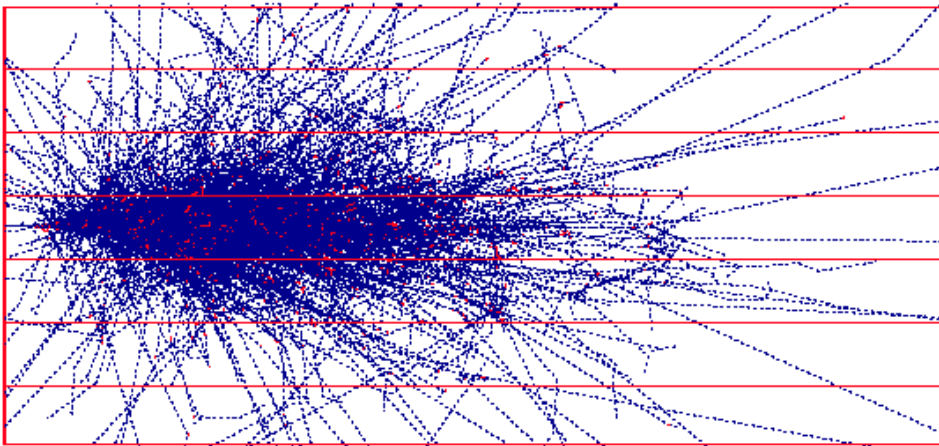
Cerenkov radiators

$$\beta > 1/n \rightarrow E_{\text{th}} \approx 0.7 \text{ MeV}$$

$$\rightarrow 10 \div 30 \text{ } \gamma/\text{MeV}$$

$$\sigma/E \sim (5 \div 10)\% / \sqrt{E} \text{ (GeV)}$$

HOMOGENOUS CALORIMETERS



All the energy is deposited in the active medium

Excellent energy resolution

No longitudinal segmentation

All e^\pm with $E_{kin} > E_{th}$ produce a signal

Scintillating crystals

$E_{th} \approx \beta \cdot E_{gap} \sim eV$

$\rightarrow 10^2 \div 10^4 \gamma/MeV$

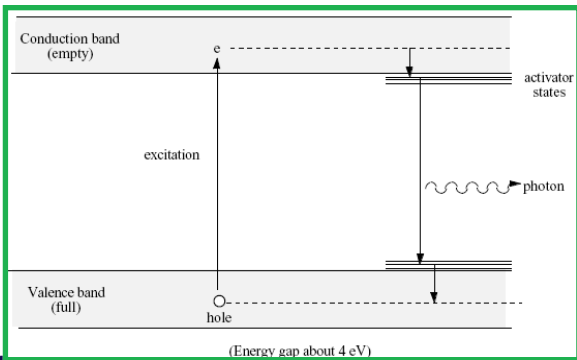
$\sigma/E \sim (1 \div 3)\% / \sqrt{E} (GeV)$

Cerenkov radiators

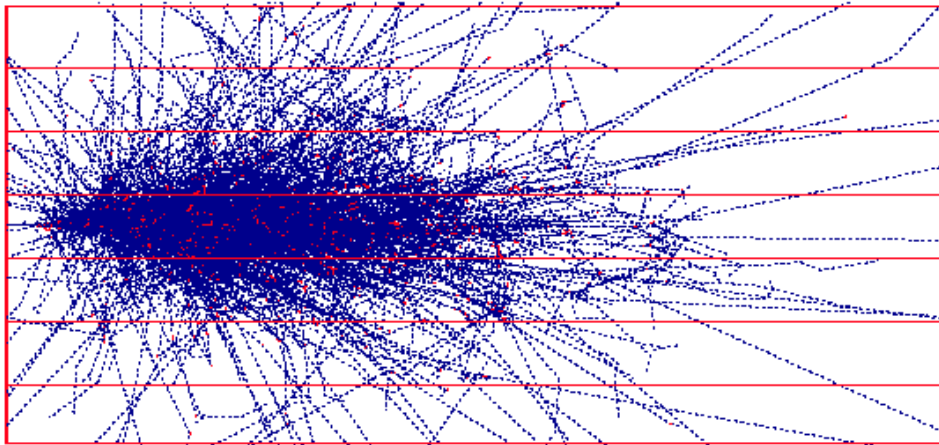
$\beta > 1/n \rightarrow E_{th} \approx 0.7 MeV$

$\rightarrow 10 \div 30 \gamma/MeV$

$\sigma/E \sim (5 \div 10)\% / \sqrt{E} (GeV)$



HOMOGENOUS CALORIMETERS



All the energy is deposited in the active medium

Excellent energy resolution

No longitudinal segmentation

All e^\pm with $E_{\text{kin}} > E_{\text{th}}$ produce a signal

Scintillating crystals

$$E_{\text{th}} \approx \beta \cdot E_{\text{gap}} \sim \text{eV}$$

$$\rightarrow 10^2 \div 10^4 \text{ } \gamma/\text{MeV}$$

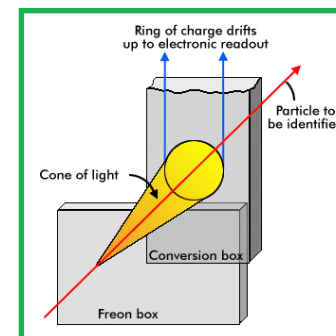
$$\sigma/E \sim (1 \div 3)\% / \sqrt{E} \text{ (GeV)}$$

Cerenkov radiators

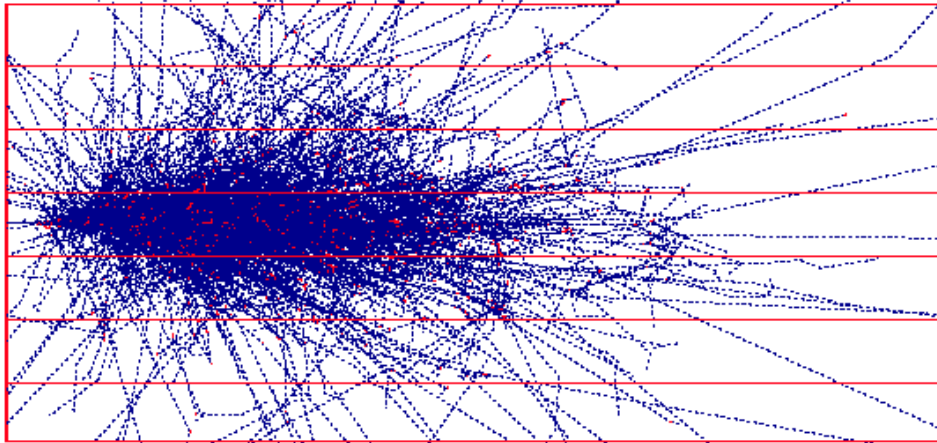
$$\beta > 1/n \rightarrow E_{\text{th}} \approx 0.7 \text{ MeV}$$

$$\rightarrow 10 \div 30 \text{ } \gamma/\text{MeV}$$

$$\sigma/E \sim (5 \div 10)\% / \sqrt{E} \text{ (GeV)}$$



HOMOGENOUS CALORIMETERS



All the energy is deposited in the active medium

Excellent energy resolution

No longitudinal segmentation

All e^\pm with $E_{\text{kin}} > E_{\text{th}}$ produce a signal

Scintillating crystals

$$E_{\text{th}} \approx \beta \cdot E_{\text{gap}} \sim \text{eV}$$

$$\rightarrow 10^2 \div 10^4 \gamma/\text{MeV}$$

$$\sigma/E \sim (1 \div 3)\% / \sqrt{E} \text{ (GeV)}$$

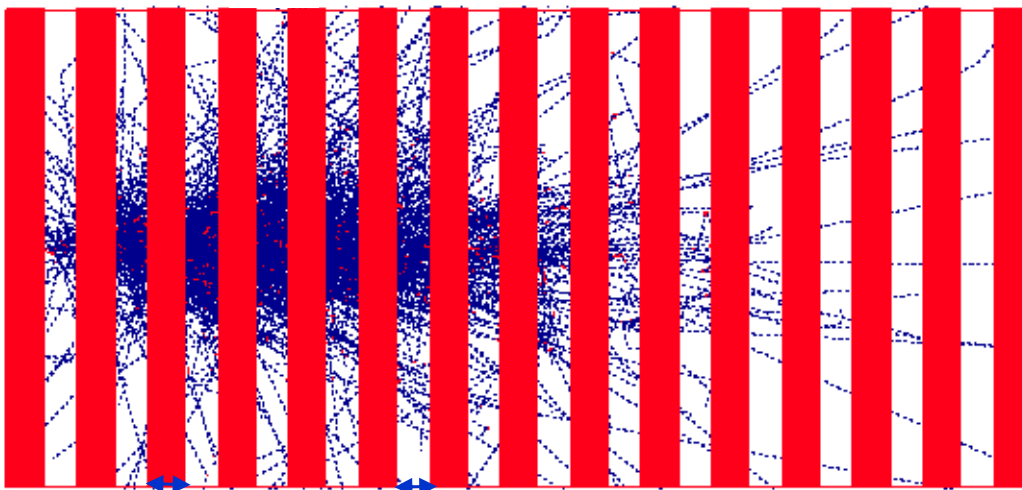
Cerenkov radiators

$$\beta > 1/n \rightarrow E_{\text{th}} \approx 0.7 \text{ MeV}$$

$$\rightarrow 10 \div 30 \gamma/\text{MeV}$$

$$\sigma/E \sim (5 \div 10)\% / \sqrt{E} \text{ (GeV)}$$

SAMPLING CALORIMETERS



Shower is sampled by layers of an active medium and dense radiator

Limited energy resolution

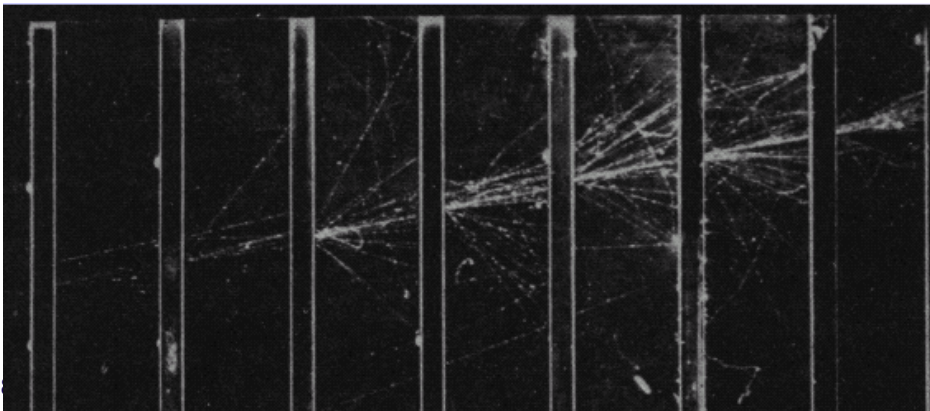
Longitudinal segmentation

Only e^\pm with $E_{\text{kin}} > E_{\text{th}}$ of the active layer produce a signal

Absorber (high Z): typically Lead, Uranium

Active medium (low Z): typically Scintillators, Liquid Argon, Wire chamber

Energy resolution of sampling calorimeter dominated by fluctuations in energy deposited in the active layers



$$\sigma(E)/E \sim (10 \div 20)\% / \sqrt{E \text{ (GeV)}}$$

SAMPLING FLUCTUATIONS



Most of detectable particles are produced in the absorber layers

Need to enter the active material to be counted/measured

Using the model of the track length

$$T_r = f_s T_0 \sim f_s \cdot E/E_c^{\text{abs}} \cdot X_0^{\text{abs}}$$

f_s : sampling fraction

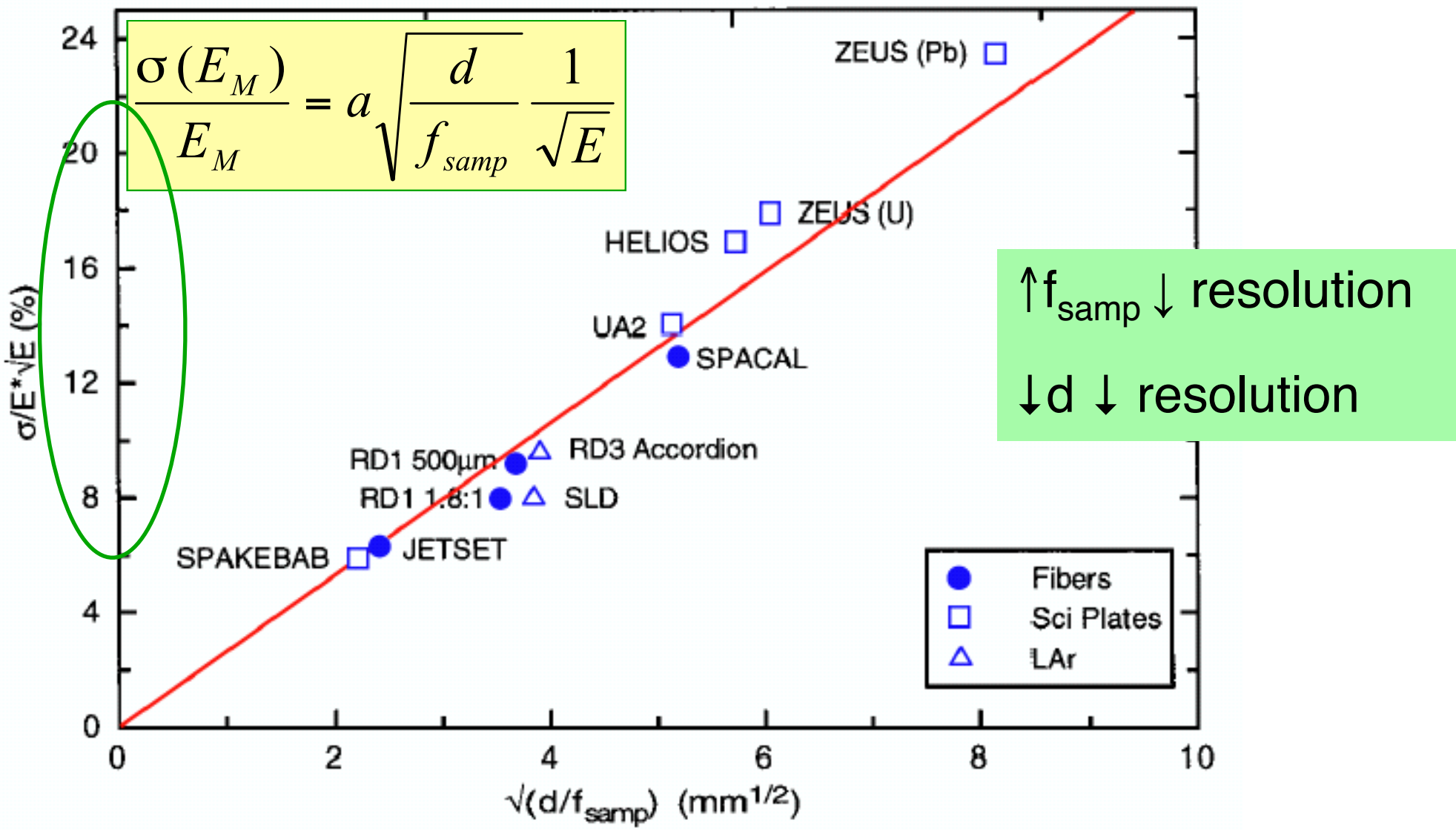
Number of detectable particles in active layer

$$N_r = T_r/d = f_s \cdot E/E_c^{\text{abs}} \cdot X_0^{\text{abs}}/d$$

Resolution scales like

$$\frac{\sigma(E_M)}{E_M} = a \sqrt{\frac{d}{f_{\text{samp}}}} \frac{1}{\sqrt{E}}$$

RESOLUTION FOR SAMPLING CALORIMETERS



ENERGY RESOLUTION

$$\frac{\sigma}{E} = \frac{a}{\sqrt{E}} \oplus \frac{b}{E} \oplus c$$

a the **stochastic term** accounts for Poisson-like fluctuations

naturally small for homogeneous calorimeters

takes into account sampling fluctuations for sampling calorimeters

b the **noise term** (hits at low energy)

mainly the energy equivalent of the electronics noise

at LHC in particular: includes fluctuation from non primary interaction (pile-up noise)

c the **constant term** (hits at high energy)

Essentially detector non homogeneities like intrinsic geometry, calibration but also energy leakage

EXAMPLE

Take a Lead Glass crystal

$$E_c = 15 \text{ MeV}$$

produces Cerenkov light

Cerenkov radiation is produced par e^\pm with $\beta > 1/n$, i.e $E > 0.7\text{MeV}$

Take a 1 GeV electron

At maximum 1000 MeV/0.7 MeV e^\pm will produce light

Fluctuation $1/\sqrt{1400} = 3\%$

One then has to take into account the photon detection efficiency which is typically 1000 photo-electrons/GeV: $1/\sqrt{1000} \sim 3\%$

Final resolution $\sigma/E \sim 5\%/\sqrt{E}$

CMS crystals: PbWO_4

Excellent energy resolution

$X_0 = 0.89\text{cm} \rightarrow$ compact calorimeter (23cm for 26 X_0)

$R_M = 2.2\text{ cm} \rightarrow$ compact shower development

Fast light emission (80% in less than 15 ns)

Radiation hard (10^5Gy)

But

Low light yield (150 γ/MeV)

Response varies with dose

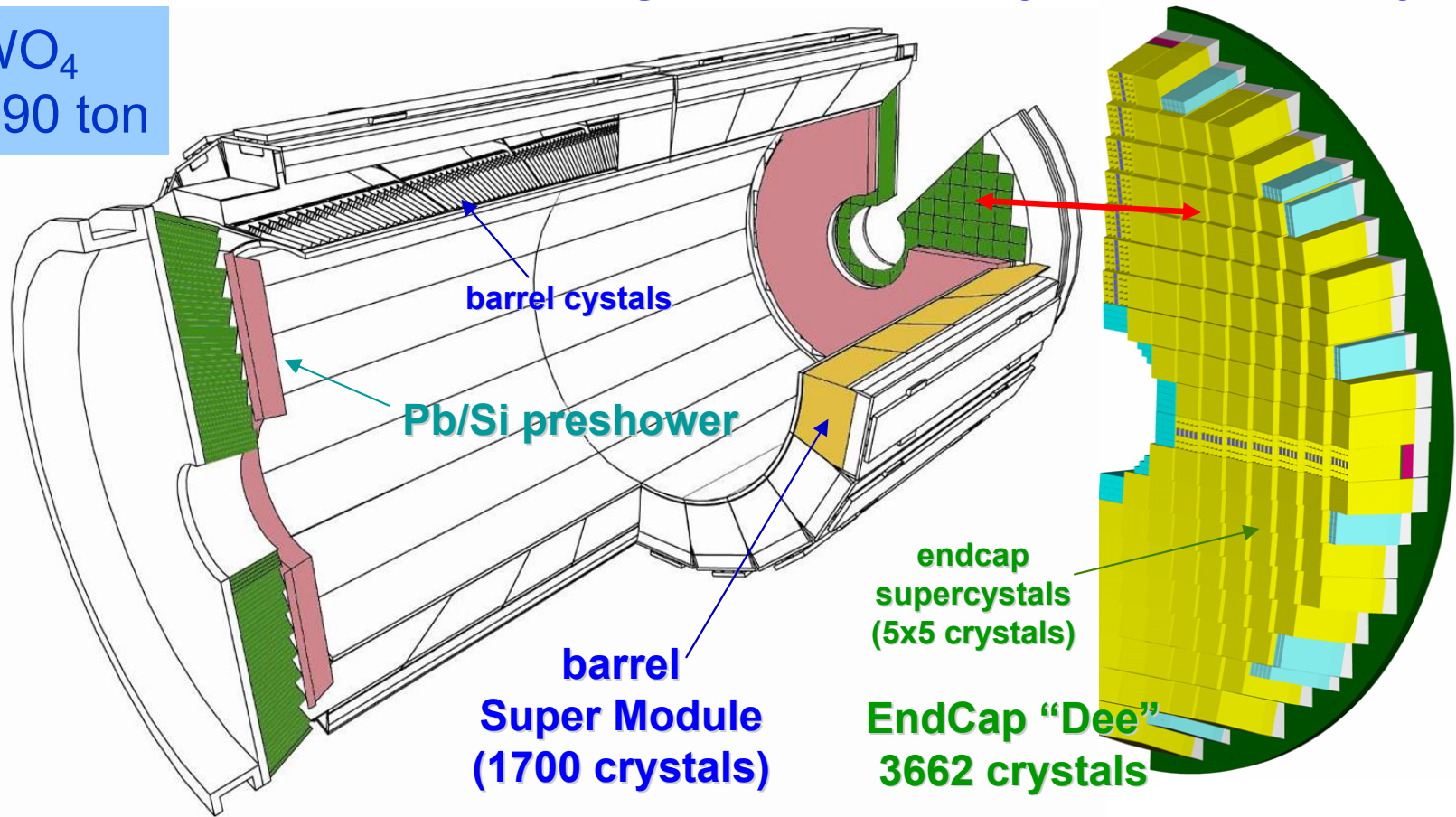
Response temperature dependance

ECAL @ CMS

Precision electromagnetic calorimetry: 75848 PWO crystals

PWO: PbWO_4
about 10 m³, 90 ton

Previous
Crystal
calorimeters:
max 1m³



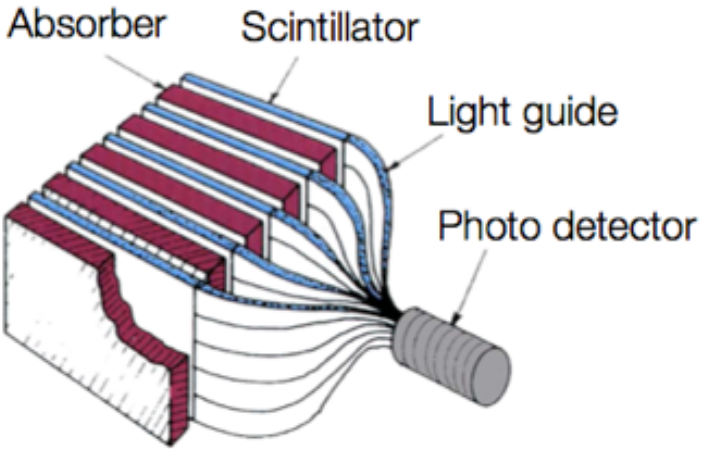
Barrel: $|\eta| < 1.48$
36 Super Modules
61200 crystals (2x2x23cm³)

EndCaps: $1.48 < |\eta| < 3.0$
4 Dees
14648 crystals (3x3x22cm³)

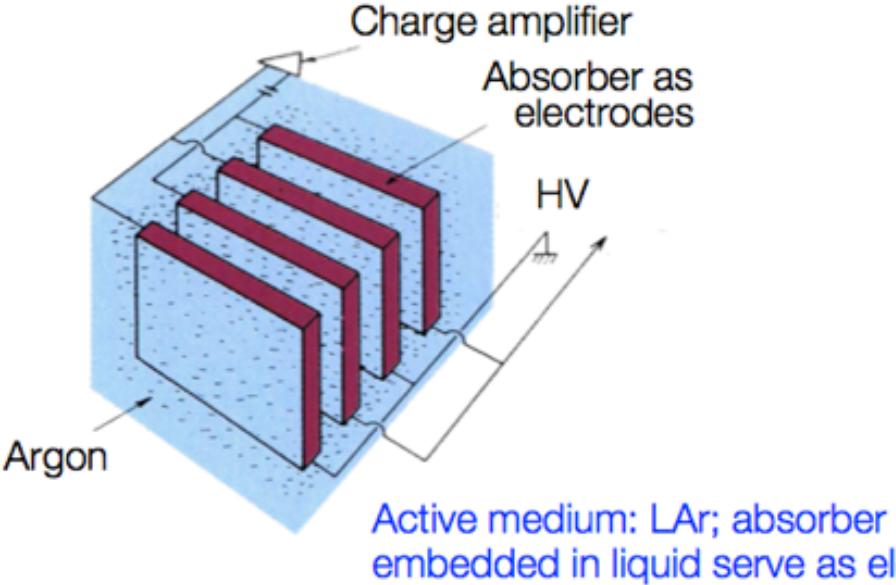
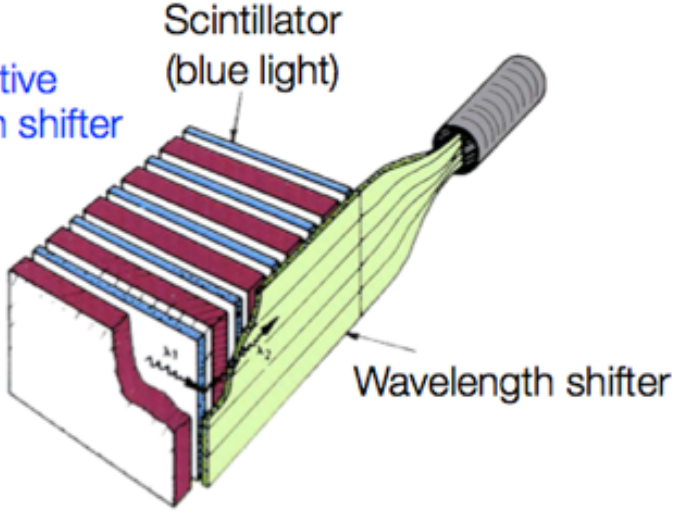
SAMPLING CALORIMETER

Possible setups

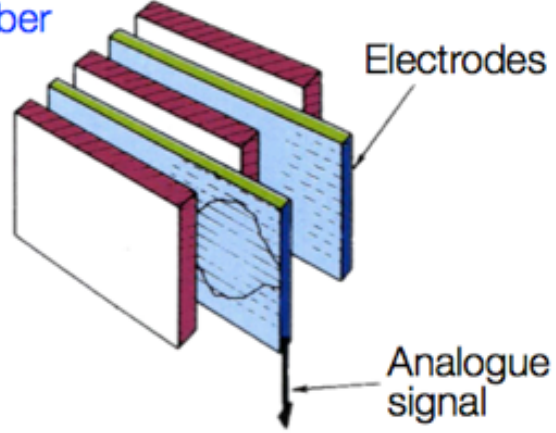
Scintillators as active layer;
signal readout via photo multipliers



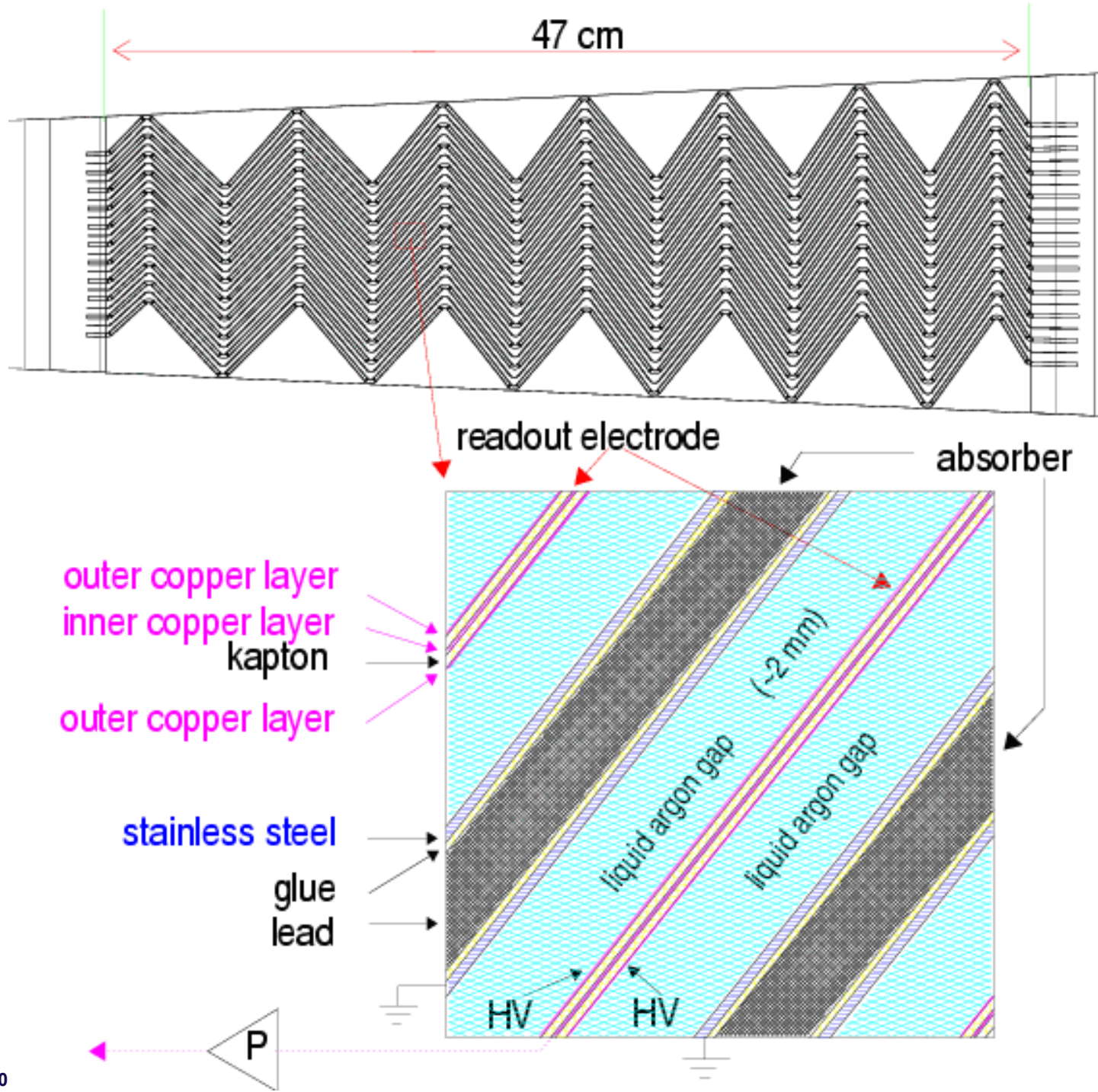
Scintillators as active layer; wave length shifter to convert light



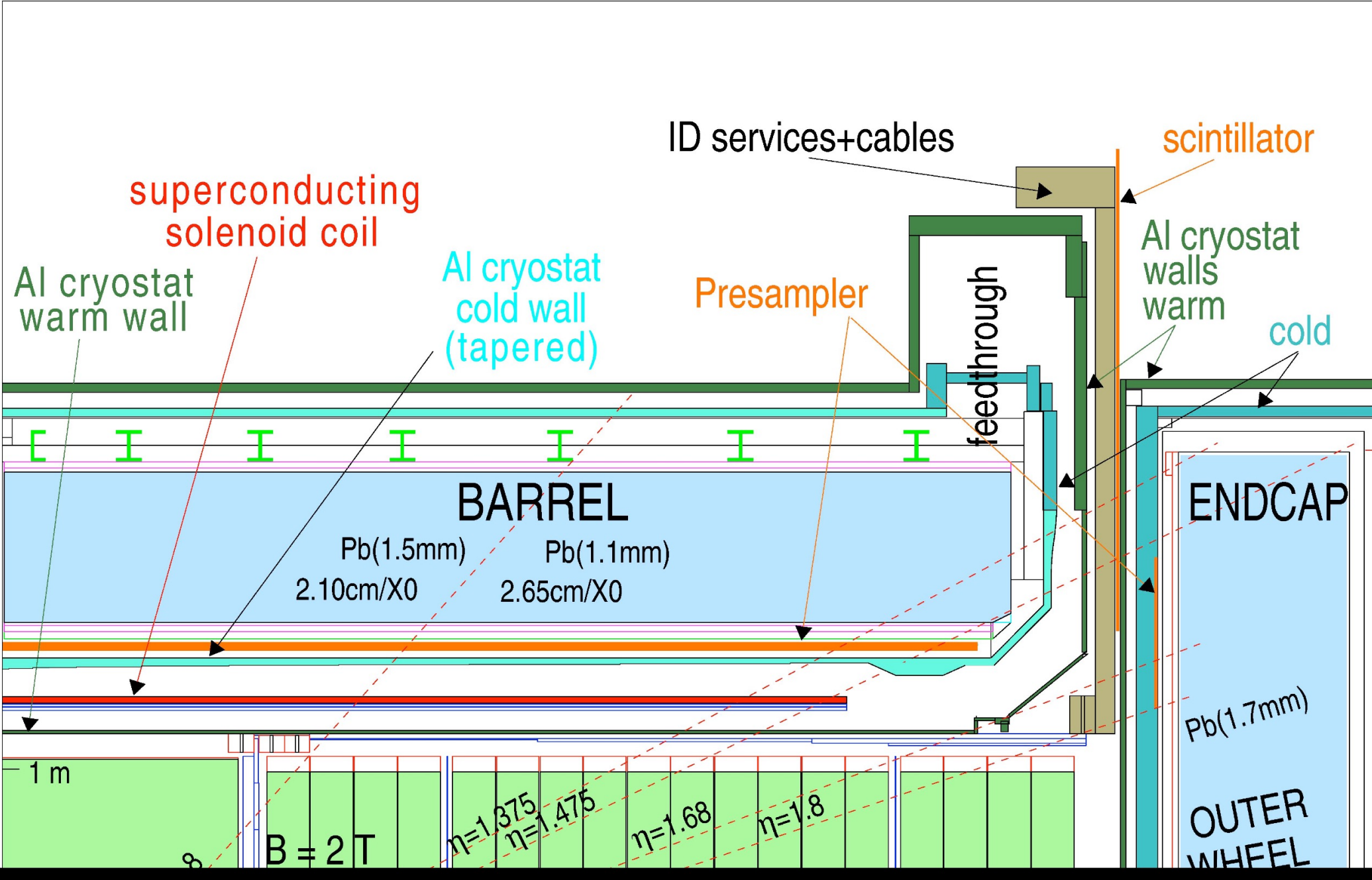
Ionization chambers
between absorber
plates



ATLAS LIQUID ARGON EM CALORIMETER



THE ATLAS CALORIMETER STRUCTURE



ATLAS ELECTROMAGNETIC CALORIMETER

Accordion Pb/LAr $|\eta| < 3.2$ ~170k channels

Precision measurement $|\eta| < 2.5$

3 layers up to $|\eta| = 2.5$ + presampler $|\eta| < 1.8$

2 layers $2.5 < |\eta| < 3.2$

Layer 1 (γ/π^0 rej. + angular meas.)

$$\Delta\eta \cdot \Delta\phi = 0.003 \times 0.1$$

Layer 2 (shower max)

$$\Delta\eta \cdot \Delta\phi = 0.025 \times 0.025$$

Layer 3 (Hadronic leakage)

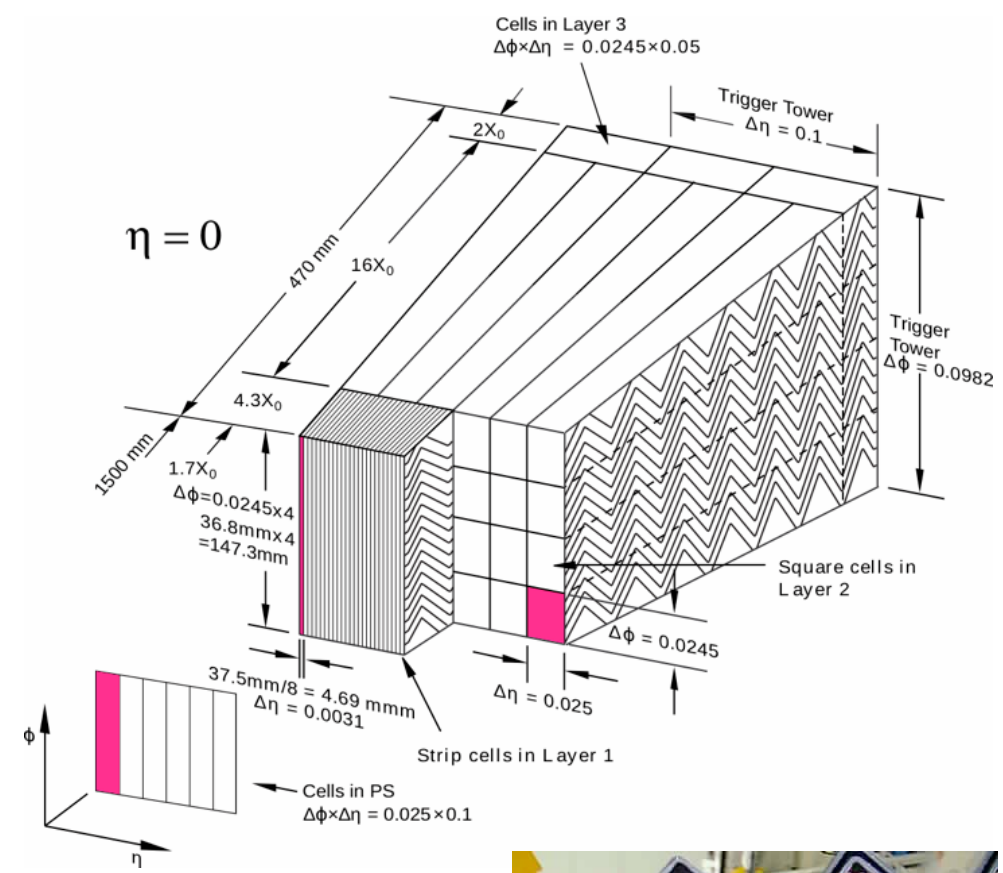
$$\Delta\eta \cdot \Delta\phi = 0.05 \times 0.025$$

Energy Resolution: design for $\eta \sim 0$

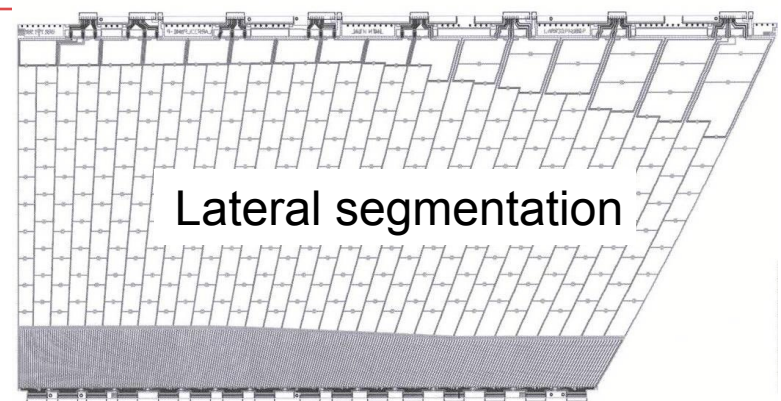
$$\Delta E/E \sim 10\%/\sqrt{E} \oplus 150 \text{ MeV}/E \oplus 0.7\%$$

Angular Resolution

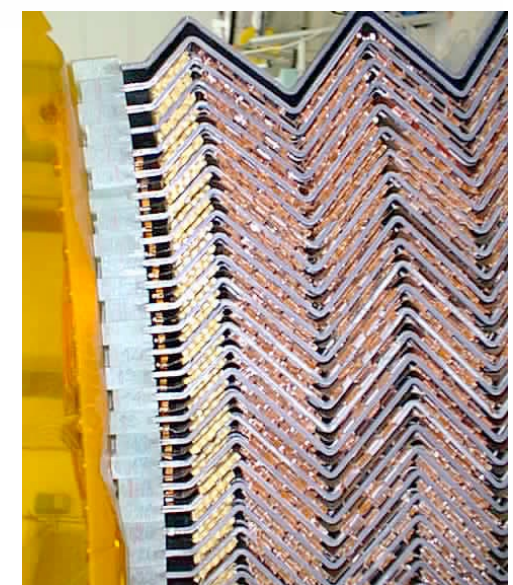
$$50 \text{ mrad}/\sqrt{E(\text{GeV})}$$



origin:27. dwg du 02/07/1999



170k channels

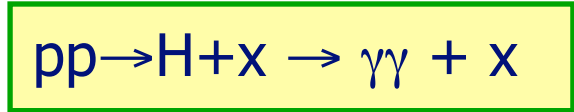
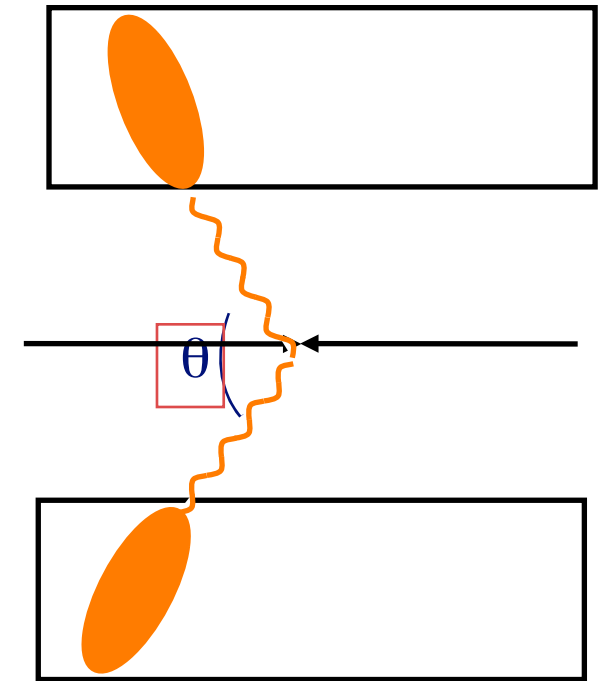
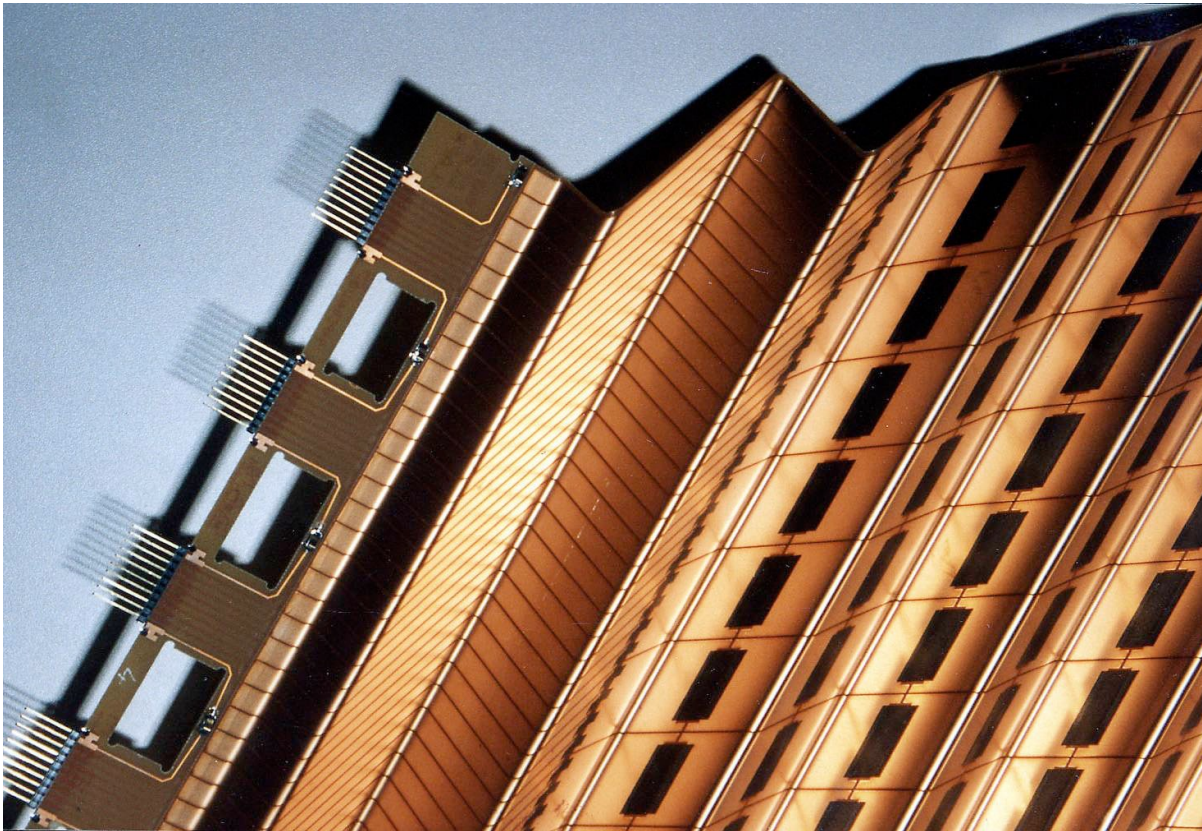


POSITION-ANGULAR RESOLUTION

Higgs Boson in ATLAS

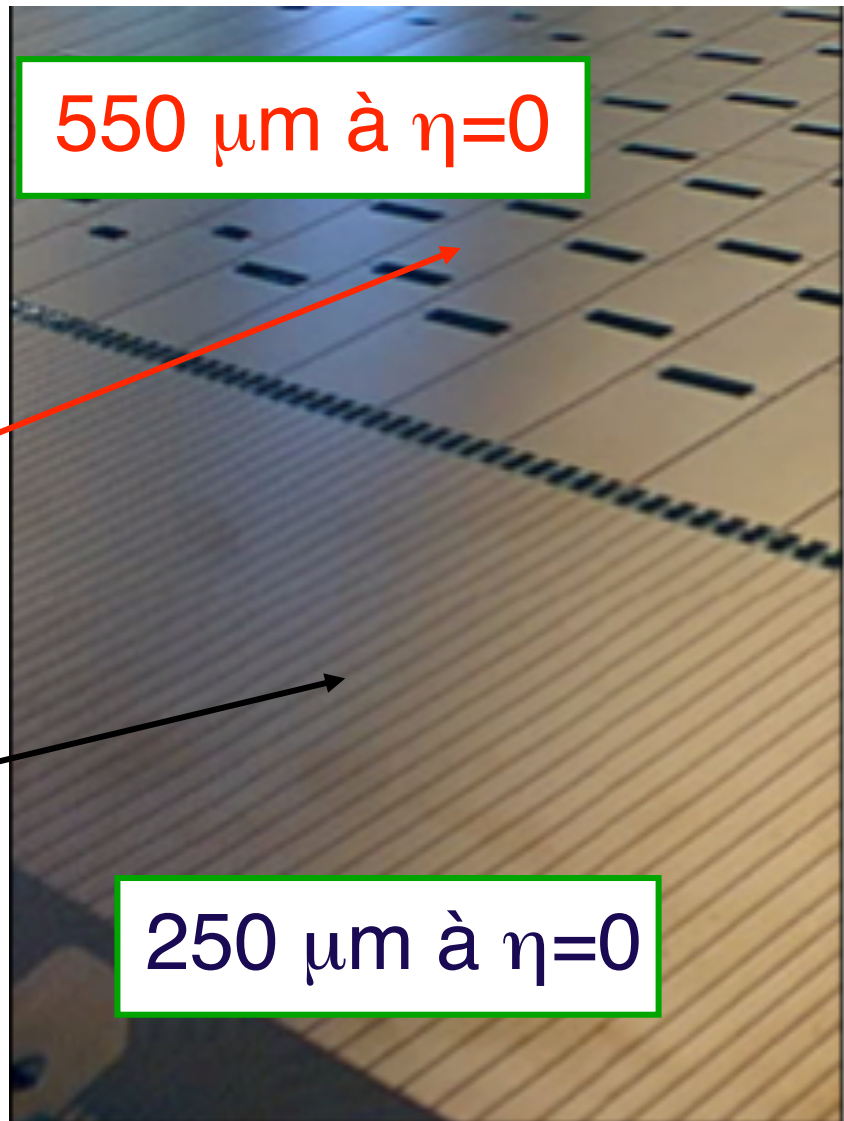
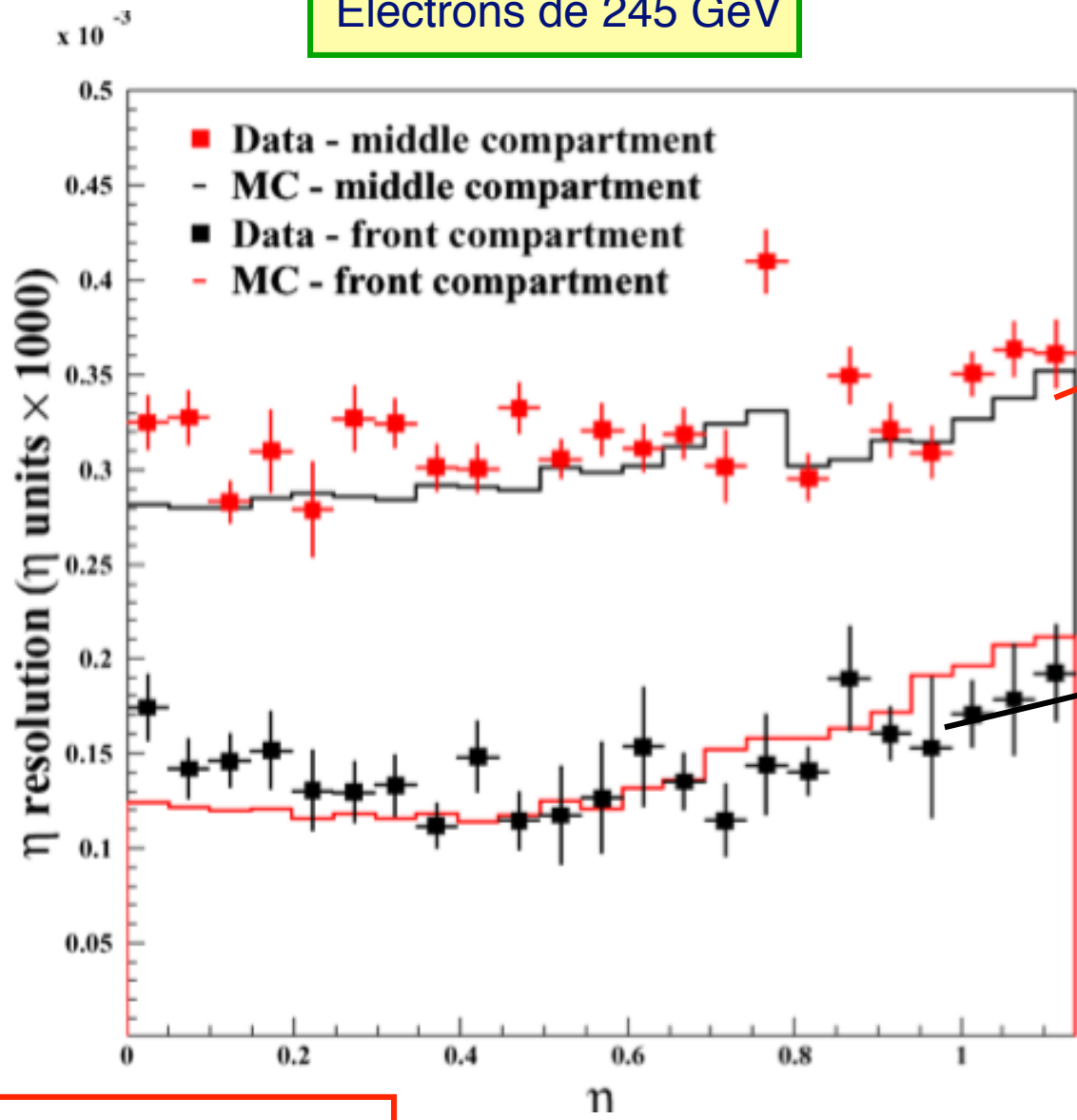
For $M_H \sim 120$ GeV, in the channel $H \rightarrow \gamma\gamma$

$$\sigma(M_H) / M_H = \frac{1}{2} [\sigma(E_{\gamma 1})/E_{\gamma 1} \oplus \sigma(E_{\gamma 2})/E_{\gamma 2} \oplus \cot(\theta/2) \sigma(\theta)]$$



SPATIAL RESOLUTION

Electrons de 245 GeV



NIM A550 96-115 (2005)

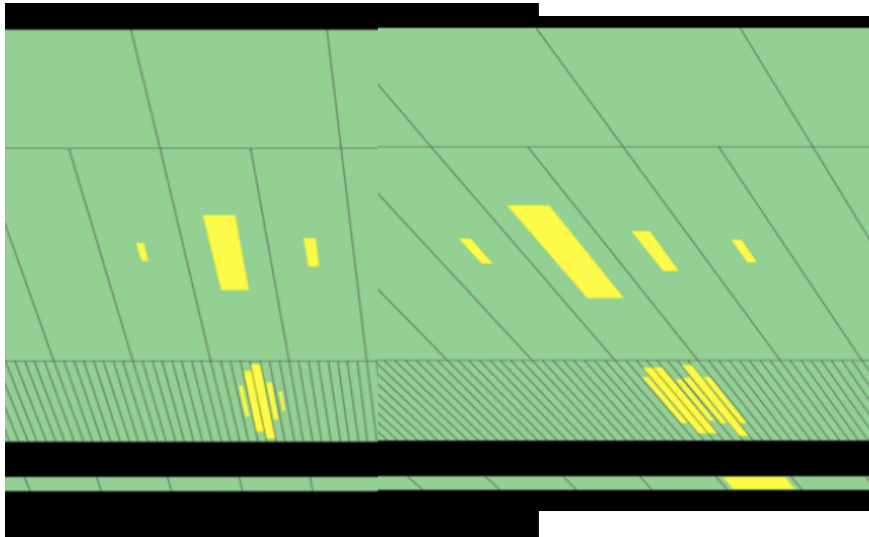
28th June-4th July 2017

PIONS REJECTION

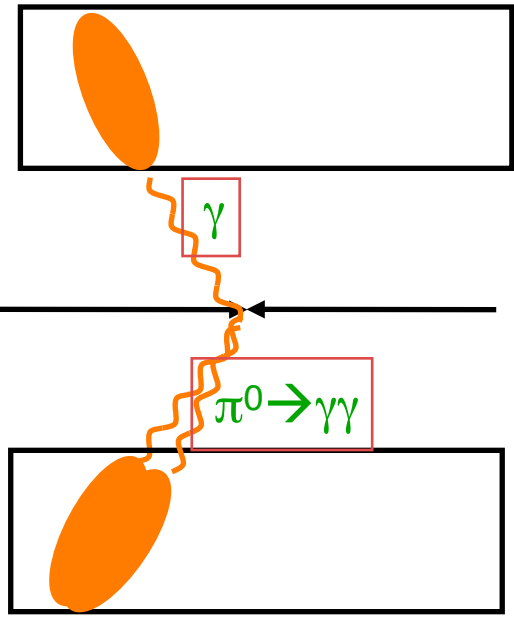
Higgs boson in ATLAS

With $M_H \sim 125$ GeV in the channel $H \rightarrow \gamma\gamma$

Background: π^0 looking like a γ



γ/π^0 rejection



$pp \rightarrow \gamma\text{-jet} \rightarrow \gamma + \pi^0 + X$

HOMOGENEOUS vs SAMPLING CALORIMETERS

| Technology (Experiment) | Depth | Energy resolution | Date |
|--|---------------------|-----------------------------------|------|
| NaI(Tl) (Crystal Ball) | 20X ₀ | 2.7%/E ^{1/4} | 1983 |
| Bi ₄ Ge ₃ O ₁₂ (BGO) (L3) | 22X ₀ | 2%/√E ⊕ 0.7% | 1993 |
| CsI (KTcV) | 27X ₀ | 2%/√E ⊕ 0.45% | 1996 |
| CsI(Tl) (BaBar) | 16–18X ₀ | 2.3%/E ^{1/4} ⊕ 1.4% | 1999 |
| CsI(Tl) (BELLE) | 16X ₀ | 1.7% for E _γ > 3.5 GeV | 1998 |
| PbWO ₄ (PWO) (CMS) | 25X ₀ | 3%/√E ⊕ 0.5% ⊕ 0.2/E | 1997 |
| Lead glass (OPAL) | 20.5X ₀ | 5%/√E | 1990 |
| Liquid Kr (NA48) | 27X ₀ | 3.2%/√E ⊕ 0.42% ⊕ 0.09/E | 1998 |
| Scintillator/depleted U (ZEUS) | 20–30X ₀ | 18%/√E | 1988 |
| Scintillator/Pb (CDF) | 18X ₀ | 13.5%/√E | 1988 |
| Scintillator fiber/Pb spaghetti (KLOE) | 15X ₀ | 5.7%/√E ⊕ 0.6% | 1995 |
| Liquid Ar/Pb (NA31) | 27X ₀ | 7.5%/√E ⊕ 0.5% ⊕ 0.1/E | 1988 |
| Liquid Ar/Pb (SLD) | 21X ₀ | 8%/√E | 1993 |
| Liquid Ar/Pb (H1) | 20–30X ₀ | 12%/√E ⊕ 1% | 1998 |
| Liquid Ar/depl. U (DØ) | 20.5X ₀ | 16%/√E ⊕ 0.3% ⊕ 0.3/E | 1993 |
| Liquid Ar/Pb accordion (ATLAS) | 25X ₀ | 10%/√E ⊕ 0.4% ⊕ 0.3/E | 1996 |

Homogeneous

Sampling

Resolution of typical electromagnetic calorimeter [E is in GeV]

HADRONIC SHOWERS

Hadronic cascades develop in an analogous way to e.m. showers

Strong interaction controls overall development

High energy hadron interacts with material, leading to multi-particle production of more hadrons

These in turn interact with further nuclei

Nuclear breakup and spallation neutrons

Multiplication continues down to the pion production threshold

$$E \sim 2m_{\pi} = 0.28 \text{ GeV}/c^2$$

Neutral pions result in an electromagnetic component (immediate decay: $\pi^0 \rightarrow \gamma\gamma$)
(also: $\eta \rightarrow \gamma\gamma$)

Energy deposited by:

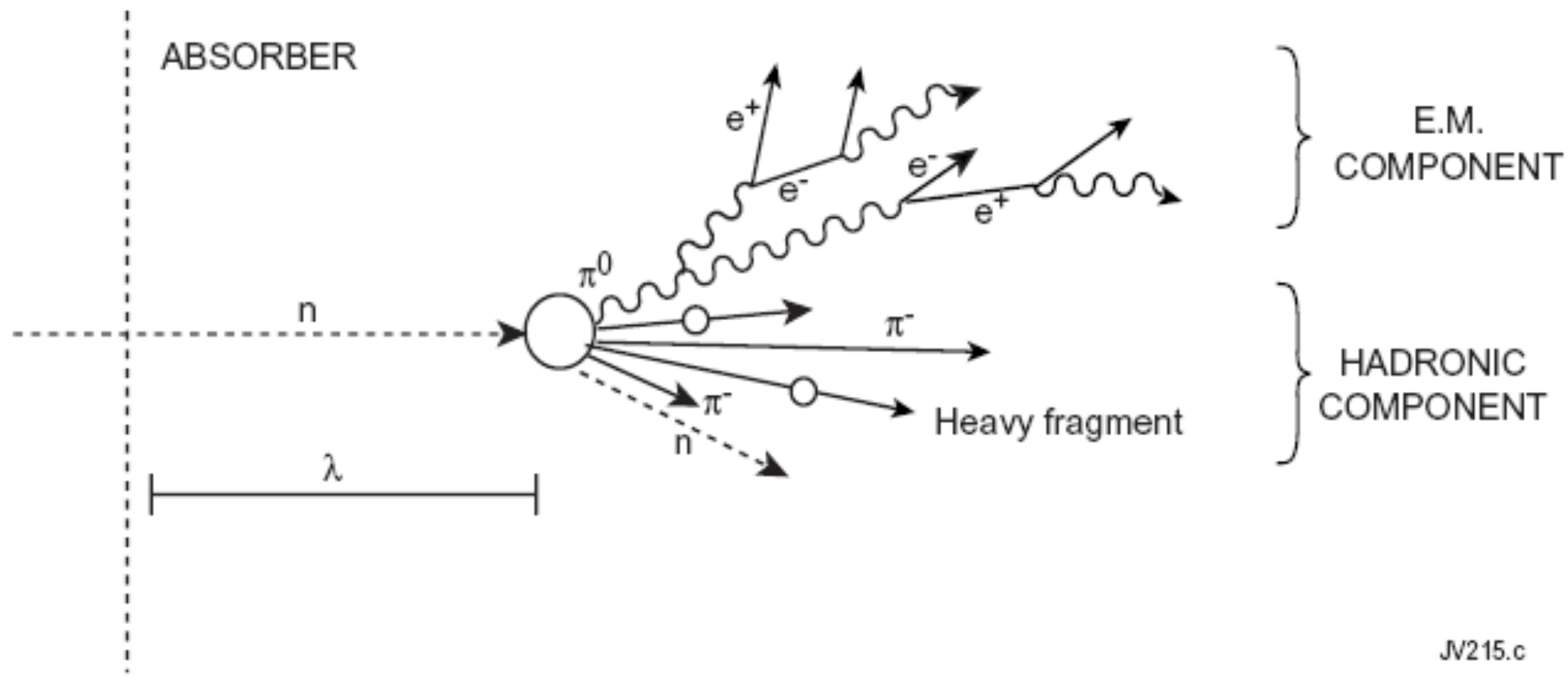
Electromagnetic component (i.e. as for e.m. showers)

Charged pions or protons

Low energy neutrons

Energy lost in breaking nuclei (nuclear binding energy)

HADRONIC CASCADE



JV215.c

As compared to electromagnetic showers, hadron showers are:

- Larger/more penetrating
- Subject to larger fluctuations – more erratic and varied

HADRONIC SHOWERS: WHERE DOES THE ENERGY GO ?

| | <i>Lead</i> | <i>Iron</i> |
|--|---------------|--------------|
| Ionization by pions | 19% | 21% |
| Ionization by protons | 37% | 53% |
| <i>Total ionization</i> | 56% | 74% |
| Nuclear binding energy loss | 32% | 16% |
| Target recoil | 2% | 5% |
| <i>Total invisible energy</i> | 34% | 21% |
| Kinetic energy evaporation neutrons | 10% | 5% |
| Number of charged pions | 0.77 | 1.4 |
| Number of protons | 3.5 | 8 |
| Number of cascade neutrons | 5.4 | 5 |
| Number of evaporation neutrons | 31.5 | 5 |
| Total number of neutrons | 36.9 | 10 |
| Neutrons/protons | 10.5/1 | 1.3/1 |

HADRONIC INTERACTION

Simple model of interaction on a disk of radius R: $\sigma_{\text{int}} = \pi R^2 \propto A^{2/3}$

$$\sigma_{\text{inel}} \approx \sigma_0 A^{0.7}, \quad \sigma_0 = 35 \text{ mb}$$

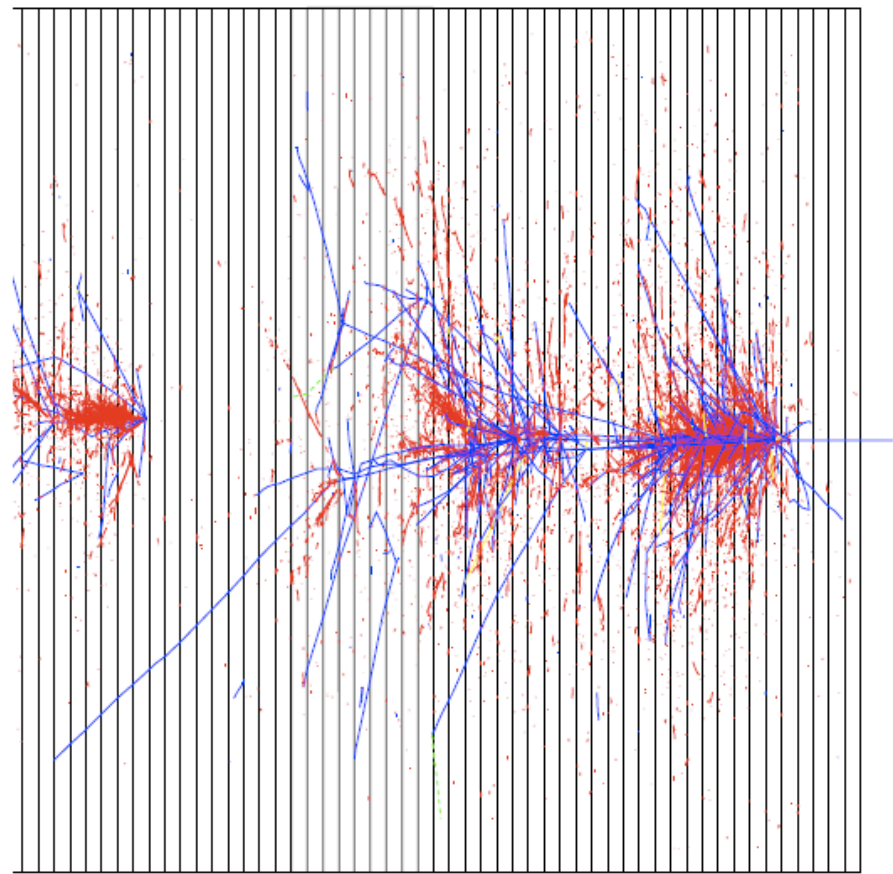
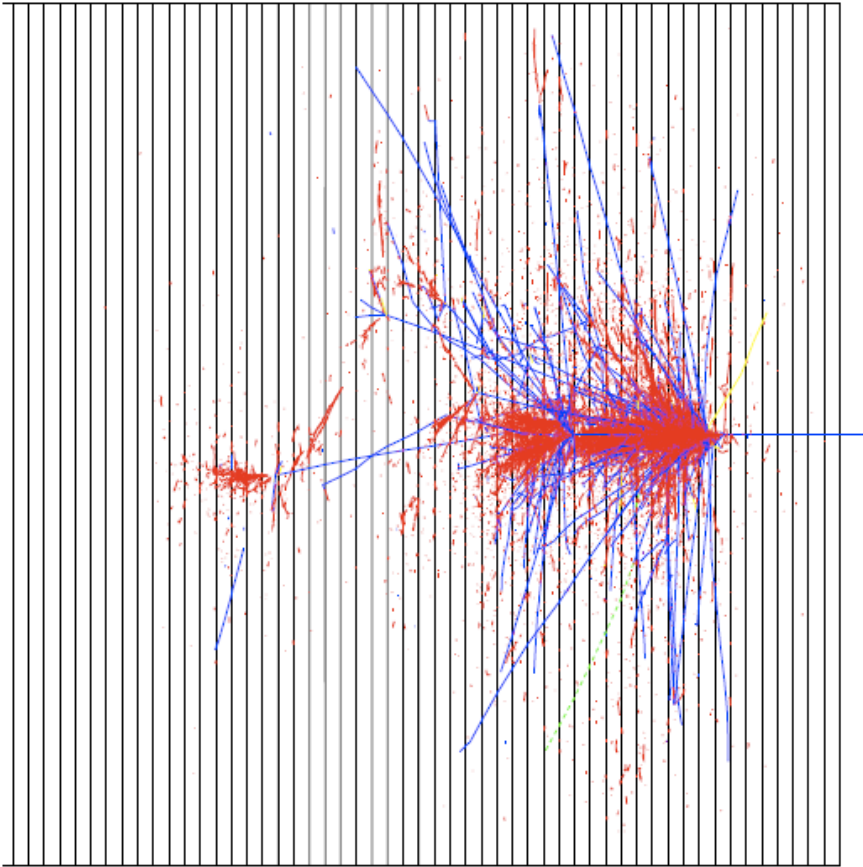
Nuclear interaction length: mean free path before inelastic interaction

$$\lambda_{\text{int}} \approx \frac{A}{N_A \sigma_{\text{int}}} \approx 35 A^{1/3} \text{ g cm}^{-2}$$

| | Z | ρ (g.cm ⁻³) | E_c (MeV) | X_0 (cm) | λ_{int} (cm) |
|-------------------|----|---------------------------------|----------------|---------------|--------------------------------|
| Air | | | | 30 420 | ~70 000 |
| Water | | | | 36 | 84 |
| PbWO ₄ | | 8.28 | | 0.89 | 22.4 |
| C | 6 | 2.3 | 103 | 18.8 | 38.1 |
| Al | 13 | 2.7 | 47 | 8.9 | 39.4 |
| L Ar | 18 | 1.4 | | 14 | 84 |
| Fe | 26 | 7.9 | 24 | 1.76 | 16.8 |
| Cu | 29 | 9 | 20 | 1.43 | 15.1 |
| W | 74 | 19.3 | 8.1 | 0.35 | 9.6 |
| Pb | 82 | 11.3 | 6.9 | 0.56 | 17.1 |
| U | 92 | 19 | 6.2 | 0.32 | 10.5 |

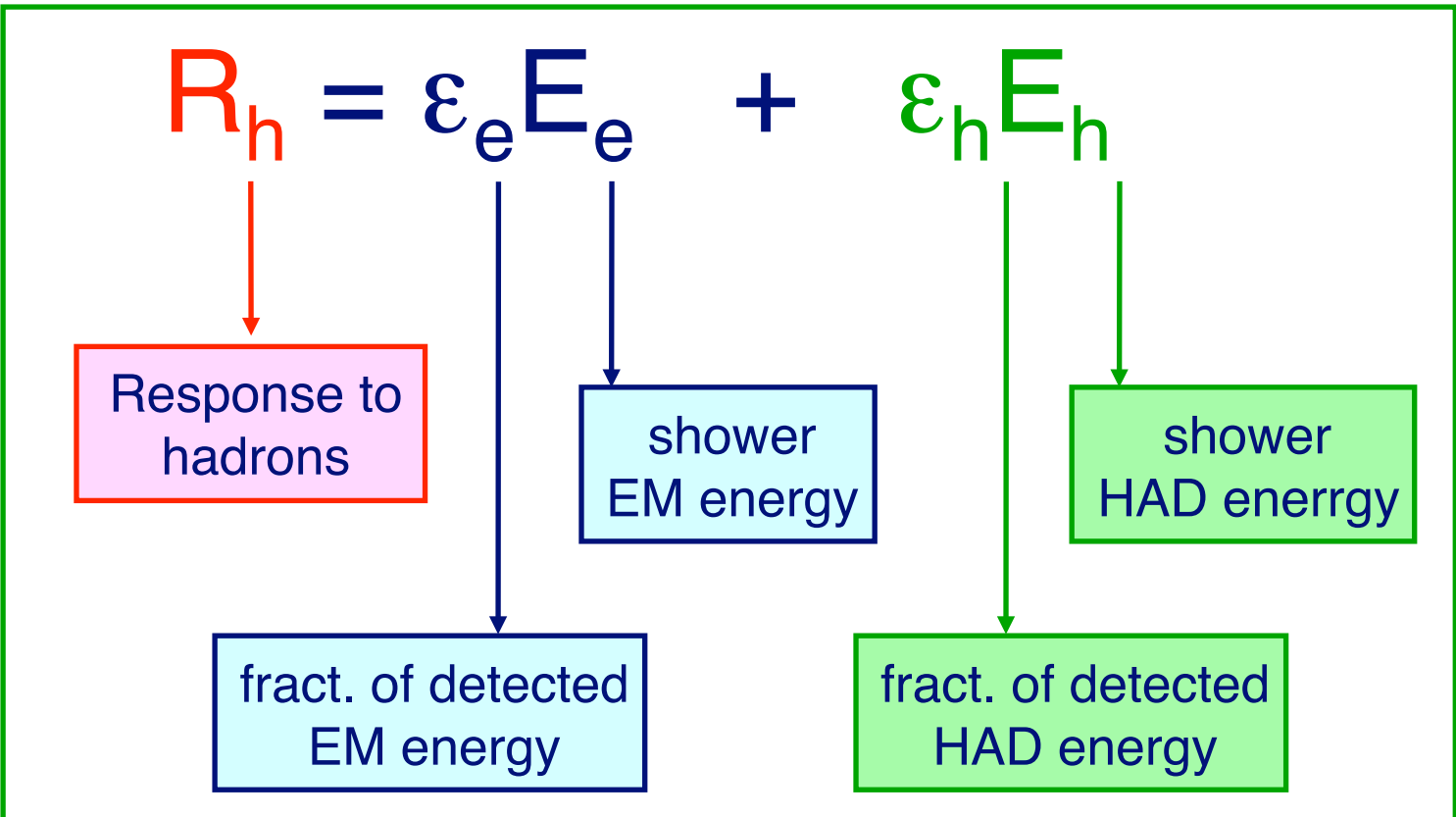
HADRONIC SHOWERS

1. Individual hadron showers are quite **2.** similar



red - e.m. component
blue - charged hadrons

HADRONIC SHOWERS and NON-COMPENSATION



$$\frac{e}{h} = \frac{\epsilon_e}{\epsilon_h}$$

≈ 1 : compensating calorimeter

> 1 : non compensating calorimeter

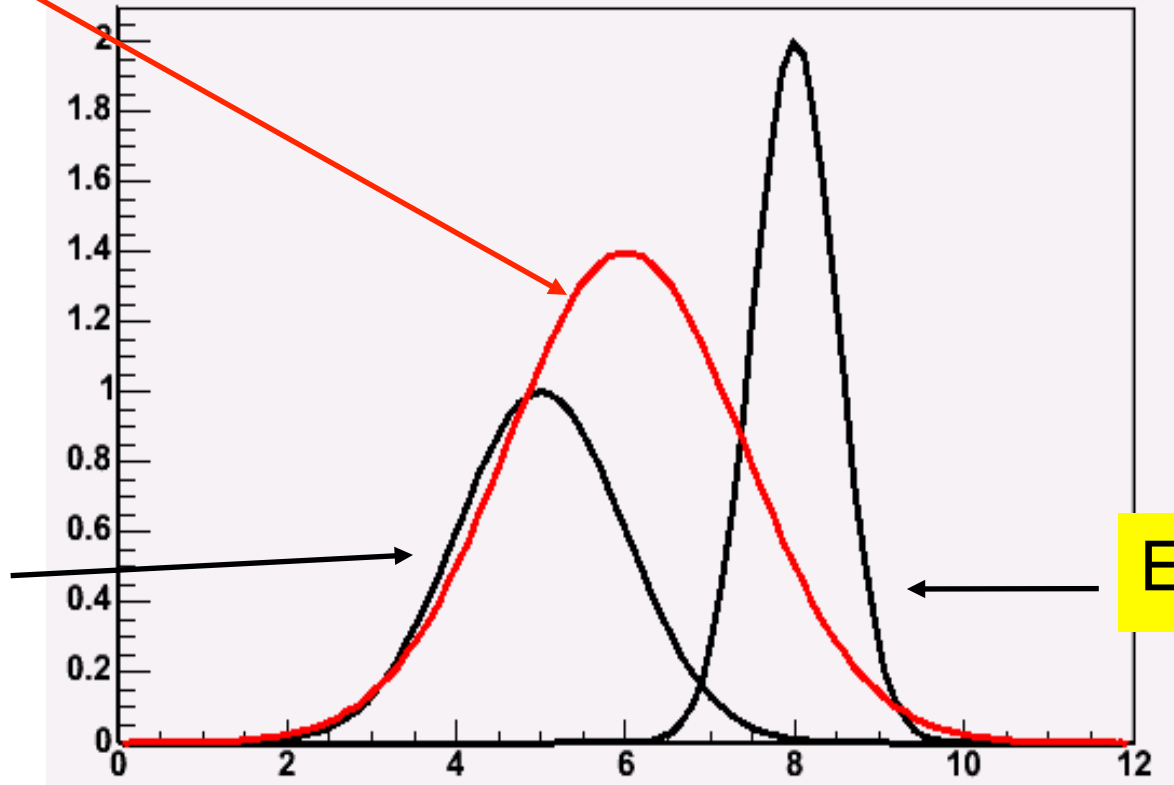
HADRONIC SHOWERS and NON-COMPENSATION

$$R_h = \epsilon_e E_e + \epsilon_h E_h$$

$$\epsilon_e > \epsilon_h$$

$$E_e \ll E_h$$

$$E_e \gg E_h$$



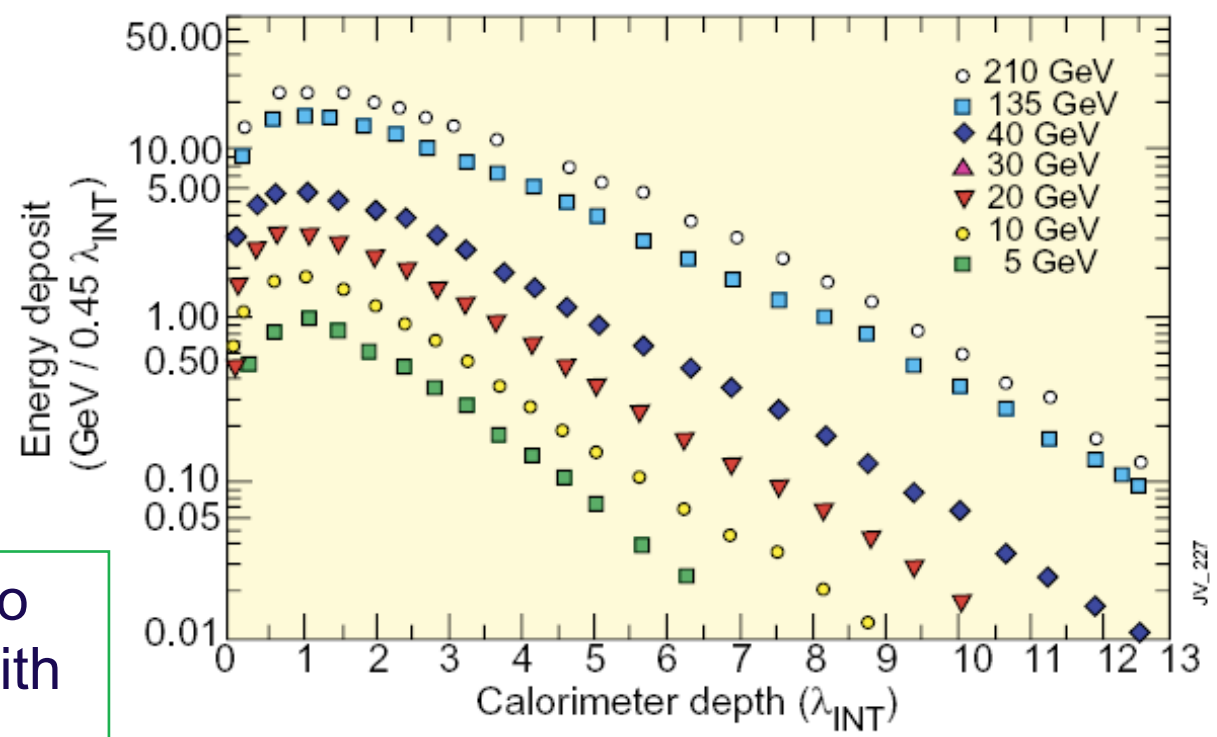
HADRONIC SHOWER LONGITUDINAL DEVELOPMENT

Longitudinal profile

Initial peak from π^0 s produced in the first interaction length

Gradual falloff characterised by the nuclear interaction length, λ_{int}

WA78 : 5.4 λ of 10mm U / 5mm Scint + 8 λ of 25mm Fe / 5mm Scint



As with e.m. showers: depth to contain a shower increases with $\log(E)$

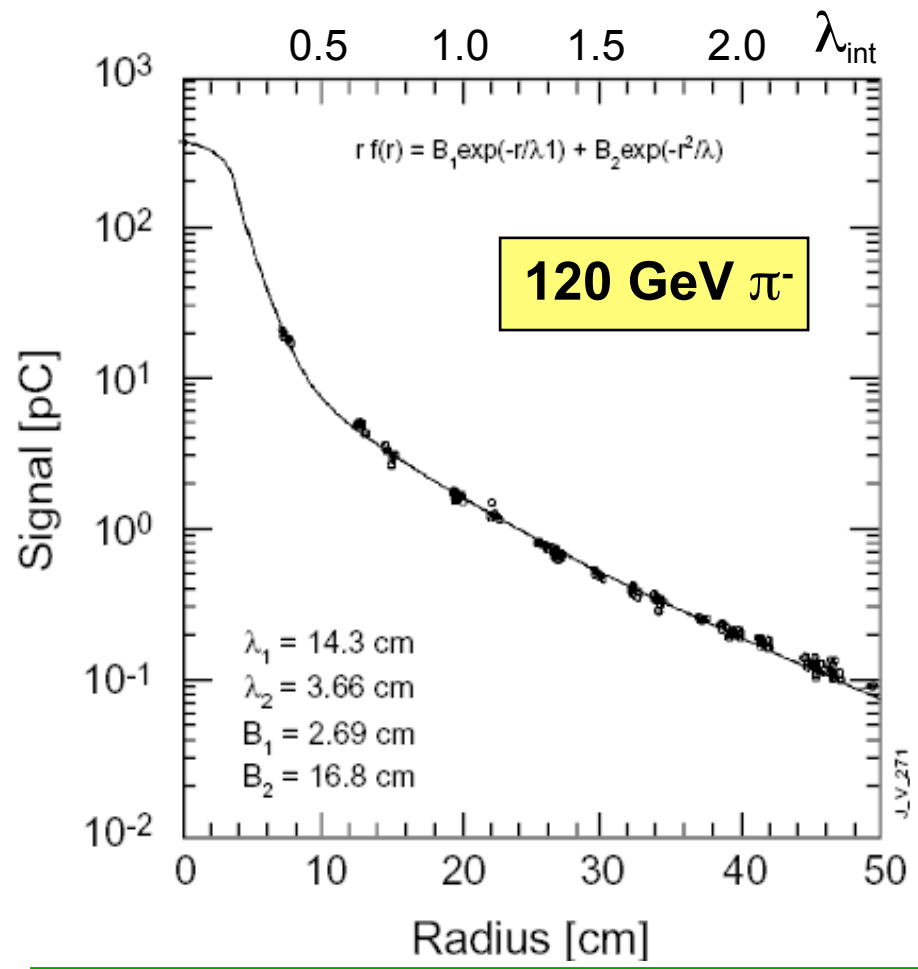
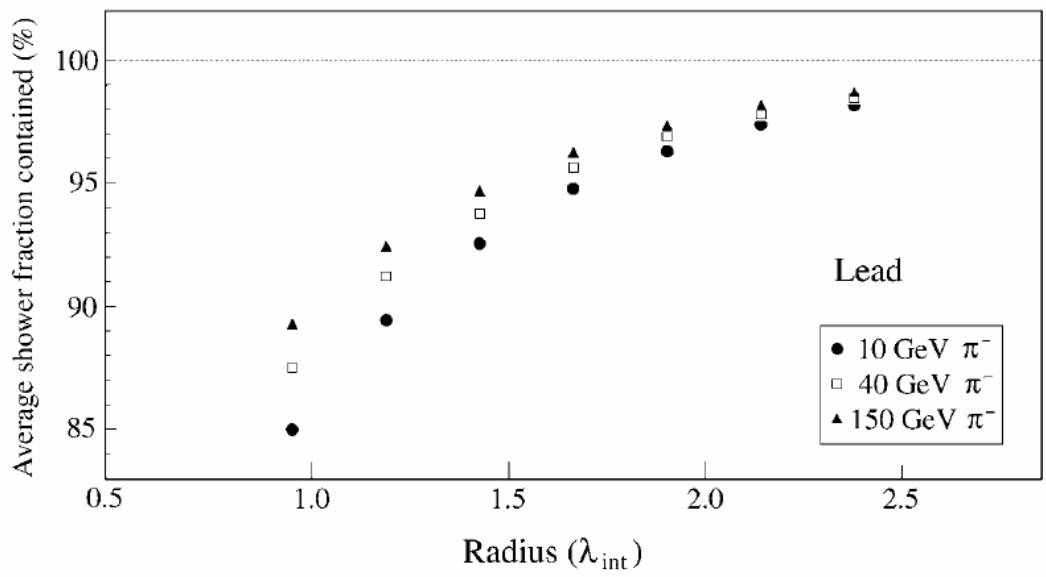
JV_227

HADRONIC SHOWERS TRANSVERSE PROFILE

Mean transverse momentum from interactions, $\langle p_T \rangle \sim 300$ MeV, is about the same magnitude as the energy lost traversing 1λ for many materials

So radial extent of the cascade is well characterized by λ

The π^0 component of the cascade results in an electromagnetic core



Lateral containment increases with energy

JETS at HIGH ENERGY COLLIDERS

At Hadronic Colliders, quarks & gluons produced, evolves (parton shower, hadronisation) to become jets

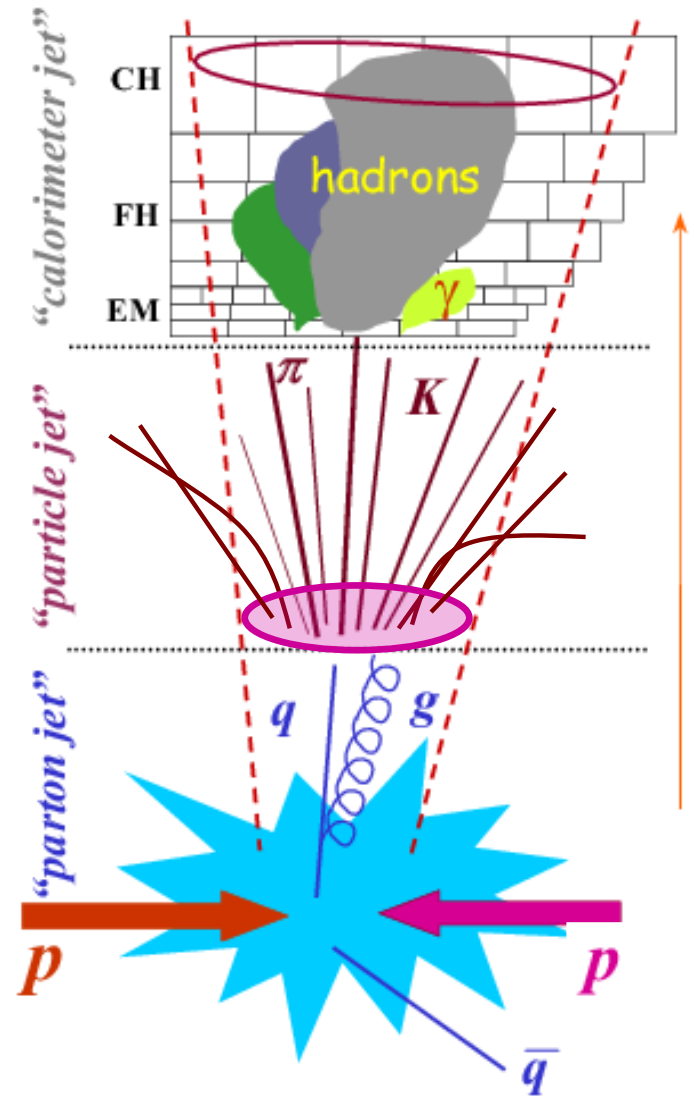
In a cone around the initial parton: high density of hadrons

LHC calorimeters cannot separate all the incoming hadrons

Use dedicated calibration schemes (based on simulation in ATLAS)

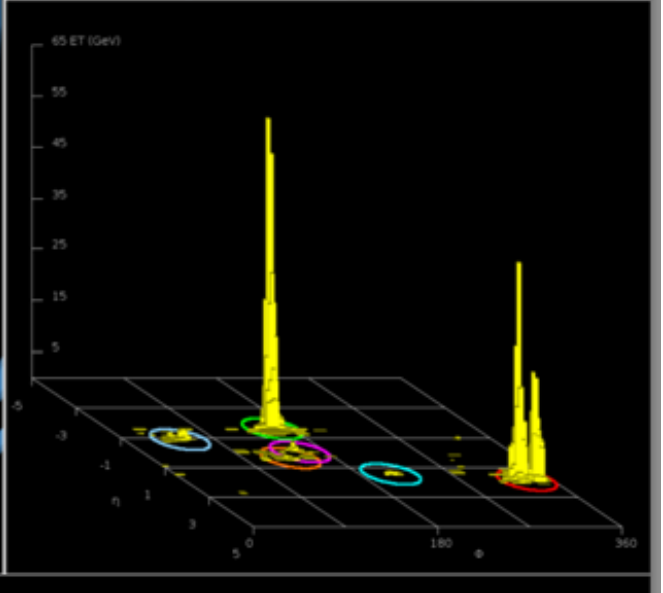
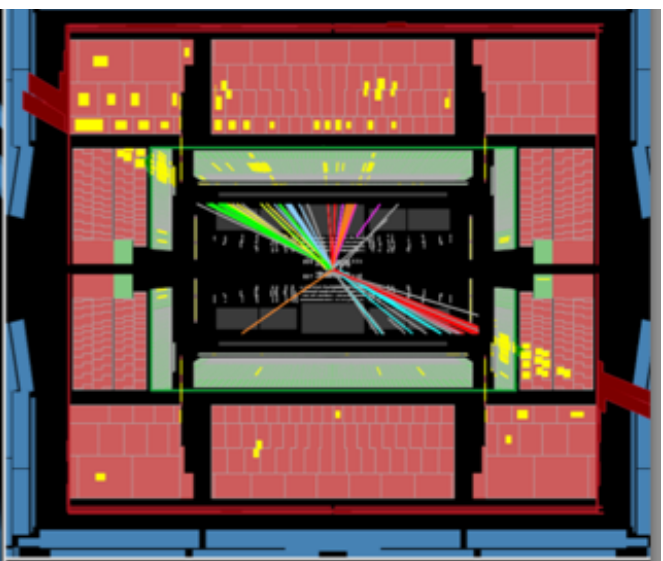
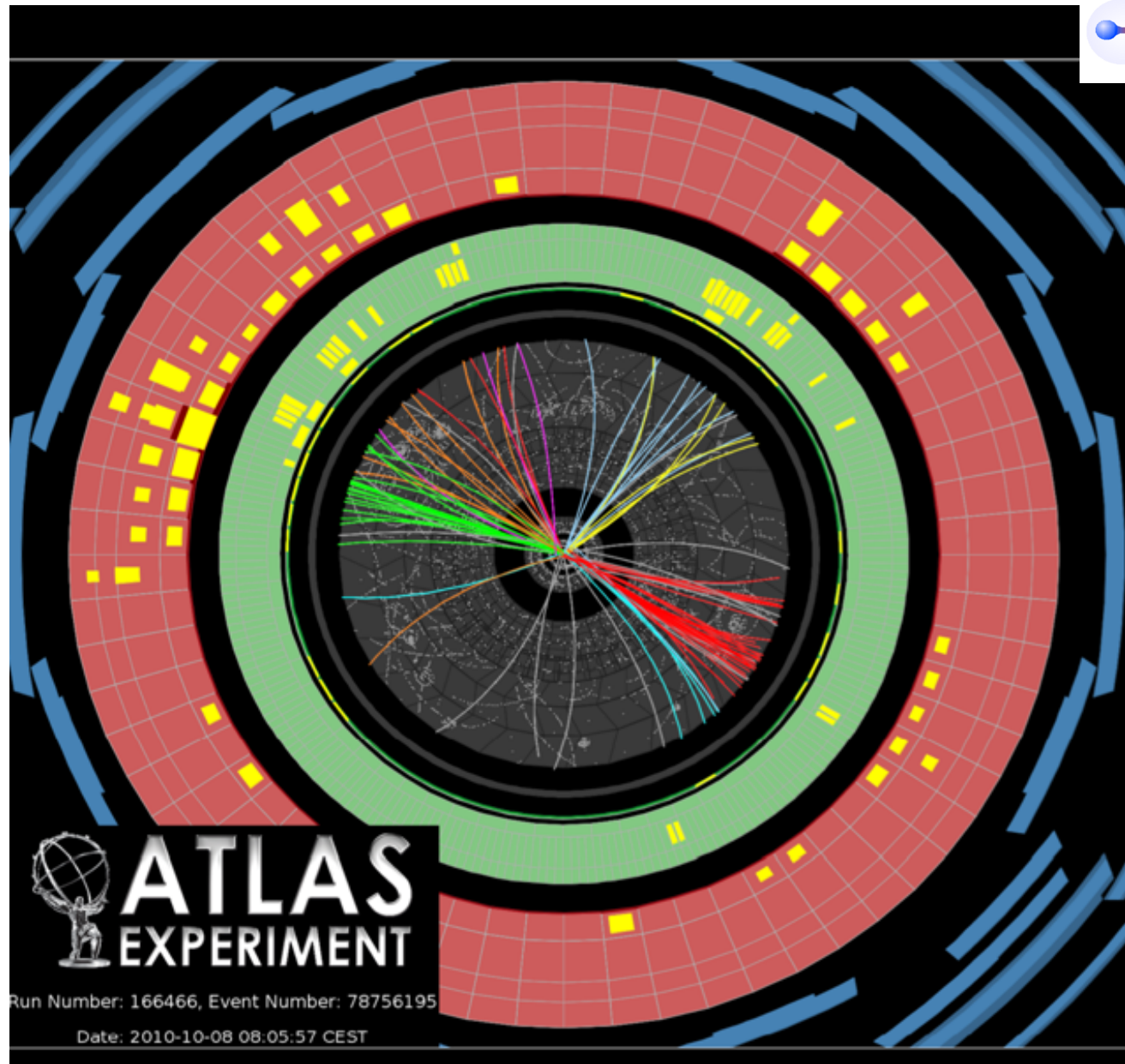
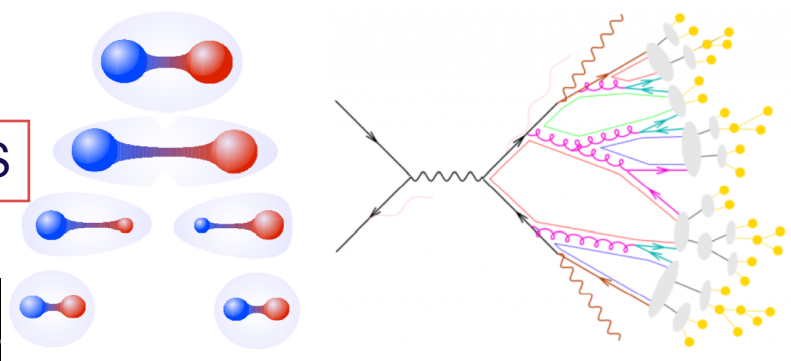
Use tracking system to identify charged hadrons (Particle Flow in CMS)

In the future, very highly segmented calorimeters

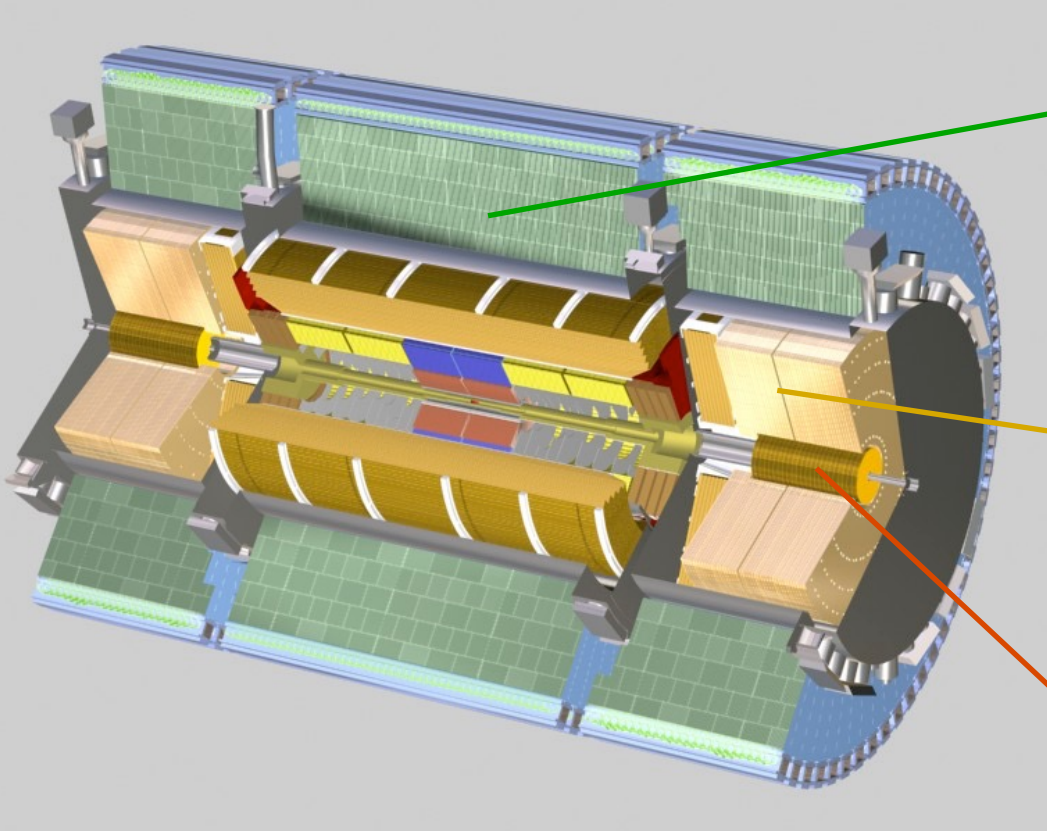


JETS

NEED a REFINED CALIBRATION PROCEDURE FOR JETS



ATLAS HADRON CALORIMETER



Tiles Calorimeter $|\eta| < 1.7$
 Fe / Scintillator
 3 layers in depth

LAr/Cu $1.7 < |\eta| < 3.2$
 4 layers in depth

Forward: 1 layer EM, 2 HAD
 LAr/Cu or W $3.2 < |\eta| < 4.9$

Total thickness: $\sim 8 - 10 \lambda$
 Use of different technics: cope with radiations in forward region

Scintillator tile calorimeter

| | Barrel | Extended barrel |
|--|------------------|----------------------|
| $ \eta $ coverage | $ \eta < 1.0$ | $0.8 < \eta < 1.7$ |
| Number of layers | 3 | 3 |
| Granularity $\Delta\eta \times \Delta\phi$ | 0.1×0.1 | 0.1×0.1 |
| Last layer | 0.2×0.1 | 0.2×0.1 |
| Readout channels | 5760 | 4092 (both sides) |

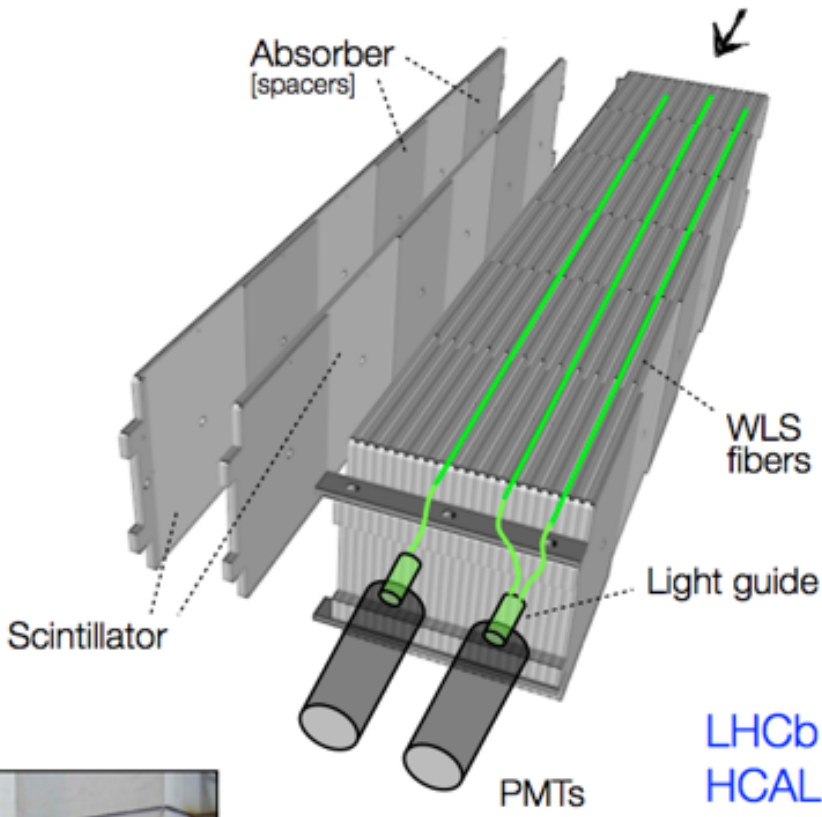
HADRONIC CALORIMETER

Most common realization: **Sampling Calorimeter**

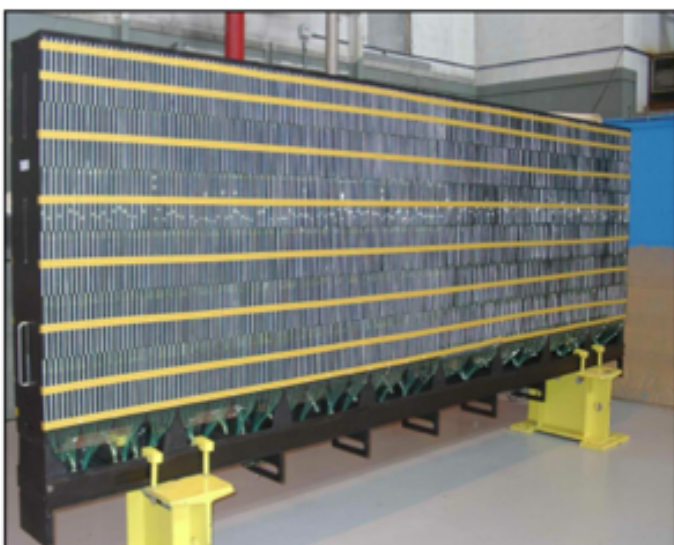
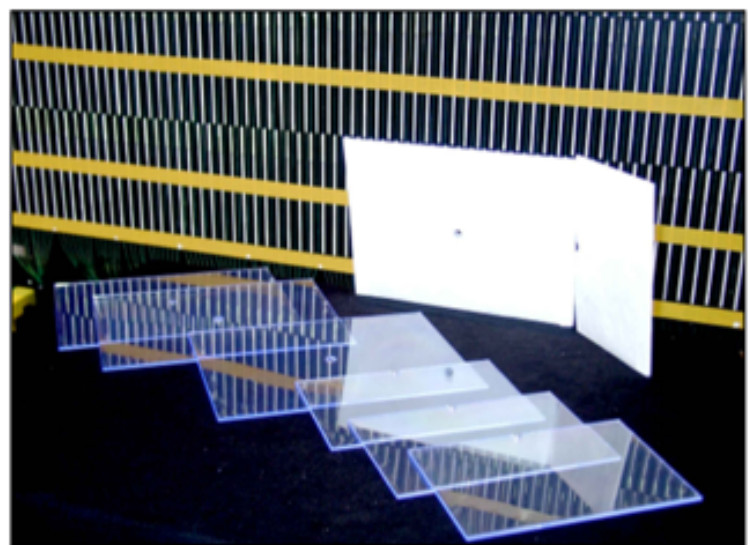
Utilization of homogenous calorimeters unnecessary (and thus too expensive) due to fluctuations of invisible shower components ...

Typical absorbers : Fe, Pb, U ...
Sampling elements : Scintillators, LAr, MWPCs ...

Typical setup:
Alternating layers of active and passive material
[also: 'spaghetti' or 'shashlik' calorimeter]



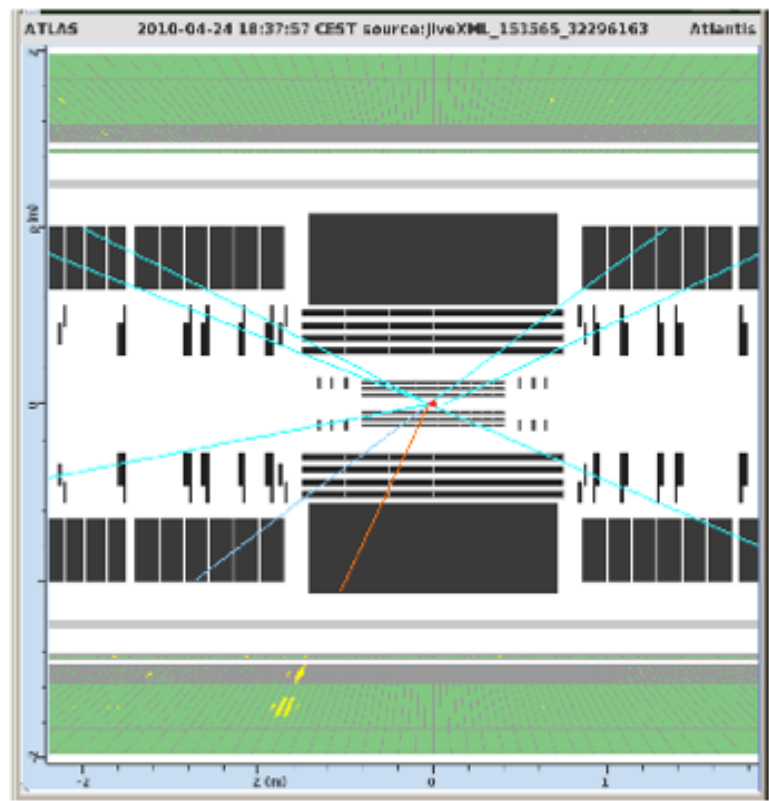
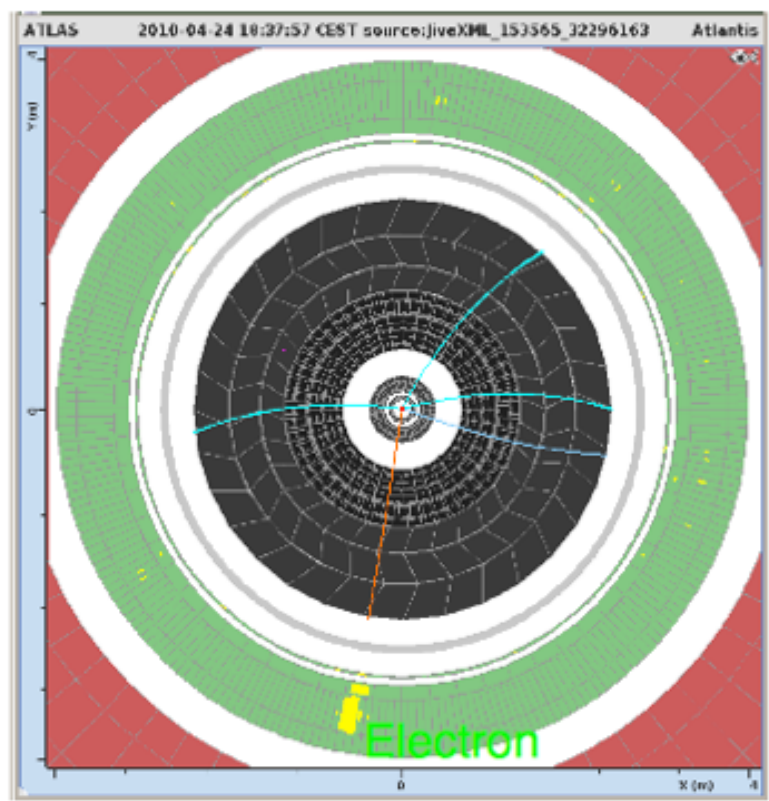
LHCb
HCAL



Example:
LHCb Hadron Calorimeter

MISSING TRANSVERSE ENERGY

Missing transverse energy : $W \rightarrow e \nu$ candidate



For a pp collision, for instance, and in the absence of escaping particles (neutrinos, neutralinos, DM,..) the transverse energy is ~balanced.

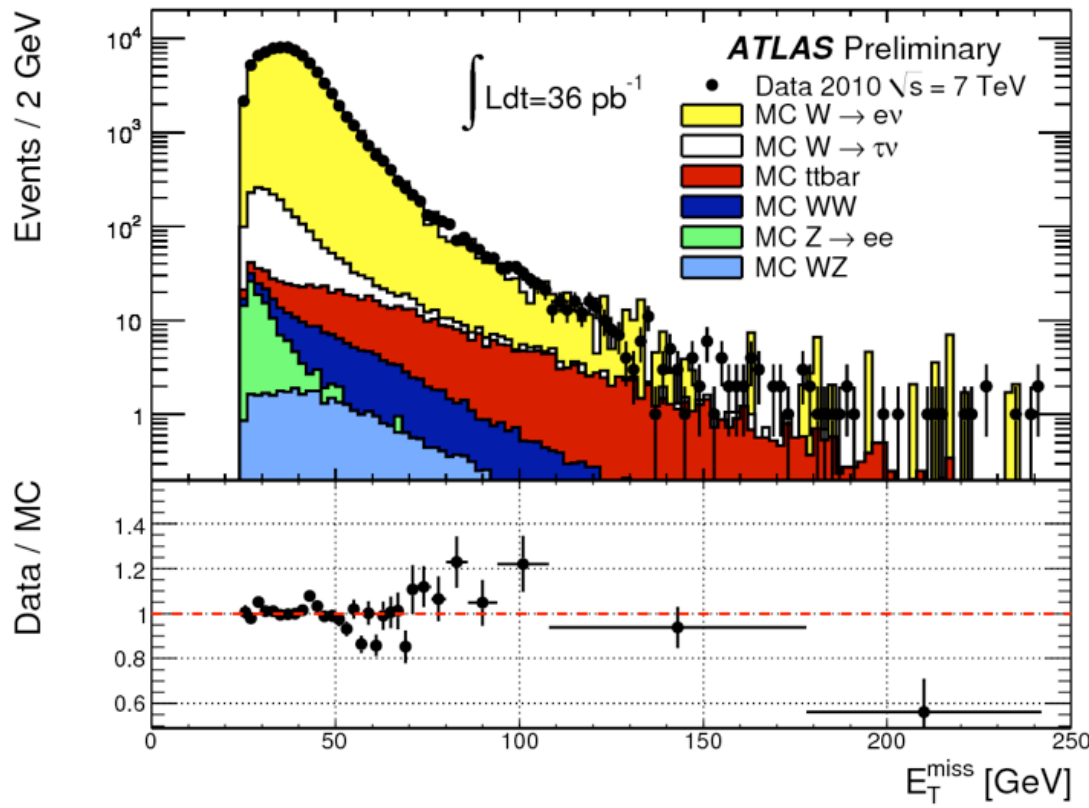
Missing transverse energy is interpreted as the presence of a neutrino.

$$\vec{E}_T^{miss} = - \sum_i^{cells} \vec{E}_T$$

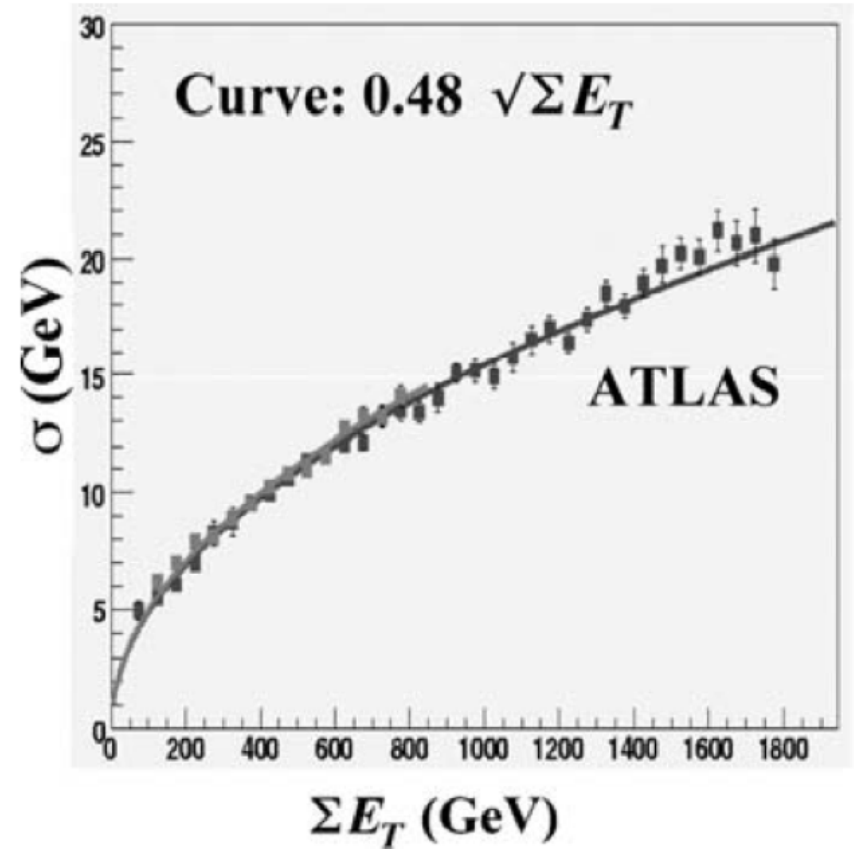
E_T^{miss} is the modulus of the vectorial sum of energy deposited in each calorimeter cell

MISSING TRANSVERSE ENERGY: CALIBRATION

Missing transverse energy in ATLAS for $W \rightarrow e\nu$ events



Missing transverse energy expected resolution in ATLAS



A FEW SUMMARY WORDS on CALORIMETERS

Calorimeters are attractive in our field for various reasons:

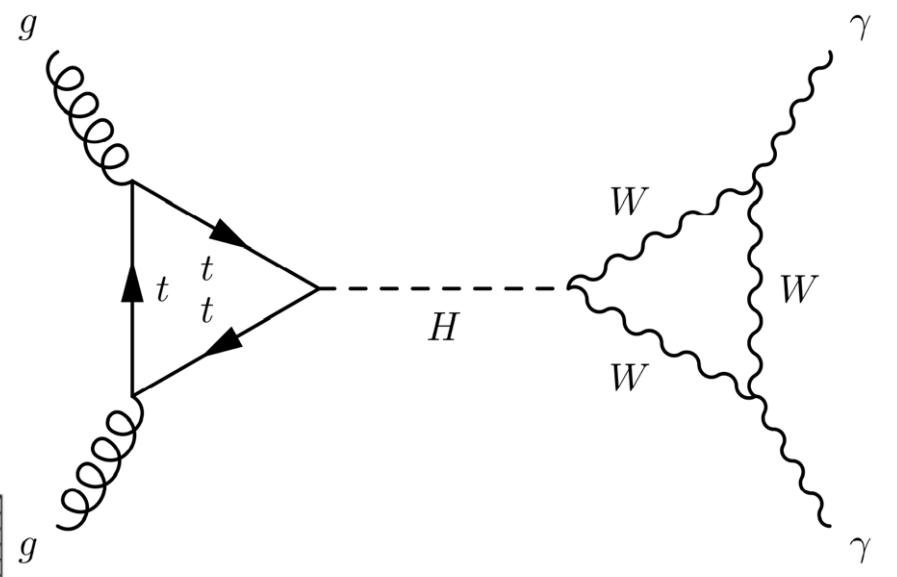
In contrast with magnet spectrometers, in which the momentum resolution deteriorates linearly with the particle momentum, on most cases the calorimeter energy resolution improves as $1/\sqrt{E}$, where E is the energy of the incident particle. Therefore calorimeters are very well suited for high-energy physics experiments.

In contrast to magnet spectrometers, calorimeters are sensitive to all types of particles, charged and neutral. They can even provide indirect detection of neutrinos and their energy through a measurement of the event missing energy.

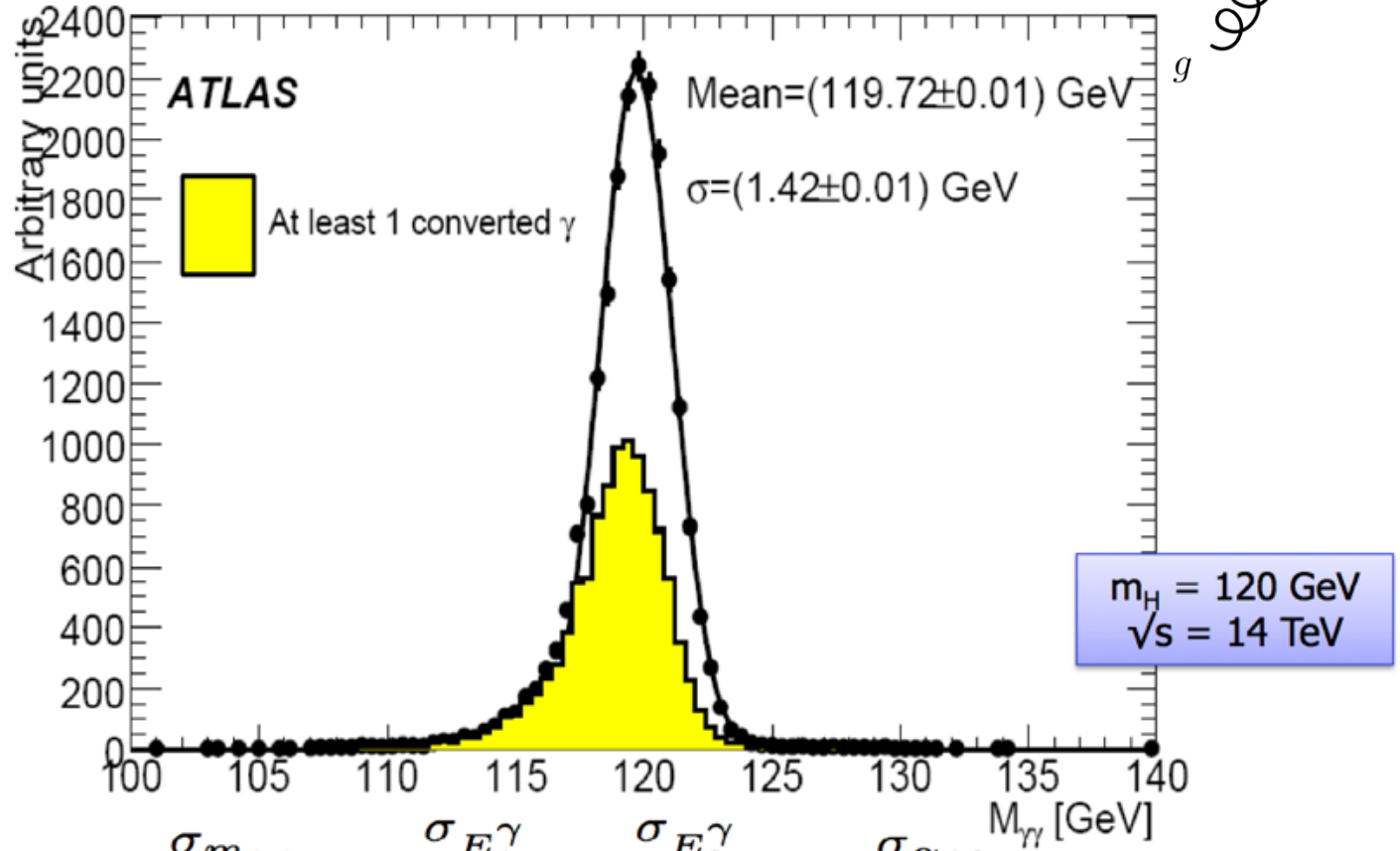
Calorimeters are commonly used for trigger purposes since they can provide fast signals that are easy to process and interpret.

They are space and therefore cost effective. Because the shower length increases only logarithmically with energy, the detector thickness needs to increase only logarithmically with the energy of the particles. In contrast for a fixed momentum resolution, the bending power BL^2 of a magnetic spectrometer must increase linearly with the particle momentum.

HIGGS MASS RESOLUTION

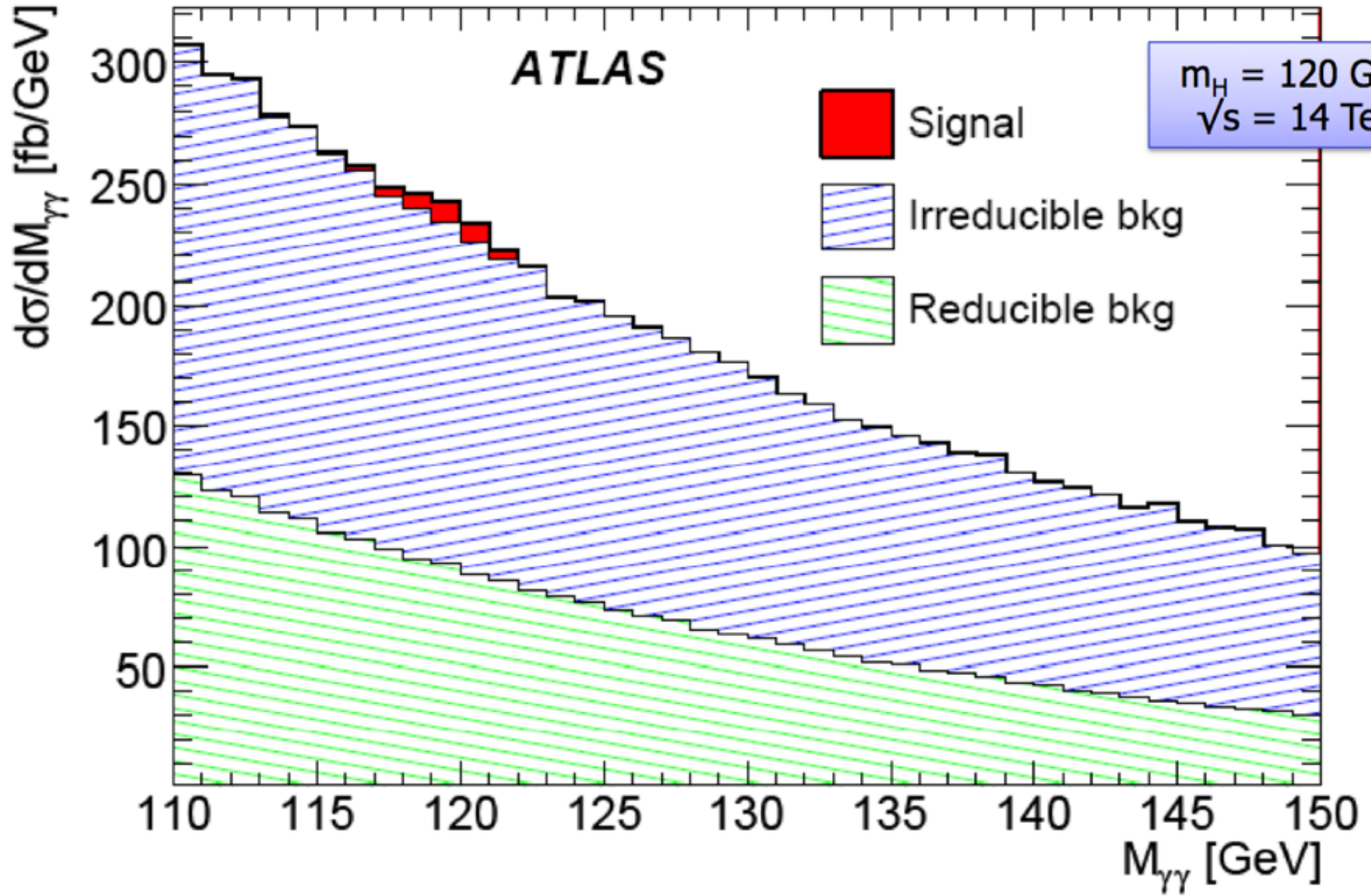


$$m_{\gamma\gamma} = \sqrt{E_1^\gamma E_2^\gamma (1 - \cos \alpha_{12})}$$



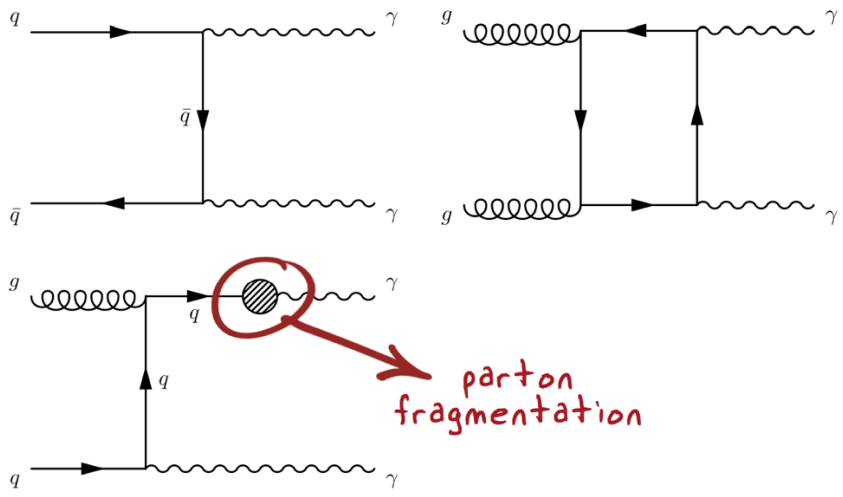
$$\frac{\sigma_{m_{\gamma\gamma}}}{m_{\gamma\gamma}} = \frac{\sigma_{E_1^\gamma}}{E_1^\gamma} \oplus \frac{\sigma_{E_2^\gamma}}{E_2^\gamma} \oplus \frac{\sigma_{\alpha_{12}}}{\tan \alpha_{12}}$$

SIGNAL on a LARGE BACKGROUND

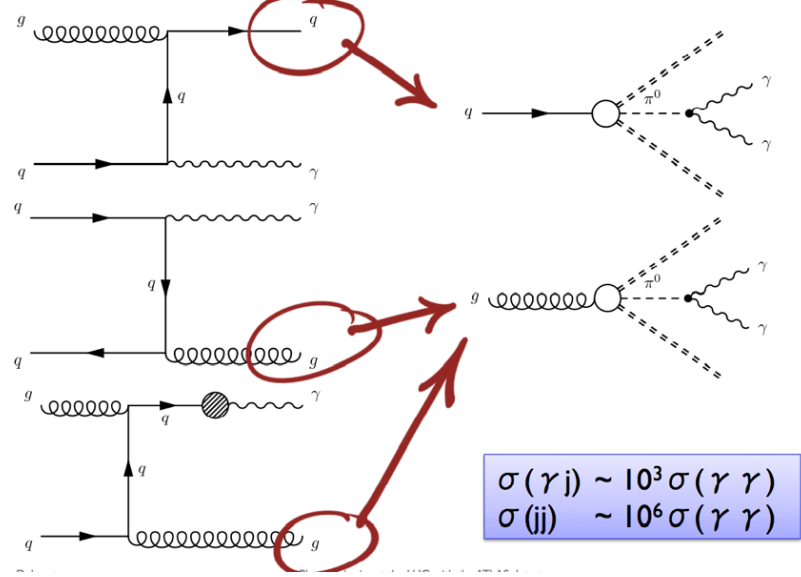


SIGNAL on a LARGE BACKGROUND

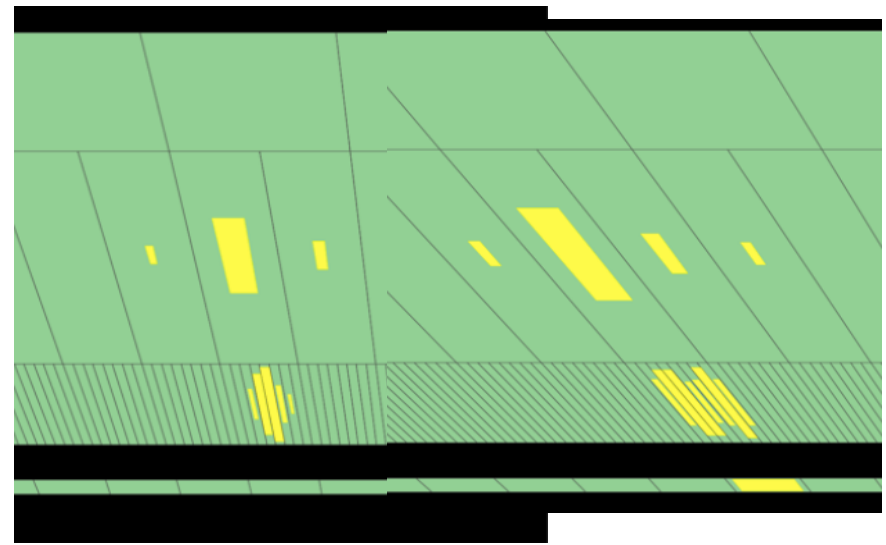
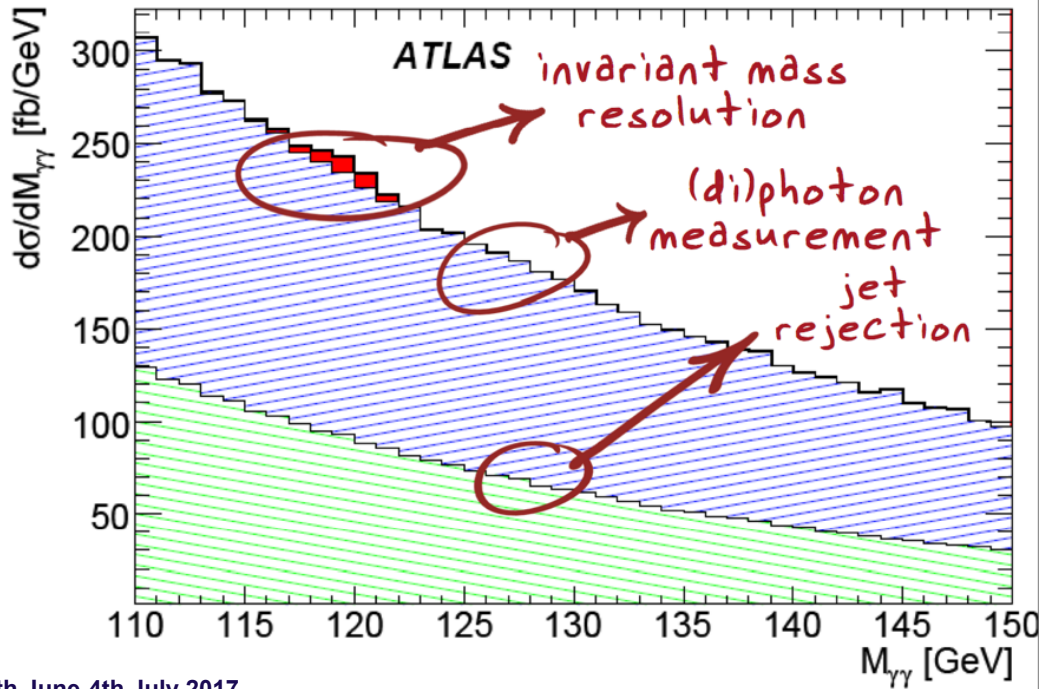
IRREDUCIBLE BACKGROUND
 γ in the FINAL STATE



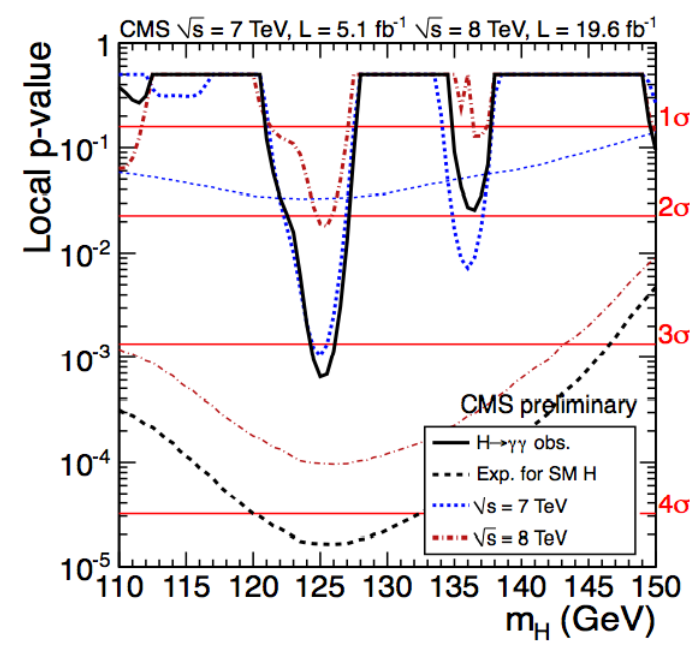
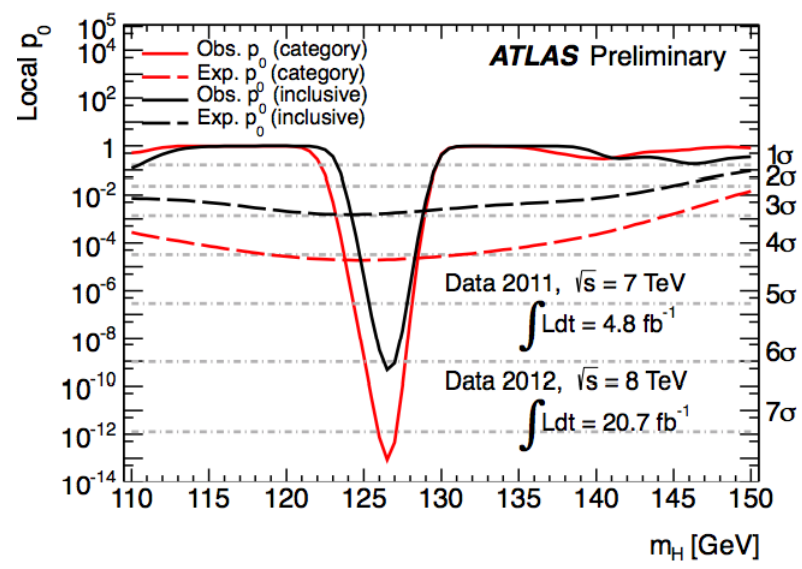
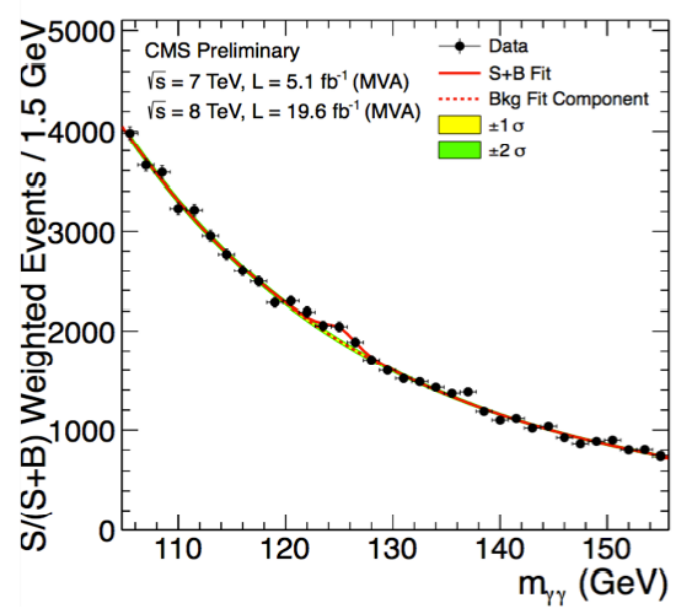
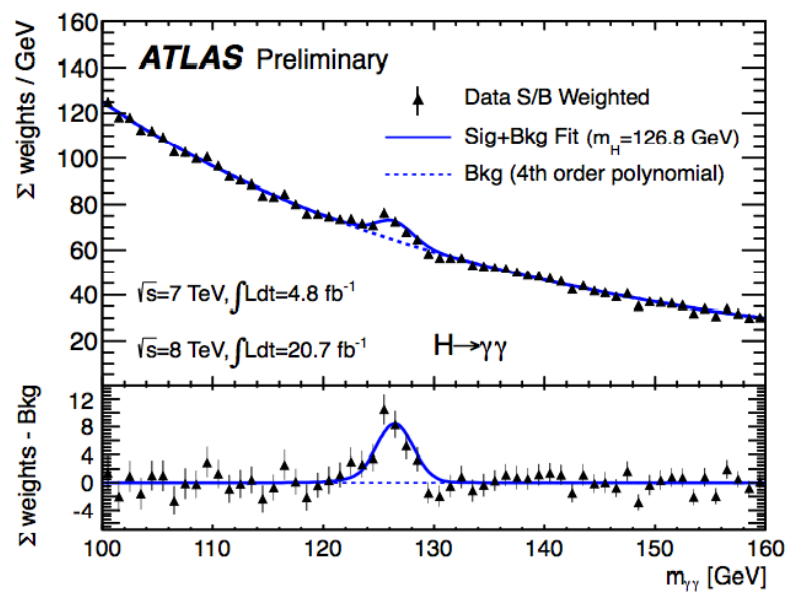
REDUCIBLE BACKGROUND
 π^0 in the FINAL STATE



$\sigma(\gamma j) \sim 10^3 \sigma(\gamma\gamma)$
 $\sigma(jj) \sim 10^6 \sigma(\gamma\gamma)$



H → γγ MASS SPECTRA & SIGNAL OBSERVATION



CONSTANT TERM

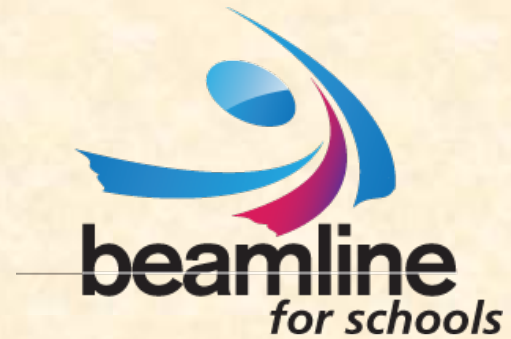
The constant term describes the level of uniformity of response of the calorimeter as a function of **position, time, temperature** and which are not corrected for.

- Geometry non uniformity
- Non uniformity in electronics response
- Signal reconstruction
- Energy leakage

Dominant term at high energy

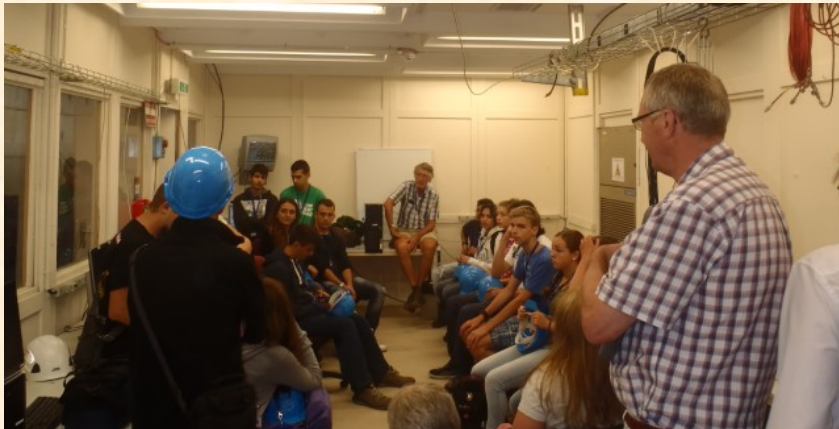
| Correlated contributions | Impact on uniformity | ATLAS LAr EMB testbeam |
|---------------------------|------------------------|------------------------|
| Calibration | 0.23% | |
| Readout electronics | 0.10% | |
| Signal reconstruction | 0.25% | |
| Monte Carlo | 0.08% | |
| Energy scheme | 0.09% | |
| Overall (data) | 0.38% (0.34%) | |
| Uncorrelated contribution | P13 | P15 |
| Lead thickness | 0.09% | 0.14% |
| Gap dispersion | 0.18% | 0.12% |
| Energy modulation | 0.14% | 0.10% |
| Time stability | 0.09% | 0.15% |
| Overall (data) | 0.26% (0.26%) | 0.25% (0.23%) |

The Beam Line for Schools competition



A competition for teams of high school students (age 16 and up)

- Teams can propose a physics experiment
- CERN provides 1 week of proton beam at the PS accelerator
- Two winning teams will be invited to CERN to carry out their experiment together with CERN scientists
- Registration closes 31 March 2018



Video: <http://cds.cern.ch/record/1757251>

<http://cern.ch/bl4s>